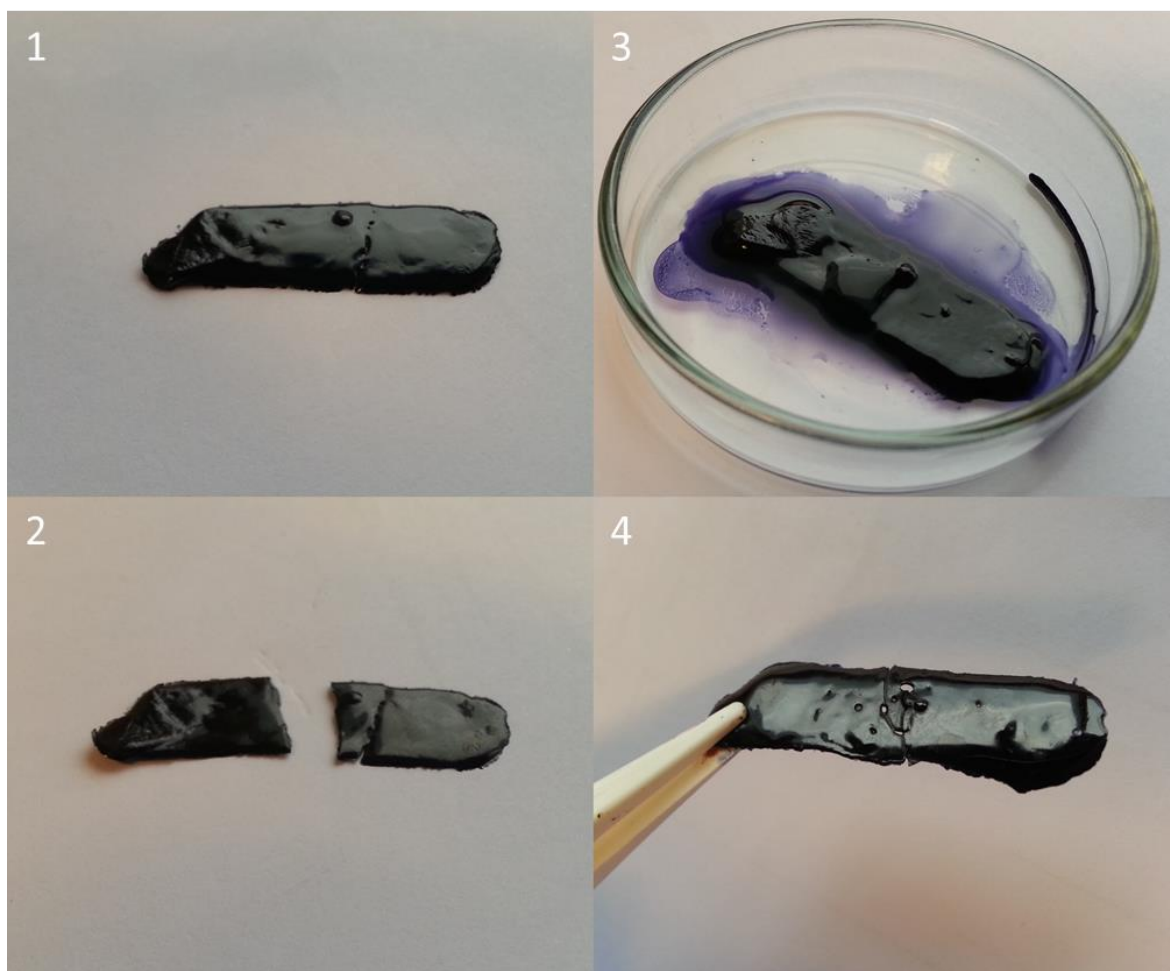


Smart self-healing polymer networks



Wouter Nielen (930414600050), Supervisors: Maarten Smulders, Fatima Garcia Melo

7/09/2015-4/03/2016

Chair group Organic Chemistry

MCs thesis ORC-80336

Figure 1: 1) Film made with compound **8** (20% w/v in DMF with 0.3 eq Fe(II)(OTf)₂). The film has already gone through one self-healing cycle which is repeated by cutting the film into two pieces (2) and putting them back together with some DMF on top (3). After three healing cycles the self-healing still works but there is visible scarring (4).

Contents

Abstract.....	3
Introduction	4
Objective	9
Results and discussion	10
Synthesis	10
Gel tests	13
Zinc.....	14
Copper.....	16
Iron.....	17
Europium.....	18
DOSY.....	19
Comparison of different metals.....	21
Dynamic imine bonds.....	22
Future prospects	22
Conclusion.....	24
Acknowledgements.....	25
References	26
Experimental details	28
Appendix	33
1. NMR, IR and MS spectra	33
NMR	33
IR	50
MS	52
2. Overview of gelation attempts	53

Abstract

A three armed molecule capable of forming hydrogen bonds, metal-ligand coordination and dynamic covalent imine bond formation was successfully synthesized. Dissolved in DMF with a 20% weight/volume ratio with a metal cross linker, this molecule is capable of forming polymer networks with its properties depending on the metal and the ratio between the molecule and the metal. With copper(II) and europium(III) soft gels were made capable of solvent-mediated self-healing. With iron(II) a sturdy solid film was created with was also able to repeatedly perform solvent-mediated self-healing. Diffusion ordered spectroscopy (DOSY) was used to monitor the amount of cross linking the europium induced at different concentrations which showed a clear trend with lower diffusion rates as the metal content increased. Overall the molecule shows very promising properties but a follow up study is required to fully measure and quantify all the possibilities.

Introduction

Self-healing materials have been of interest for a lot of researchers for quite some time now, since they offer a lot of new possibilities and have a lot of applications.^{1, 2} The main advantage of a self-healing material is, that it can maintain and repair itself so that less time and money is needed for maintenance costs. When properly made these materials can be significantly more durable than ordinary materials.

Current advances in the field of self-healing materials have identified two major criteria by which self-healing materials can be classified. The first is whether the self-healing is autonomous, and the second being the replicability of the self-healing.² The first property addresses whether the material is truly “self” healing or if it needs an external influence to initiate the healing process. It is preferable to have a fully autonomous self-healing material so there is no need to check the material for damage. However fully autonomous self-healing often comes with the drawback of having a very low replicability, which means that most fully autonomous self-healing materials can repair themselves once when damaged but when damaged again in the same area they are often unable to do so again.² There are currently multiple mechanisms available to make a self-healing material. The traditional way to achieve self-healing is with pockets of unreacted material inside the material itself.² More recently, self-healing materials relying on supramolecular interactions or reversible covalent bonds have been developed.^{3, 4-5, 6} It is important to note that the supramolecular and dynamic covalent methods create mostly “soft” materials like gels which have different applications than the “hard” materials made with techniques that use pockets or vascular systems with healing agents.

The approach of making self-healing materials by including pockets of unreacted components of the material inside of the material is an excellent example of fully autonomous self-healing as shown in Figure 2.⁷ When the material is damaged, materials are released from the pockets which then react to form a fresh layer of the material in the damaged area. This method can very efficiently heal even the smallest amounts of damage to the material. Unfortunately the healing capacity is limited to the amount of reactive components inside it, which means that it will be unable to heal large amounts of damage. Additionally it will only work once in the same spot since the reactive materials inside the material cannot be renewed. Nevertheless its limitations, it is still a very efficient way of making fully autonomous self-healing materials, which can have a wide variety of applications from ordinary applications such as chairs to the hull of spacecraft.⁸

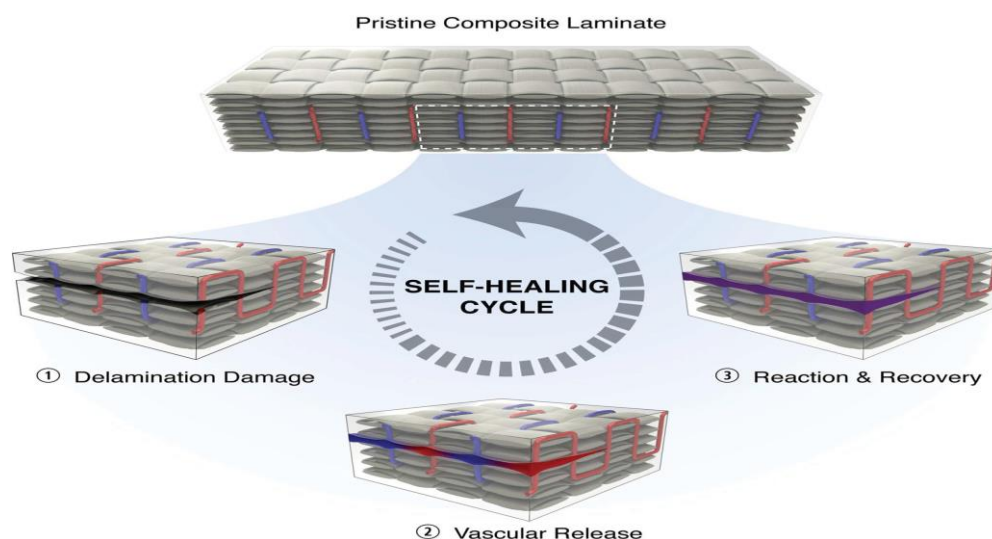


Figure 2: Self-healing with vascularized structural composites, taken from Patrick et al. ⁷

Non-autonomous self-healing has the disadvantage that an external influence is needed to induce the self-healing of the material. The advantage is that often the damaging and healing of the material can be repeated multiple times. The most common stimuli for inducing self-healing are: heat, photo irradiation, pH change or pressure. Most non-autonomous self-healing materials have bonds which can be activated or have a natural equilibrium which can be influenced to recreate the bonds between damaged parts of the material. In polymer gels there are two popular ways in which this can be achieved, with supramolecular interactions between different polymers or with dynamic covalent bonds.^{5, 6, 9}

Supramolecular interactions have the advantage that they are always fully reversible which means that there is potentially no limit to how many times the damaging and repairing cycle can be repeated. Unfortunately, this is often not feasible because there is often also some damage to the non-supramolecular bonds and depending on which method is used there is also the possibility that contamination can compete with the material for the supramolecular interactions which can prevent the self-healing. One of the most commonly used supramolecular motifs is hydrogen bonding.^{4, 10, 11} Often these motifs are designed to have complementary donor-acceptor interactions creating a relative strong bond by effectively combining multiple weak bonds together as seen in Figure 3.⁴

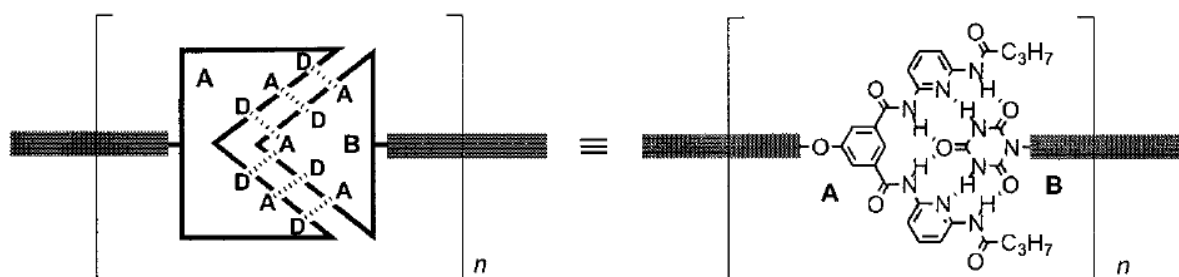


Figure 3: hydrogen bonding motif, taken from Berl et al.⁴

In biological systems metal ions are an integral part in a lot of enzymes to provide catalysis or stability.¹² This illustrates how interesting and important metal-ligand (M-L) coordination is and why it is interesting to determine how we can make use of it in different ways. Metal ions have very distinct coordination geometry which allows for systems to be more predictable, which in combination with rational design of the ligands, complex self-assembled three dimensional structures can be made.^{13 14,}¹⁵ Because every metal ion has multiple coordination sites, multiple ligands can bind to a single metal ion which gives it interesting cross linking properties. This can be used to make large polymer networks where the monomers are bound together using a metal ion. When trying to make such polymer networks some metals are more suitable than others which mostly depends on their coordination number. Same as with the hydrogen bonding motif in the previous paragraph, a ligand which can make multiple coordination bonds will offer a lot more stability. Therefore metals such as copper(I) and platinum(II) can make up to four coordination bonds are less suitable compared to metals such as copper(II) and zinc(II) which can have up to six bonds. This allows two bonds per ligand when using the metal ion as a branching point for the network or three when using it as a linear linker. Lanthanides are also very interesting metals for cross linking networks since they can form up to nine coordination bonds. Next to the coordination number the size of the metal and the ligand also play a role because when the sizes match more stable coordination bonds are formed. In addition to cross linking some metals can also give other interesting properties to polymer networks such as the absorption and emission of light (UV/vis). An example is the work of Pangkuan Chen *et. al.* where they used europium and terbium as cross linkers in their network to make white light emitting gels.¹⁶

There are also other possibilities for supramolecular interactions which do not involve hydrogen bonds or M-L coordination. An example is host-guest interactions with molecules like cyclodextrins and various guest molecules.^{3, 14, 17} In a recent paper, Miyamae *et al.* used host-guest interactions combined with M-L coordination to create a self-healing hydrogel.³ Additionally to self-healing properties, it also displayed shape memory due to the M-L coordination. This was achieved by creating polymer layers with cyclodextrin groups alternated by adamantane and ferrocene, combining two different host-guest interactions (Figure 4). Both adamantane and ferrocene have binding interactions with cyclodextrin but the interaction of ferrocene can also be tuned with its redox potential. Oxidised ferrocene has slightly larger dimensions which means it will no longer fit inside the cyclodextrin effectively terminating the interaction. When afterwards the ferrocene is reduced it will again be able to undergo the interaction with cyclodextrin, making this a “smart” reversible supramolecular bond.

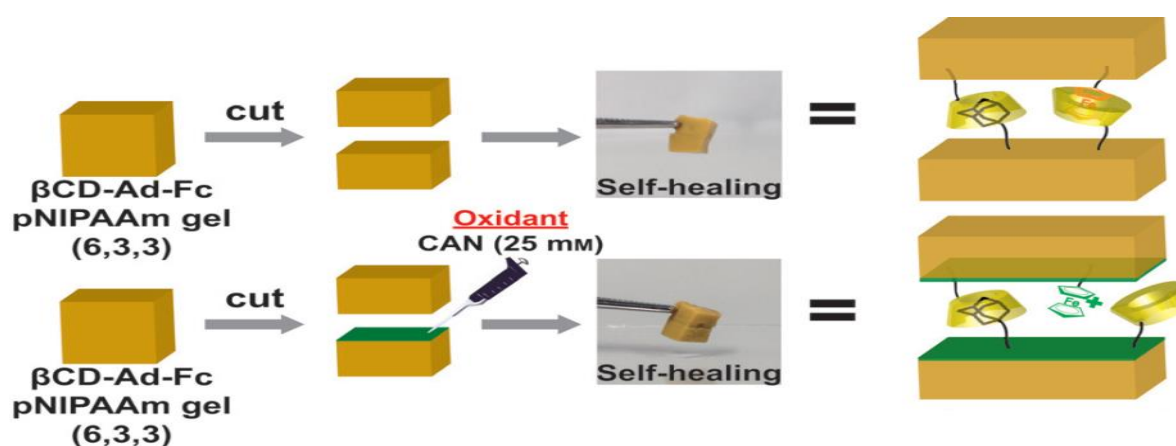


Figure 4: Smart self-healing gel based on host-guest interactions, taken from Miyamae *et al.*³

Dynamic covalent bonds have the innate property that, while the bonds are as strong as any covalent bond, they are also dynamic under the right conditions. As stated by Rowan *et al.*: “Dynamic covalent chemistry relates to chemical reactions carried out reversibly under conditions of equilibrium control.”¹⁸ For dynamic covalent bonds to be useful this equilibrium should be easily influenced from outside for instance: light, heat, pH, or an added catalyst.^{5, 6, 9, 10} With dynamic covalent bonds it is possible to create a complex polymer network consisting of monomers bonded together reversible bonds. This network can then be triggered to collapse by cleaving all the dynamic bonds and afterwards to reassemble with a different trigger. Because the covalent bonds of these dynamic polymers, also known as “dynamers”, are in a dynamic equilibrium there will always be some exchange between the bonded and the cleaved form.¹⁹ By using these dynamers it is easier to make materials with self-healing properties. There are multiple types of reactions which can be used to create dynamers including: aldol reactions, Diels-Alders reactions, cycloadditions, imine bond formation, ester formation, thioacetal exchange and many more.⁵ The combination of multiple dynamic bonds and supramolecular interactions has proven to be an interesting subject for research since it allows for a more precise tuning of the properties of the material.^{3, 17}

Here we will mostly focus on the imine bond because in addition to being a dynamic covalent bond the imine group can also coordinate with metals, thus combining multiple dynamic binding mechanisms.²⁰ Also there is previous work done in the group combining imine bonds with metal coordination.²¹ Imine bonds are formed by a Schiff-base reaction when an amino group reacts with an aldehyde or ketone group with elimination of water.²² The Schiff-base reaction is an equilibrium reaction and its stability is dependent on the groups that surround the imine bond, aromaticity, and the pK_a of the amino group.²³ It has also been shown that the pH and the temperature highly influence

the equilibrium of the reaction; a decrease in pH causes the imine bonds to hydrolyse while an increase in temperature favours the formation of them.²² Because the imine bonds are in a constant equilibrium it is easy to substitute one the amino groups in an imine bond with a more stable form.^{21, 23} It has also been shown that complexation with metal improves the stability of the imine bonds by preventing hydrolysis.²¹ This makes imine bonds an excellent form of dynamic covalent binding to be used in combination with M-L bonding to make dynamic systems.²⁰

The bases of this project lies in previous work done in the group as well as the research done by Kotova *et al.*^{21, 24, 25} In the previous work done by the group, a pincer moiety with imine bonds was attached to a polymer chain which was reversibly crosslinked using metal ions and diamine groups (Figure 5). The pincer moiety can form three coordination bonds, one with the nitrogen from the pyridine and two with the imine groups. The imine bonds are stabilized when the metal is coordinated but retain their dynamic nature making it possible to exchange them (Figure 5).

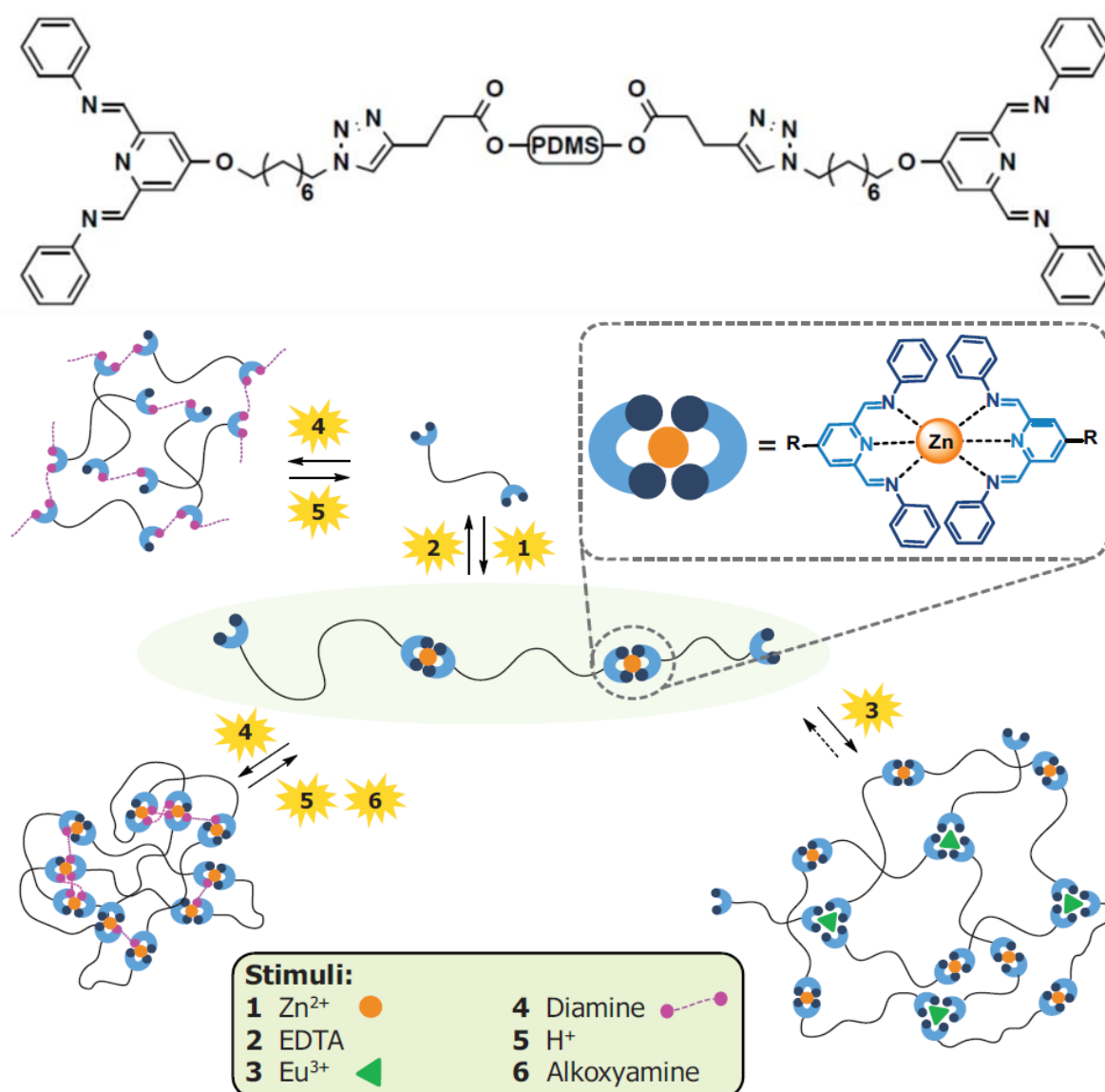


Figure 5: On top: the linear polymer with the pincer moieties. At the bottom: scheme of the possible interactions with the polymer.²¹

Kotova *et al.* combined metal-ligand coordination with hydrogen bonding to create a metallogel which is purely based on supramolecular interactions without any covalent linkage between the molecules.²⁴ This was achieved by creating a tripodal terpyridine ligand which was capable to self-assemble by hydrogen bonding and π - π stacking as well as to coordinate with metals using the terpyridine groups as ligand, Figure 6. Through the hydrogen bonding and π - π stacking the molecule was already able to form a fibrous gel. The addition of d-metal ions resulted in an increased width of the fibres and a shift in fluorescence.

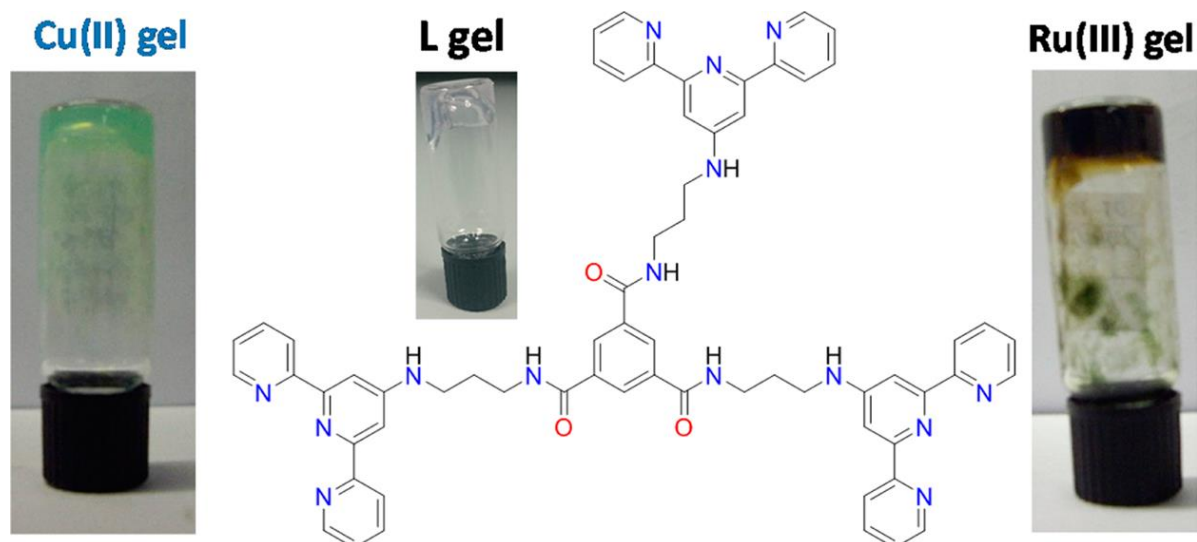


Figure 6: Tripodal ligand molecule (L) used in the formation of metallogels with Cu(II) and Ru(III), taken from Kotova *et al.*²⁵

Our goal is to create a similar molecule which for some extent will also be able to have supramolecular interactions through hydrogen bonding and π - π stacking but instead of using terpyridine, a 2,6 diiminopyridine motif will be used, Figure 7. This design introduces another dynamic interaction with the imine bonds which allows an increase in the responsiveness of the final system. By combining the hydrogen bonding, π - π stacking and metal coordination with dynamic imine bonds we aim to create a “smart” self-healing gel. The “smart” aspect of the gel will be that it is possible to externally and reversibly influence the gel by for instance changing the pH.

Objective

The main objective is to create a molecule which is capable of self-assembly through hydrogen bonding, π - π stacking and metal-ligand coordination while also using dynamic covalent imine bonds (Figure 7) and make a “smart” self-healing gel with that molecule.

The first part is to successfully synthesize the molecule. Then, gelation of the target molecule in combination with different metals will be explored. The imine bonds are sensitive to pH, this will be used to determine how the dynamic bonds have an effect on the gel. Due to the dynamic nature of these bonds it is also possible to use different compounds with amine groups to change the properties of the molecule.

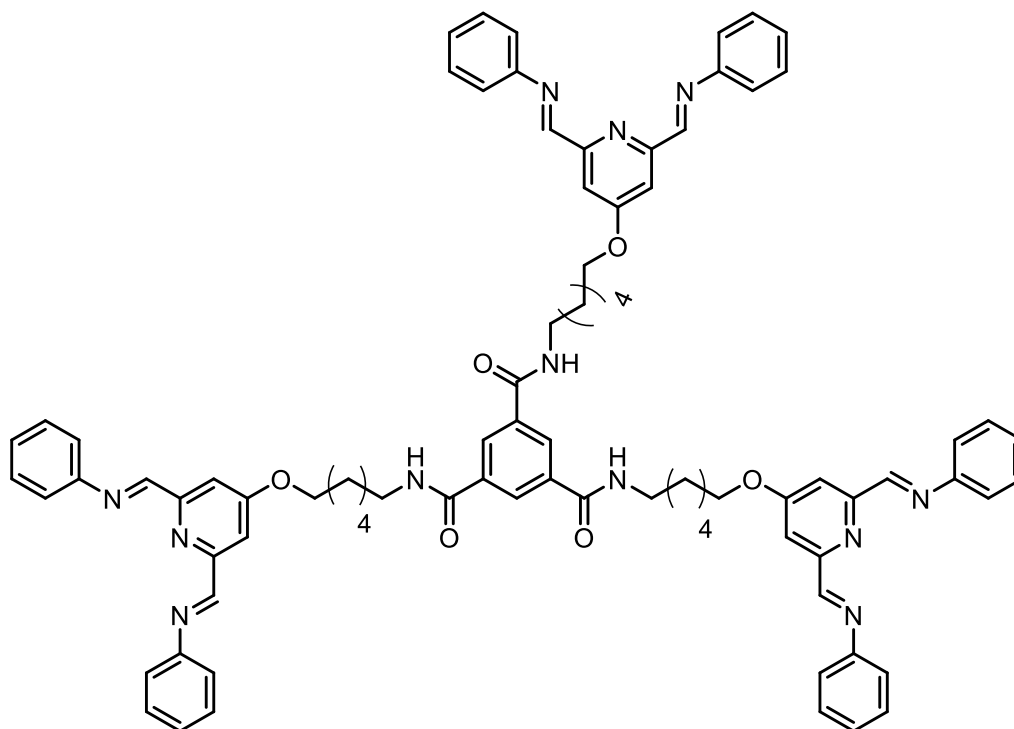


Figure 7: Target molecule.

Results and discussion

Synthesis

The first five steps of the synthesis (Figure 8) were quite straightforward since they were based on previous work done in the lab.²¹ The only difference was that compound **2** has a C6 instead of a C8 linker to make the target molecule slightly more compact. This required slightly different conditions during the purification by chromatographic column but posed no great difficulties.

Starting from chelidamic acid, an acid catalysed esterification with ethanol yielded the diester **1**. 1-azido-bromohexane (**2**) was made with a nucleophilic substitution of 1,6-dibromohexane with NaN₃, the mono adduct was purified from the di-adduct with column chromatography. Then with a nucleophilic substitution of the diester **1** with **2**, compound **3** was made. Next the ester groups were first reduced to alcohols with NaBH₄ (**4**) after which they were oxidized with Dess-Martin periodinane to form the completed pincer unit **5**.

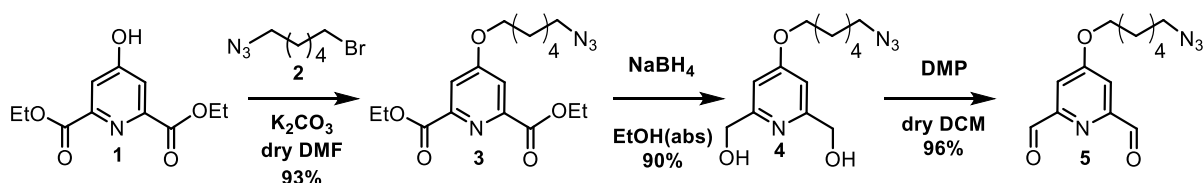


Figure 8: Pathway used to synthesise compound (**8**) which was used to form the gels.

In the following step the aldehyde groups were protected with hemiacetals to prevent polymerization in the step afterwards where the azide would be reduced to an amine (Figure 9). Unfortunately this step was unsuccessful. An excess (1.5 eq.) of triphenylphosphine (PPh₃) was added to a solution of **6a** in THF/H₂O (4/1) and stirred at RT for four hours. On TLC the azide was no longer observed but ¹H NMR showed a lot of contamination even after column purification. MS showed that there is a lot of the intermediate compound, where the PPh₃ is bound to the molecule and still needs to be hydrolysed with water, but no completed product. Several reaction parameters were changed (time, temperature and solvent) however the desired product **7a** was not obtained.

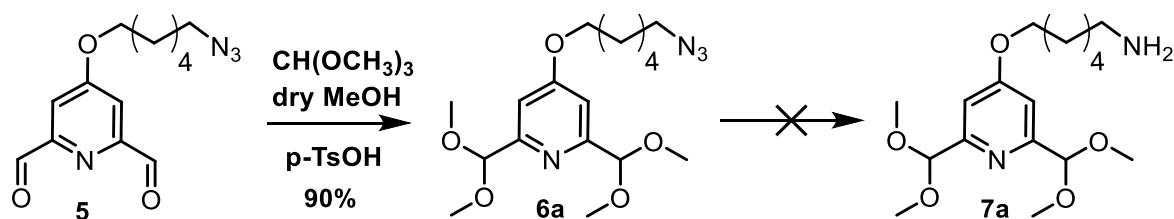


Figure 9: Reaction steps to protect the aldehydes and reduce the azide.

After several failed attempts it was decided that a click reaction might be better suited since we already have the azide derivative **5**. This required us to make some small modifications to the target molecule described in the Objective section. It was hypothesized that the addition of the triazole group would not severely impact the molecule's self-healing and dynamic properties (Figure 10). The new pathway is described in Figure 11.

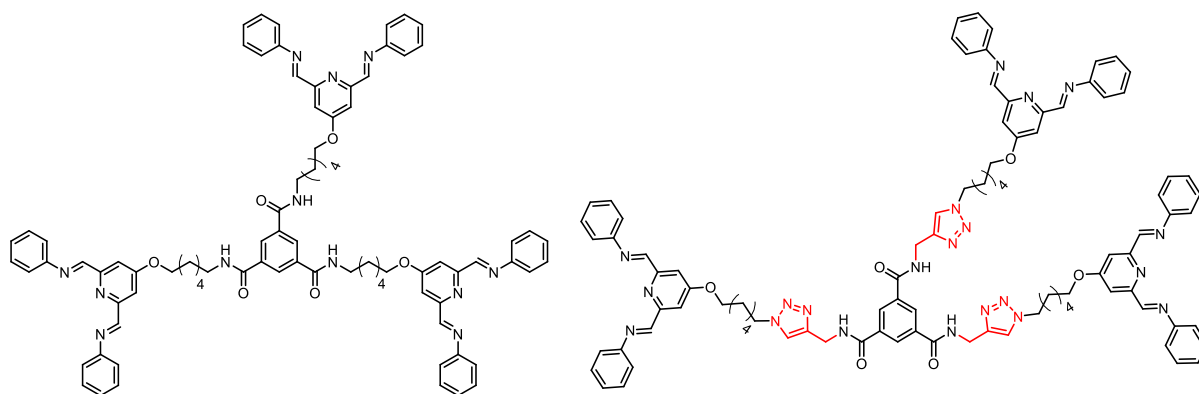


Figure 10: Comparison between the original target molecule (left) and the redesigned molecule (right), the difference is indicated in red.

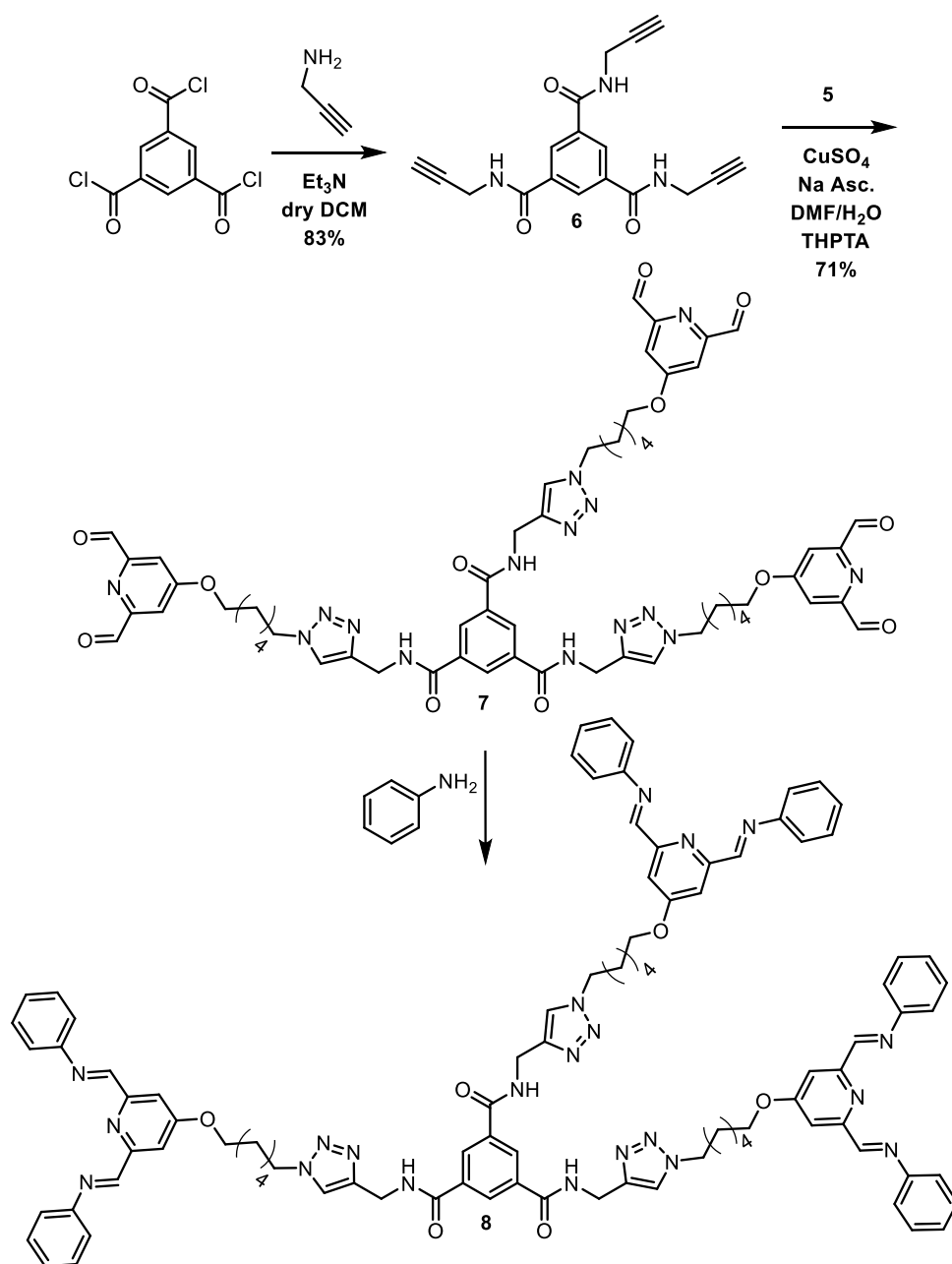


Figure 11: Revised pathway for the new target molecule.

To obtain the tri-substituted core group bearing alkyne groups (compound **6**), 1,3,5-benzenetricarbonyl trichloride was reacted with propargylamine. This reaction is quite straightforward, and its purification only involved several washing steps of the formed precipitate with ethyl acetate and 1M H₂SO₄ to get rid of the excess of propargylamine and the Et₃N.

In these steps it is important to make sure that all three groups have reacted since having two instead of three arms will severely affect the properties of the molecule. The click reaction between the pincer and the core group proved to be a lot more difficult than anticipated. The main problem was that the copper(I) used to catalyse the reaction coordinated with the pincer groups and caused them to precipitate before the completion of the reaction. Only a small amount of product remained in solution which could be purified with a yield of less than 5%. From the precipitate no product could be purified. Multiple test reactions were done with different parameters such as the reaction temperature, solvent and catalyst concentration. These changes were unfortunately of little help and it was also noticed that the reaction did not go to full completion as a small amount of alkyne groups remained visible on the ¹H NMR spectrum. The addition of the tris(3-hydroxypropyltriazolylmethyl)amine (THPTA) ligand dramatically improved the yield and drove the reaction to full completion. Another series of test reactions were done to find the optimal conditions using as little as possible of the THPTA ligand due to its steep price. The next challenge was to purify the product by removing the excess of the azide pincer **5**. The main problem here was that compound **5** has similar properties as compound **7** which made it infeasible to separate them with liquid-liquid extraction and no suitable conditions for silica column chromatography could be found. Because of the polarity of compound **7** it does not run in apolar solvents and when methanol is used the aldehyde groups quickly react to form acetal groups which gives incredible amount of band broadening. Therefore size exclusion chromatography (S-X3 Bio-Beads) was used which cleanly separated the product from the starting compounds and also made sure any molecules with only one or two reacted groups were also separated. In the end a yield of 71% was achieved (Figure 12).

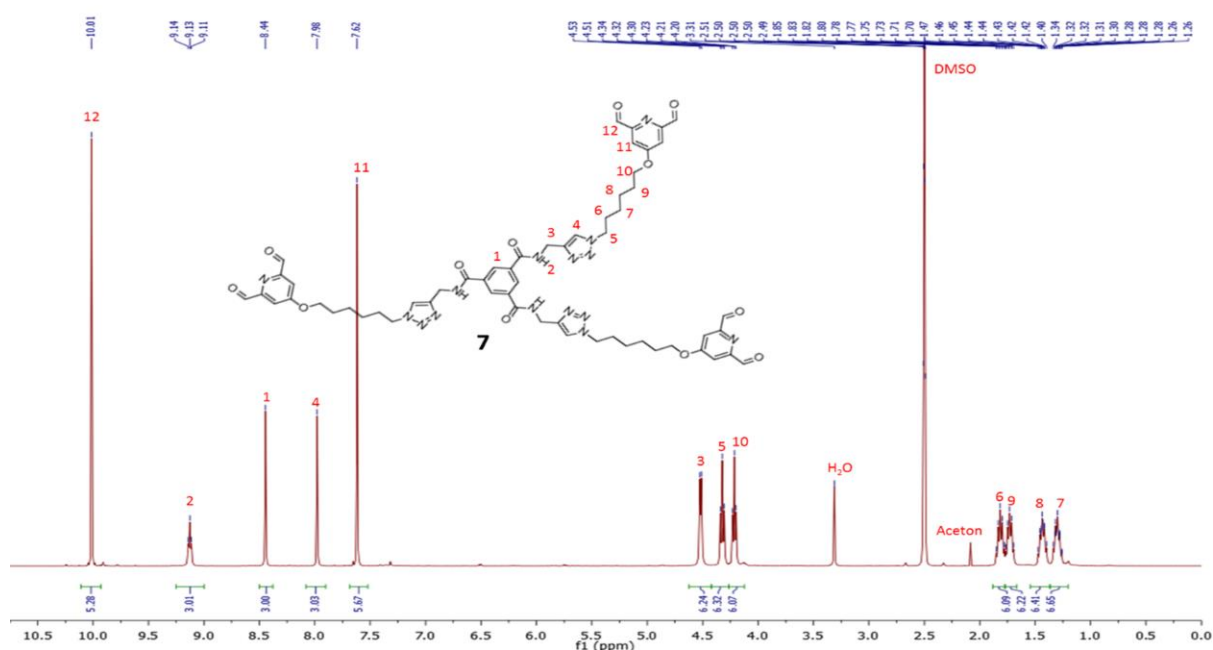


Figure 12: ¹H NMR spectrum of compound **7** in DMSO after purification. It is observed that the protons on the pincer group (11 and 12) have a lower integral than expected, 5.28 and 5.67 instead of 6. It is possible that this is caused by rotation of the molecule, MS shows that the product is complete without missing arms (Figure 25).

The last step to make the final product **8**, was the easiest as it only required the addition of aniline to the solution of compound **7** and gently heating which was done by using a heat gun for several seconds (Figure 13).

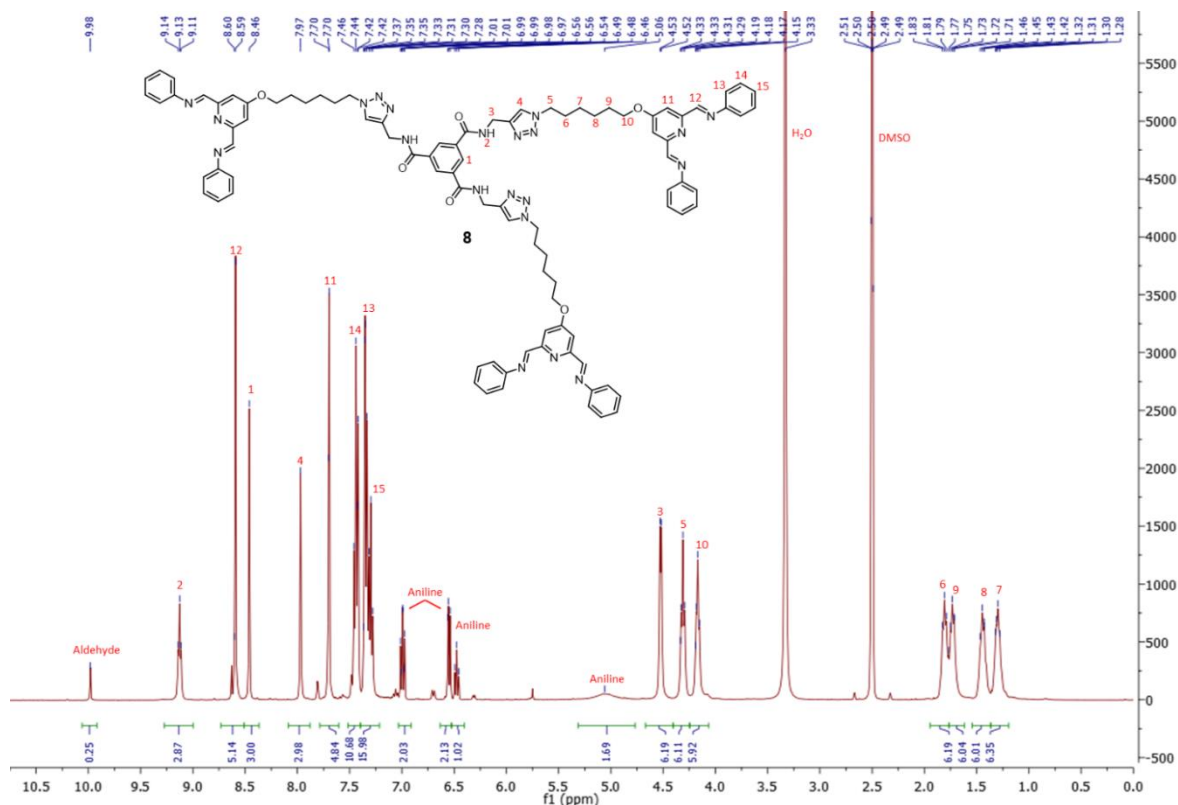


Figure 13: ^1H NMR spectrum of compound **8** in DMSO.

The new molecules described in this report were characterized by NMR, MS and FTIR except for compound **8** since it was made in situ and never purified. For the compounds already described in the group previously, ^1H NMR were compared with those reported.

Gel tests

Compound **7** was subsequently dissolved in different solvents at different concentrations with aniline and different metals ions at different ratios, and heated with a heat gun for several seconds to determine the conditions in which it would form a gel. In the study by Kotova *et al.* the compound was dissolved in MeOH/H₂O at 0.3 weight/volume % (w/v %) and left to evaporate to open air.²⁵ Therefore this was tested first but it did not work because when the imine bonds were formed the compound became insoluble. A multitude of different conditions and solvents was tested, but in most cases compound **8** remained in solution or precipitated. However when the concentration was increased up to 20% w/v, gels were formed. Table 1, shows the conditions tested which were successful, a complete overview of all tests can be found in Appendix 2. The high concentration needed to obtain a gel in comparison to the reported conditions by Kotova *et al.* indicate compound **8** is not as good a gelator.²⁵ This large difference is possibly caused by the long aliphatic carbon chains that links the core to the pincer moieties and the lower number of amide groups which makes the stacking with hydrogen bonding less effective. These chains give the molecule distinct regions in which its polarity changes drastically which makes it difficult to find a proper solvent and it likely decreases the solvent capture ability of the molecule. Whether the addition of the triazole has a positive or negative effect on the gelation properties of the molecule remains uncertain and additional research will have to be performed to determine if a better version of this molecule can be designed and made.

Table 1: Conditions tested to obtain gels from compound **8**. To each sample 6 equivalents of aniline was added to form the imine bonds.

Metal	Metal equivalent ¹	Solvent	Gel %	Solubility
Zn(OTf)₂	0.15	DMF	20	soluble
	0.30	DMF	20	soluble/gel
	0.40	DMF	20	gel
Cu(OTf)₂	0.15	DMF	20	soluble
	0.30	DMF	20	gel/solid
Fe(II)(OTf)₂	0.15	DMF	20	soluble
	0.23	DMF	20	soluble
	0.30	DMF	20	gel/film
Eu(III)(OTf)₃	0.10	DMF	20	soluble
	0.20	DMF	20	soluble
	0.30	DMF	20	soluble
	0.40	DMF	20	gel

²: The metal equivalent is the molar ratio of the metal ions to compound **8**.

After checking the conditions under which compound **8** forms gels, their properties were studied. Since the conditions in all further gel test were kept the same, the conditions of each gel referred to will be the ones at which point it first showed gelification as described in Table 1. There is a clear difference in the behaviour of each metal which is why in the next part the experiments performed with each metal are discussed in further detail.

Zinc

The gels with zinc were made with 20% w/v solutions of compound **8**. To the solutions Zn(OTf)₂ was added stepwise, either dissolved in DMF or as its powdered form. When the zinc was added in solution the gelification was observed when 0.40 eq. of the metal was added. When the metal was added in its powdered form gel formation was already observed after the addition of 0.3 eq. This is most likely caused by the dilution of the 20% w/v to a 17% w/v by the amount of DMF used to dissolve the zinc. Adding the zinc as a solid does make it more difficult to completely homogenize the solution with heating before it starts to form a gel but it keeps the w/v% constant which is why this method was used for all further gelation attempts. The gels formed have a transparent brown colour (Figure 14a).

It was determined that upon heating the DMF evaporates from the gel which leaves a brittle solid with a light brown colour (Figure 14b). It was not possible to redissolve it upon heating up to 130 °C. The solid showed no signs of self-healing under increased temperature or presence of solvent (Figure 14c). To another gel 6 eq. of TFA was added to determine the effect of acid on the imine bonds. Upon the addition of the acid the gel slowly solidified in the same way the zinc gels solidified when the DMF was evaporated (Figure 14d). This solid was also brittle and light brown like with heating but the colour changed to purple when left to open air. Also the film on the sides of the vial had a purple colour instead of the brown colour it had with the other brittle sample. Why the TFA has this effect on the gel is unknown, it is possible that because there was no water added the acid could not properly catalyse the hydrolysis of the imine bonds. That TFA addition and heating the gel have a very similar effect might indicate that they both somehow strengthen the crosslinking, thus inducing solidification. This could indicate that during heating it is not the evaporation of DMF that causes the solidification

but that there is some sort of a transition to a more strongly crosslinked system which requires heating or TFA to activate. However, this is speculation and will require further research.

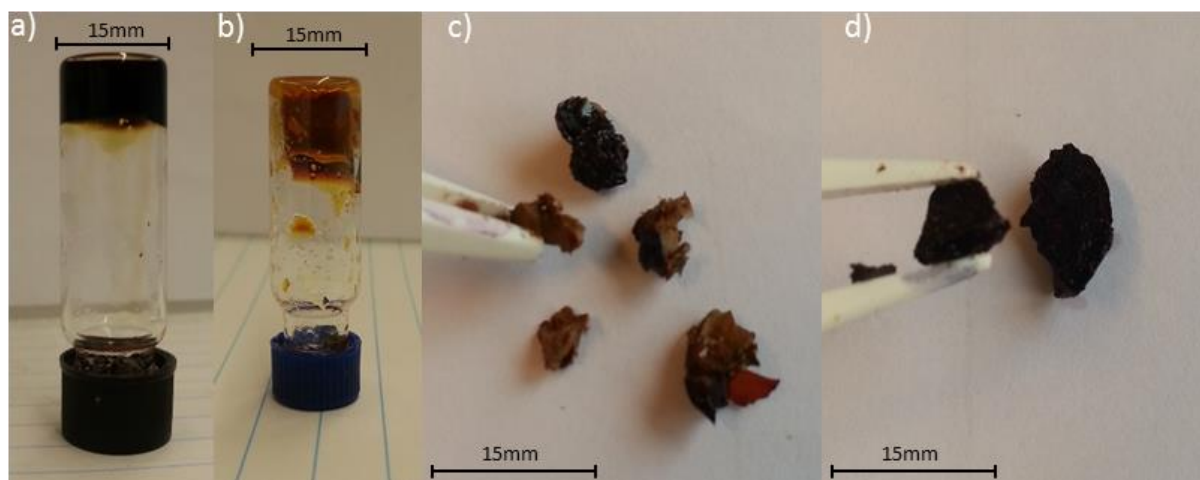


Figure 14: a) Gel formed with 20% w/v compound **8** in DMF with 6 eq. of aniline and 0.3 eq. of $Zn(OTf)_2$. b) A gel made under the same conditions as (a) after being heated. c) Brittle fragments from a gel such as (b) when removed from the vial and air dried. d) Fragments of the solid that was formed when a gel such as (a) was exposed to 6 eq. TFA.

In another attempt the solution was cast in a Teflon mould (40x5x5mm) after the addition of zinc to make a rectangular gel (Figure 15a). The solution was allowed to form a gel in contact with open air. Although a gel was formed overnight it took six days for the gel to dry and become strong enough to be handled properly without tearing it. It appears that when the DMF evaporates, the gel becomes harder and stronger until it reaches a point where it is more a solid than a gel (Figure 15b). Interesting is that even when dried out, as soon as some DMF is put on the solid it is quickly reabsorbed returning to a more gel like state. When the film is cut and the pieces are put back together with DMF the pieces heal back together. This means that the formed material has solvent mediated self-healing properties. Unfortunately, it sticks quite well to glass which is why it was slightly damaged again after the healing (Figure 15c,d). The disadvantage is that after the self-healing most of the DMF needs to be evaporated for the gel to become solid again to gain some structural integrity. When DMF is added and the material becomes soft it is also possible to reshape it (Figure 15f-h).

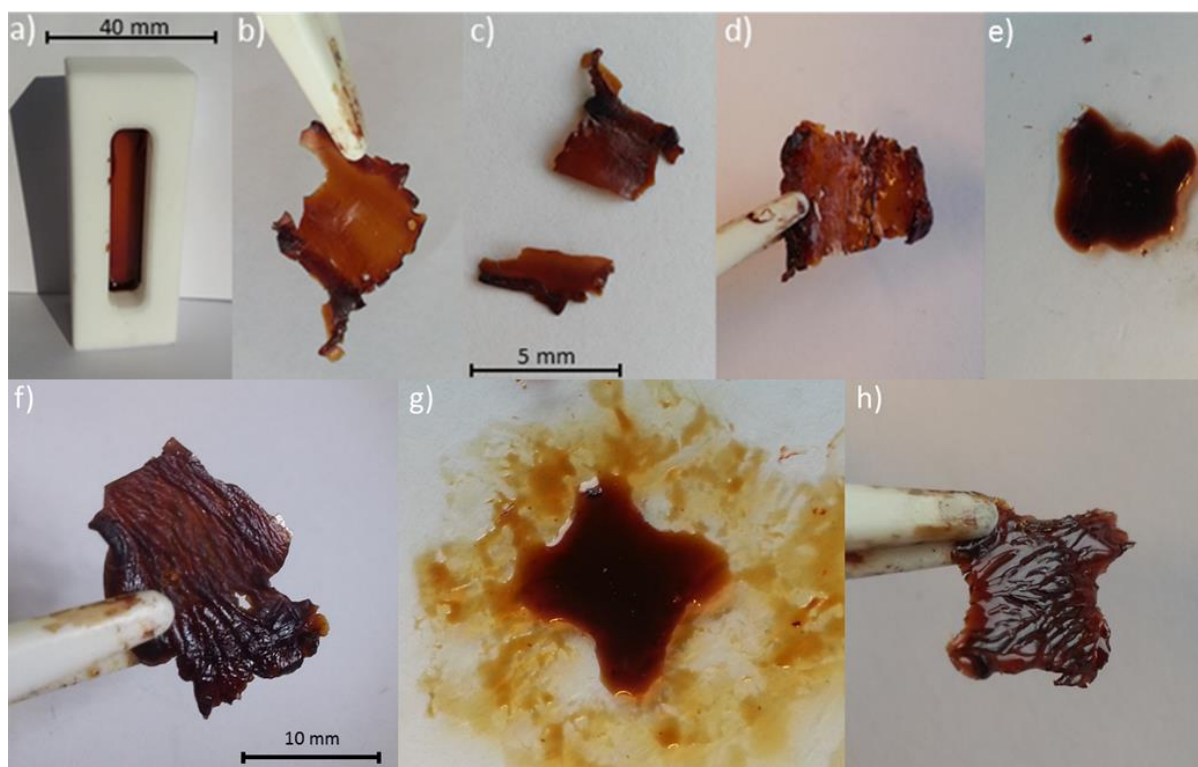


Figure 15: a) Zinc gel in the Teflon mould. The gel remained very sticky was torn to pieces when the attempt was made to remove it (b). The different pieces of the gel showed capabilities of reabsorbing DMF after which self-healing was possible (c-d). In (e) DMF was applied again which smoothed the rough features formed after the gel piece (d) was removed from the glass plate completely healing all damage done. In (f) a dried gel piece was wet with DMF after which its shape was formed and it dried in its new shape (g-h).

Copper

To make gels with copper the same conditions were used as with zinc, 20% w/v solutions of compound **8**. The metal content was stepwise increased with 0.15 eq of $\text{Cu}(\text{OTf})_2$ dissolved in DMF. At 0.3 eq. (20 μL added, 19.2% w/v) the solution formed a red/brown gel within seconds (Figure 16a). When left to dry to the gel solidified (Figure 16b), becoming a brittle solid without self-healing capabilities.

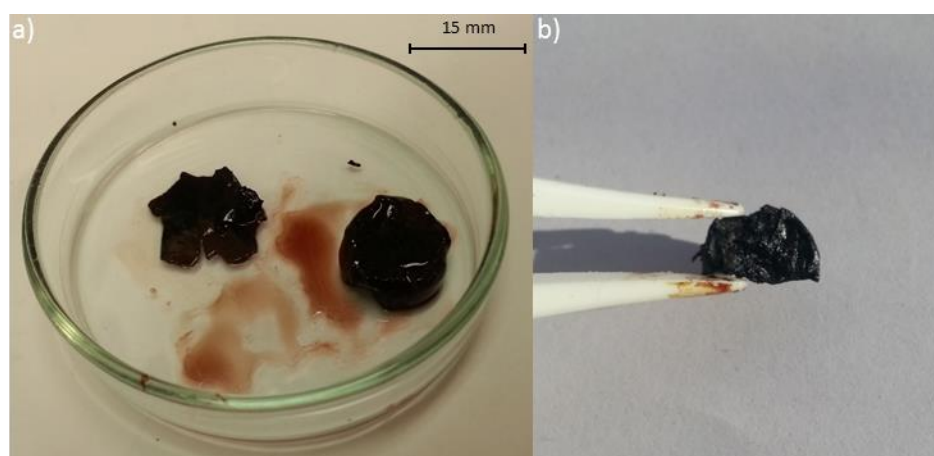


Figure 16: a) The gel and film formed with copper were removed from the vial quickly after it was made, at this point they were still flexible. After drying to open air the gel solidified becoming black and brittle with no signs of self-healing (b).

Apparently copper coordinates quite strongly with compound **8** which adversely affects the dynamic nature of the material which makes it unable to self-heal. It could be possible that when a smaller amount of copper is used the material will be more dynamic and have self-healing properties.

Unfortunately not enough time and material was available to fully explore the properties of the material with copper. It could be that there is an optimal concentration of copper which unlocks the “smart” and self-healing properties of the material that has not yet been found.

Iron

A 20% w/v solution of compound **8** in DMF with 0.3 eq. Fe(II)(OTf)_2 was cast in a mould (40x5x5mm). The solution was left overnight, and instead of a gel a thin (0.5 mm) film was formed with some DMF as supernatant (Figure 17). When removed from the mould the film was still soft and elastic being swollen in DMF. After drying the film to open air more of the DMF evaporated, hardening the film, making it stronger but less elastic. When the film was cut into two pieces and the pieces were put together with some DMF it was observed that some of the DMF gets reabsorbed by the film and that it gets partially dissolved. When the film was left like this overnight to the open air the DMF evaporated and the film had healed (Figure 17b-d). This was repeated several times and each time the two parts of the film reattached to each other indicating repeatable solvent mediated self-healing. It is important to note that already after one cycle there is visible scarring on the film which gets worse after multiple cycles, indicating that the healing cannot be repeated endlessly (Figure 17e).

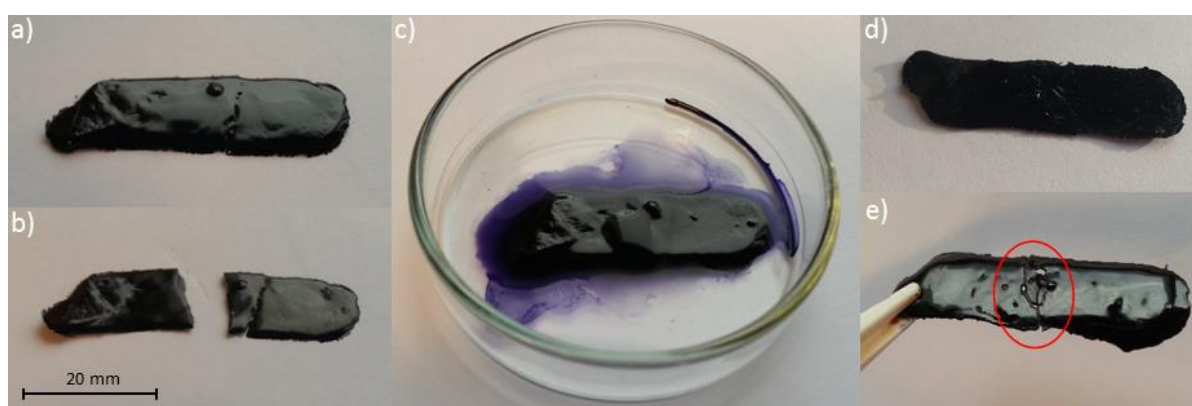


Figure 17: a) The film made from a 20% w/v compound **8** solution in DMF with 6 eq. aniline and 0.3 eq. Fe(II)(OTf)_2 after one healing cycle. The film cut into two pieces (b) after which the film is soaked in some DMF (c). The DMF partially absorbed by the film and also dissolves the film a little. This is what allows the solvent mediated self-healing of the gel resulting in one whole piece after 24 hours (d). After three healing cycles the film still self-heals but visible scarring increases (e).

This shows that compound **8** behaves differently with iron as a cross linker than with zinc since not a gel but a film is formed. Like with the zinc the material is capable reabsorbing DMF after it has been dried although it is less effective. It seems to be a balance in the properties of the material depending on the amount of DMF. More DMF makes the material softer and enables its self-healing capabilities, and less DMF strengthens the material making it more resistant to strain and stress. Due to lack of time and resources no quantitative measurements were done but qualitative experiments. They showed that when the film is swollen on DMF it is easy to break the material by pulling on direct opposite ends by hand. However when the material was allowed to dry for at least five days to air it was not possible to damage the material in this way without applying excessive force. The strength of the dried film is similar to that of a sheet of paper, hard to break it by stretching it but easy to tear. It was observed that when the material was dried for six days it started to curl on the flat side (bottom), it is uncertain what causes this behaviour (Figure 18a). It is observed that the material still has very good solvent mediated self-healing properties after it was dried to open air for five days. (Figure 18b-d). A piece of the film was left at 60 °C for 3 days to explore the possibility of heat as a stimuli for self-healing. It was observed that there was no self-healing and that afterwards solvent mediated self-healing no longer worked. This indicates that when the material is completely dried it can no longer

reabsorb the solvent effectively, which blocks its self-healing capabilities. Whether this also happens when the material is left at room temperature for extended periods (months) has not yet been tested.

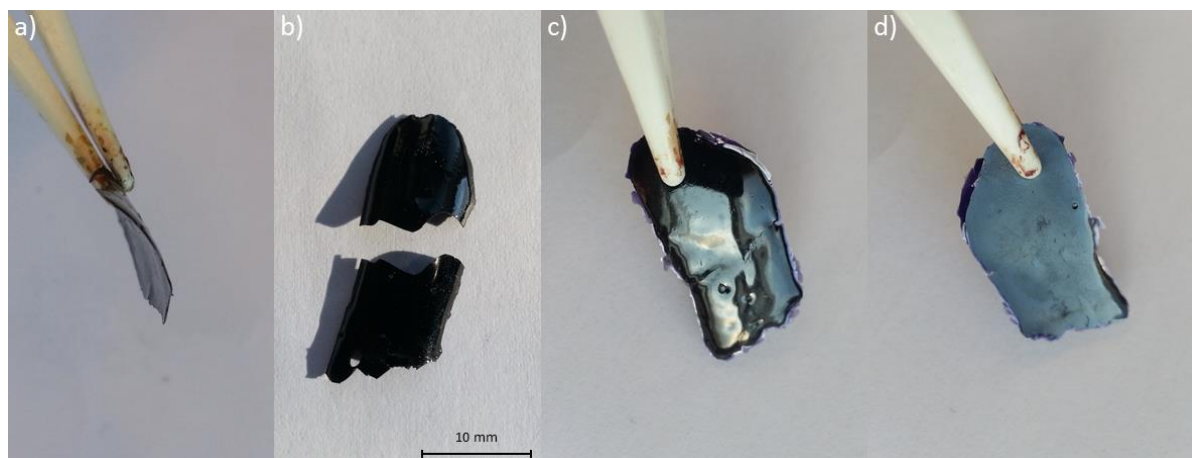


Figure 18: a) The iron film starts to curl after almost all the DMF has been evaporated at room temperature. Even though the film has dried out it is still capable of reabsorbing DMF and almost completely self-heal (b-d).

Europium

The gels with europium were made with 20% w/v of compound **8** with 0.4 eq. of Eu(III)(OTf)_3 in DMF-d₇. Deuterated DMF was used to be able to perform DOSY measurements on the sample while the metal content was stepwise increased from 0 to 0.4 eq. at which point it quickly formed a gel (Figure 19a,b). The gel made was at first soft and flexible, when the gel was cut both pieces weakly stuck back together after being overnight in contact with DMF, it is unlikely this is actual self-healing (Figure 19c,d).

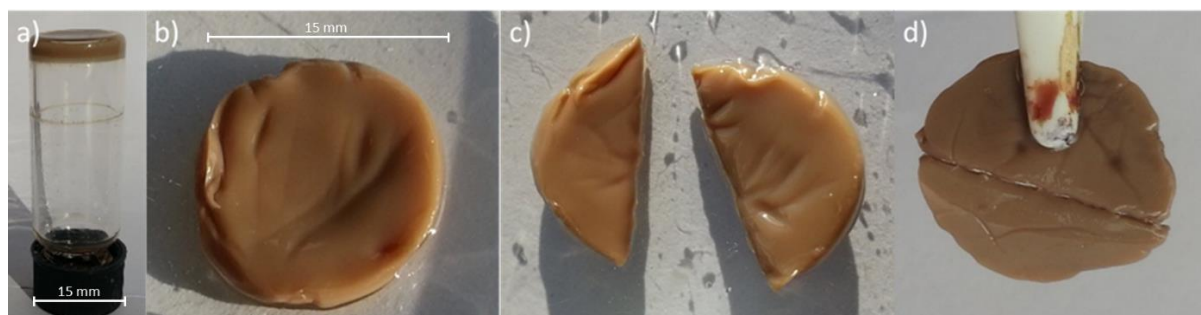


Figure 19: a) With 0.4 eq. of europium a soft and flexible gel was formed which could be removed from the vial without breaking (b). The gel pieces weakly stuck back together after they were cut and DMF was added (c and d).

After the second day in contact with open air the structure of the gel changed drastically into a somewhat sticky, more solid material similar to the materials formed with the zinc gels (Figure 20a). When this material was cut and treated with DMF it did show a much more complete form of solvent mediated self-healing (Figure 20b-e). Because the pieces were a bit deformed it was not possible to fit them back together precisely which is why some deformation is observed.

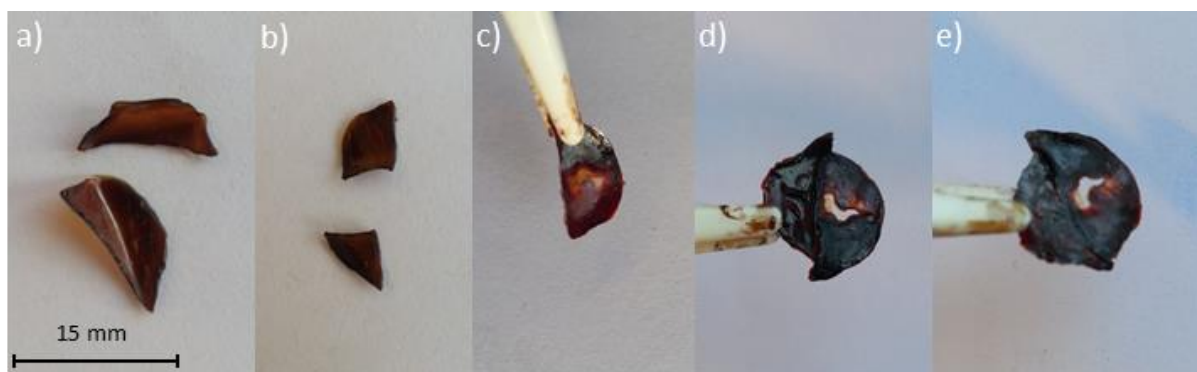


Figure 20: a) The europium gel pieces after two days in contact with open air. One of the pieces was cut again (b) and the self-healing properties under influence of DMF were tested (c-e).

DOSY

To investigate the amount of crosslinking between the different monomers of compound **8** under different conditions a series of DOSY experiments were performed. These experiments show that the diffusion coefficient of compound **8** is concentration dependent, where a higher concentration equals a lower diffusion rate (Figure 21). For the low concentration of 2% w/v a diffusion coefficient of $2.5 \cdot 10^{-10}$ (m^2/s) was obtained, whereas a diffusion coefficient of $8.7 \cdot 10^{-11}$ (m^2/s) was obtained for the 20% w/v. This clear difference in diffusion rate means that either the concentration is so high that the individual molecules of compound **8** hamper each other's movement or that there is some sort of interaction between them. The molecule was designed with a BTA core to make it possible to stack on itself. Therefore we can assume that at higher concentrations the molecule stacks and therefore has a lower diffusion coefficient.

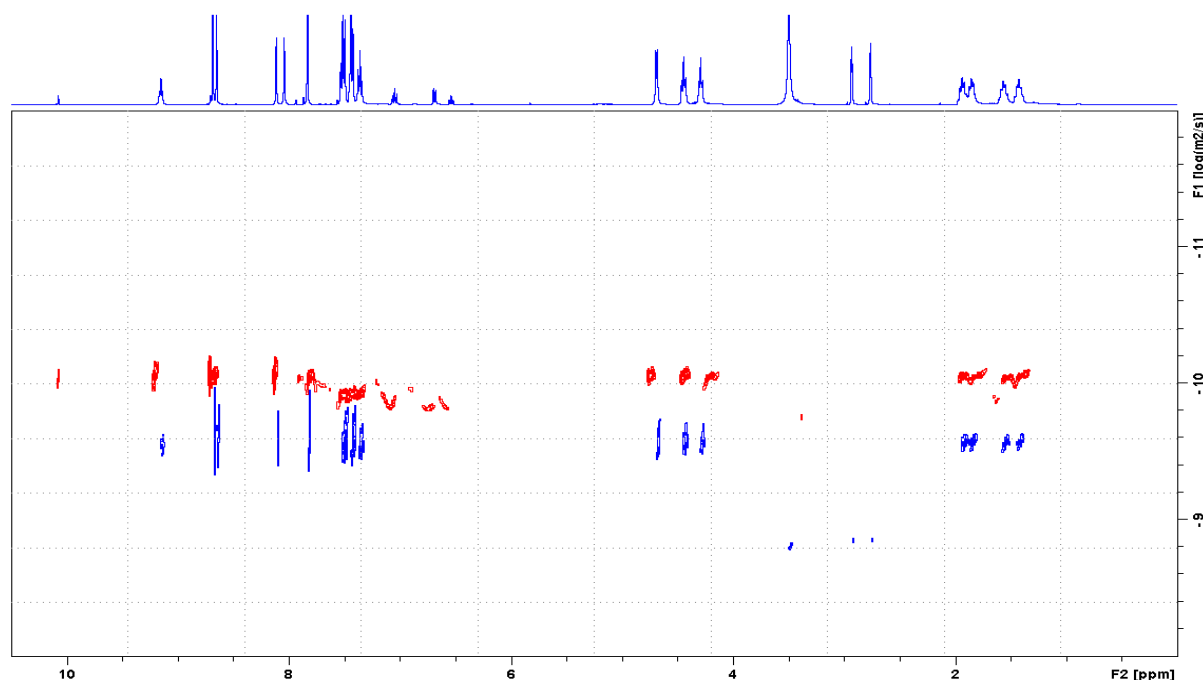


Figure 21: Overlaid DOSY spectra of compound **8** in a 2% w/v solution of DMF-d7 (blue), and that of a 20% w/v solution (red). The signals between 2.5 and 3.5 ppm originate from the solvent (DMF-d7), those between 6 and 7 belong to free aniline.

When the metal is added to the sample there is large amount of peak broadening especially the peaks around the imine bond (Figure 22).

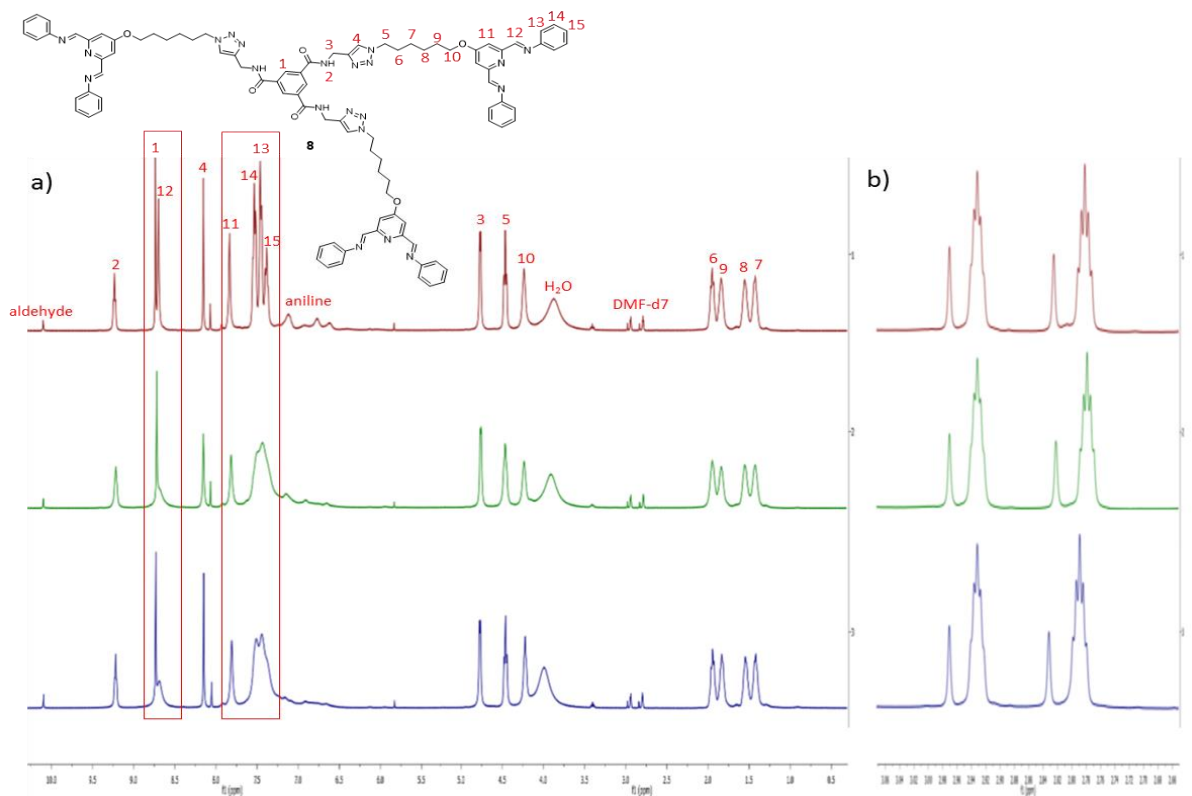


Figure 22: a) ^1H NMR spectra of compound **8** 20% w/v in DMF-d7 without metal (red), with 0.15 eq. Zinc (green) and 0.1 eq. Europium (blue). Highlighted are the protons belonging to peaks around the imine bond which shows peak broadening upon metal complexation. b) Zoomed in on the DMF-d7 resonances to highlight that the broadening of the peaks is not due to bad shimming.

In addition to the peak broadening the diffusion coefficient also drops significantly when increasing the amount of metal added (Figure 23). When 0.1 eq. of europium is added the diffusion coefficient drops from $8.7 \cdot 10^{-11}$ to $6.8 \cdot 10^{-11}$ m^2/s . When the europium concentration is further increased, the diffusion coefficient also drops further, to $4.7 \cdot 10^{-11}$ and $3.6 \cdot 10^{-11}$ m^2/s for 0.2 and 0.3 eq. respectively. At higher concentrations of europium gelification occurred. This clearly shows that the metal is successfully acting as a cross linking agent. The resonances around 7.5 ppm have a larger diffusion coefficient than the rest, which is probably caused by the equilibrium between the hydrolysis of the imine bond and its reformation.

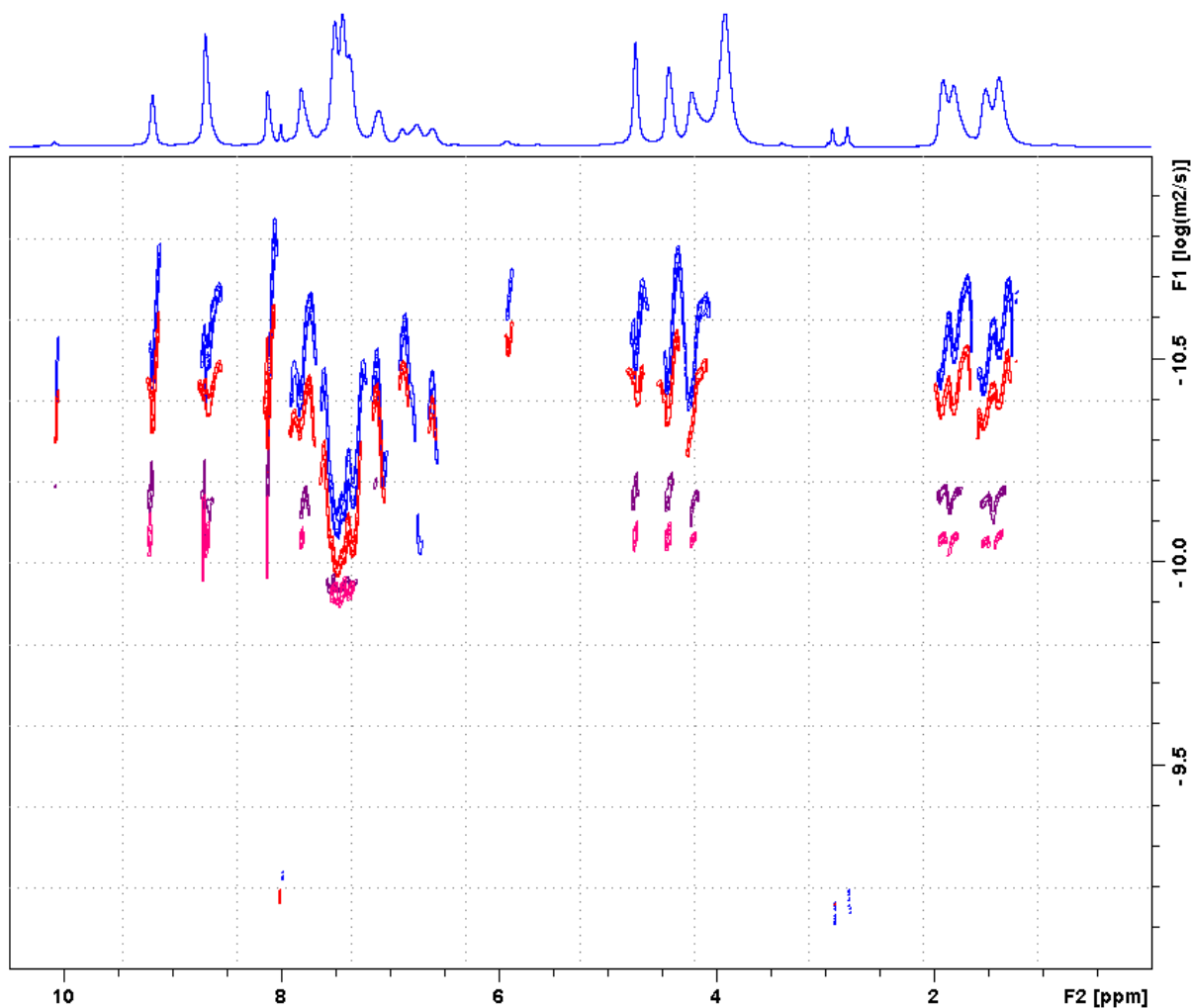


Figure 23: Overlaid DOSY spectra of compound **8** in a 20% w/v solution of DMF-d7 (pink), and with an addition of 0.1 (purple), 0.2 (red) and 0.3 (blue) equivalents of Eu(III)(OTf)₃. With the chemical shift on the x-axis and the 10Log of the diffusion coefficient on the y-axis. The signals with a ppm between 2.5 and 3.5, and the one at 8 originate from the solvent (DMF-d7), those between 6 and 7 belong to free aniline.

Comparison of different metals

Three distinctive materials were made using compound **8** in combination with copper(II), europium(III), iron(II) and zinc(II). When zinc and europium were used a soft sticky gel-like substance was formed which becomes stronger when the solvent evaporates. When iron was used a non-sticky film was created which is a lot stronger than the gels with zinc and europium. When it is dried it becomes even stronger and quite resistant versus linear stress. Copper induced the fastest gelation, however the formed gel dries fast and become quite brittle. These materials have different properties and two of them show solvent mediated self-healing. It is quite likely these deviating properties are caused by the difference in metal, in addition it is likely that the concentration of the metal also plays a large role. This could mean that there are three stages in the material, depended on the metal concentration. A soft stage where it forms more gel like materials, a stronger stage where it forms films and a final stage where it only forms solids. To determine which possibility is true or a possible combination of them, more research will have to be done examining the behaviour of compound **8** at more different metal ratios.

It is observed that the speed at which the solutions form gels is quite different depending on the metal that is used. The copper solution forms a gel within seconds after the metal content was increased

from 0.15 to 0.30 while the zinc gel with the same conditions did not after being left overnight with very similar conditions (19.2% w/v with 0.3 eq. for the copper and 17% w/v with 0.3 eq. for the zinc). Under the conditions that copper does form gels zinc and europium do not. This means it is likely that the binding stability of the metal determines at which point the gelification occurs and not the kinetics of the M-L interaction.

It is also interesting to see that the amount of europium needed to induce gelation is a lot higher than was originally expected. Since europium can form up to nine coordination bonds which means it should crosslink a lot more effectively than the other metals. That we do not see gelation at the expected 0.2 equivalent indicates that either the coordination of three pincer units does not happen or that the bonds are very weak compared to the bonds formed with the other metals. Other work done in the same lab shows that these type of pincer moieties are able to form triple coordination bonds with europium when fit on a linear polymer.²¹ This means that possibly there is some steric hindrance due to the triple arms and small size of the molecule which makes triple coordination unfavourable.

Dynamic imine bonds

The dynamic nature of the imine bonds was unfortunately not fully explored due to a lack of time. The aniline molecule in the pincer unit can easily be replaced by another molecule with an amine which can give a whole range of new properties to the molecule. One attempt was made using 1,12-diaminododecane to induce additional crosslinking however this proved to be insoluble in DMF. It will be interesting to see how compound **8** behaves when in addition to metal it is also crosslinked using for instance two aniline groups linked together by a PEG chain. There are of course a lot more possibilities which is why it will be interesting to do more research in this direction.

Future prospects

In this project we successfully made compound **8** and managed to make gels and films of which some most even have solvent mediated self-healing capabilities. This is very interesting but there is still a lot of work that needs to be done. The exact amount of metal and w/v % which causes gelation need to be determined and it needs to be checked how the metal concentration has an influence on the material's properties. The strength of the materials made needs to be quantified with methods like rheology for the gels and tensile strength measurements for the film. With this we can determine how strong the materials are and we can observe how effective the self-healing is and how often it can be repeated. In the objective and introduction we also talked about the dynamic imine bonds and how interesting these are but we never got the time to test it with compound **8** apart from that they are formed with aniline. To test compound **8** with different types of amines when making and after the gel has been made will be very interesting. There is also the issue that the materials that were made cannot yet be classified as really "smart" materials since we still need to do more experiments to determine how we can influence them. With further research it might be possible to determine how "smart" the materials actually are and how this can be used or improved. It is perhaps possible to also induce the self-healing with UV light instead of solvent. It will also be interesting to determine if there are more solvents in which compound **8** will make gels or films. In the research done by Kotova *et al.* they observed that the gel structure was needle like due to the stacking.^{24, 25} It might be interesting to see what the exact structure of compound **8** is in the gels since not all the molecules are linked together via the M-L coordination. There were also plans to make small variations on the molecule to see how these affect the properties, for instance it would be interesting to see how the molecule behaves when the BTA core is replaced with something which cannot stack with hydrogen bonding. In addition there is still room to improve the synthesis of compound **8** to obtain even higher yields and use less of the THPTA ligand which is quite expensive.

Overall there is a multitude of possibilities to continue with this project. In my opinion the most interesting ways to continue are with the dynamic imine bonds, to test the exact strength of the materials and repeatability of the self-healing.

Conclusion

Compound **8** was successfully synthesized in moderate to good yields for each step and combined with different metals to form gel-like materials. Depending on the metal and solvent it either quickly formed a solid after gelation (copper(II)), a film (iron(II)) or a gel (zinc(II) and europium(III)). The gels and the film are able to perform solvent-mediated self-healing. It was observed that these self-healing properties rely upon the reabsorption of the solvent and cease when it is completely evaporated. Overall compound **8** shows a lot of promising properties but there is still a lot of research needed to fully quantify all the possibilities and properties.

Acknowledgements

I would like to thank Maarten Smulders and Fatima Garcia Melo for supervising me during my thesis. Fatima was always there ready to help and answer questions in the lab and Maarten was always full of ideas to tackle any problem. Furthermore I would thank Ester van Andel, Medea Kosian and Zanhua Wang for a nice time working in the lab; Jona Merx, Iris van Marwijk and Rijo da Costa Carvalho for great time in the office; Pepijn Geutjes and Barend van Lagen for the help with the NMR and other equipment. And of course everyone in the ORC department for making my time there really enjoyable.

References

1. Yang Y, Urban MW. Self-healing polymeric materials. *Chem Soc Rev* 2013, **42**(17): 7446-7467.
2. Wool RP. Self-healing materials: a review. *Soft Matter* 2008, **4**(3): 400-418.
3. Miyamae K, Nakahata M, Takashima Y, Harada A. Self-Healing, Expansion–Contraction, and Shape-Memory Properties of a Preorganized Supramolecular Hydrogel through Host–Guest Interactions. *Angew Chem Int Ed* 2015, **127**(31): 9112-9115.
4. Berl V, Schmutz M, Krische MJ, Khoury RG, Lehn JM. Supramolecular Polymers Generated from Heterocomplementary Monomers Linked through Multiple Hydrogen-Bonding Arrays—Formation, Characterization, and Properties. *Chem Eur J* 2002, **8**(5): 1227-1244.
5. Jin Y, Yu C, Denman RJ, Zhang W. Recent advances in dynamic covalent chemistry. *Chem Soc Rev* 2013, **42**(16): 6634-6654.
6. Zhang Y, Barboiu M. Constitutional Dynamic Materials-Toward Natural Selection of Function. *Chem Rev* 2016, **116**(3): 809-834.
7. Patrick JF, Hart KR, Krull BP, Diesendruck CE, Moore JS, White SR, *et al.* Continuous Self-Healing Life Cycle in Vascularized Structural Composites. *Adv Mater* 2014, **26**(25): 4302-4308.
8. Francesconi A, Giacomuzzo C, Grande A, Mudric T, Zaccariotto M, Etemadi E, *et al.* Comparison of self-healing ionomer to aluminium-alloy bumpers for protecting spacecraft equipment from space debris impacts. *Adv Space Res* 2013, **51**(5): 930-940.
9. Maeda T, Otsuka H, Takahara A. Dynamic covalent polymers: reorganizable polymers with dynamic covalent bonds. *Prog Polym Sci* 2009, **34**(7): 581-604.
10. Roy N, Bruchmann B, Lehn J-M. DYNAMERS: dynamic polymers as self-healing materials. *Chem Soc Rev* 2015, **44**(11): 3786-3807.
11. Herbst F, Seiffert S, Binder WH. Dynamic supramolecular poly (isobutylene) s for self-healing materials. *Polym Chem* 2012, **3**(11): 3084-3092.
12. Williams RJ. Metal ions in biological systems. *Biol Rev* 1953, **28**(4): 381-412.
13. Smulders MM, Riddell IA, Browne C, Nitschke JR. Building on architectural principles for three-dimensional metallosupramolecular construction. *Chem Soc Rev* 2013, **42**(4): 1728-1754.
14. Cook TR, Stang PJ. Recent Developments in the Preparation and Chemistry of Metallacycles and Metallacages via Coordination. *Chem Rev* 2015, **115**: 7001-7045.

15. Chakrabarty R, Mukherjee PS, Stang PJ. Supramolecular coordination: self-assembly of finite two-and three-dimensional ensembles. *Chem Rev* 2011, **111**(11): 6810-6918.
16. Chen P, Li Q, Grindy S, Holten-Andersen N. White-Light-Emitting Lanthanide Metallogels with Tunable Luminescence and Reversible Stimuli-Responsive Properties. *J Am Chem Soc* 2015, **137**(36): 11590-11593.
17. Xu N, Han J, Zhu Z, Song B, Lu X, Cai Y. Directional supracolloidal self-assembly via dynamic covalent bonds and metal coordination. *Soft Matter* 2015, **11**(27): 5546-5553.
18. Rowan SJ, Cantrill SJ, Cousins GR, Sanders JK, Stoddart JF. Dynamic covalent chemistry. *Angew Chem Int Ed* 2002, **41**(6): 898-952.
19. Skene WG, Lehn J-MP. Dynamers: Polyacylhydrazone reversible covalent polymers, component exchange, and constitutional diversity. *Proc Natl Acad Sci U S A* 2004, **101**(22): 8270-8275.
20. Sarma RJ, Otto S, Nitschke JR. Disulfides, imines, and metal coordination within a single system: Interplay between three dynamic equilibria. *Chem Eur J* 2007, **13**(34): 9542-9546.
21. Garcia F, Pelss J, Zuilhof H, Smulders MMJ. Multi-responsive coordination polymers utilising metal-stabilised, dynamic covalent imine bonds. *Chem Commun* 2016, **ASAP**(DOI: 10.1039/c6cc00500d).
22. Xin Y, Yuan J. Schiff's base as a stimuli-responsive linker in polymer chemistry. *Polym Chem* 2012, **3**(11): 3045-3055.
23. Godoy-Alcántar C, Yatsimirsky AK, Lehn JM. Structure-stability correlations for imine formation in aqueous solution. *J Phys Org Chem* 2005, **18**(10): 979-985.
24. Kotova O, Daly R, dos Santos CM, Boese M, Kruger PE, Boland JJ, *et al.* Europium-directed self-assembly of a luminescent supramolecular gel from a tripodal terpyridine-based ligand. *Angew Chem Int Ed* 2012, **51**(29): 7208-7212.
25. Kotova O, Daly R, dos Santos CIM, Kruger PE, Boland JJ, Gunnlaugsson T. Cross-Linking the Fibers of Supramolecular Gels Formed from a Tripodal Terpyridine Derived Ligand with d-Block Metal Ions. *Inorg Chem* 2015, **54**(16): 7735-7741.

Experimental details

All solvents and chemicals were purchased from commercial sources (Sigma Aldrich, Fisher Scientific) and used without further purification. Water was purified using a Millipore Milli-Q water purification system. The synthesis pathway for the pincer unit (**1-5**) was based on the route previously described in the group.²¹

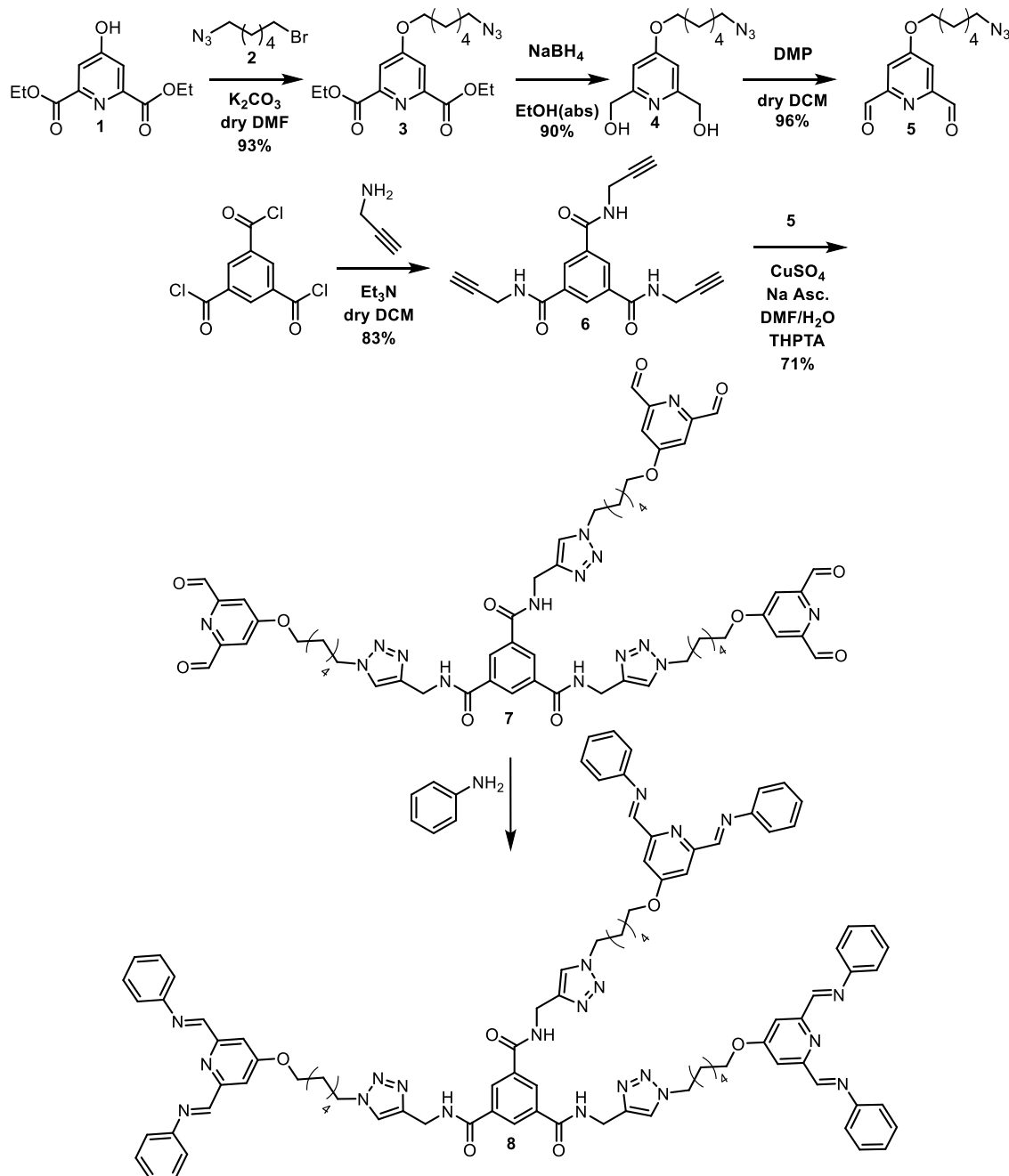
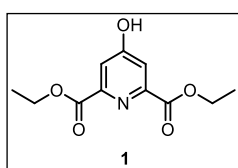


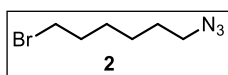
Figure 24: Revised pathway for the synthesis of the new target molecule.



To a solution of dried chelidamic acid (5.00 g, 26.7 mmol) (dried overnight with a high vacuum pump to remove the water) in absolute ethanol (250 mL), concentrated sulfuric acid was added (0.3 mL). The mixture was stirred and refluxed for 4 hours. The reaction was monitored with TLC, and although the

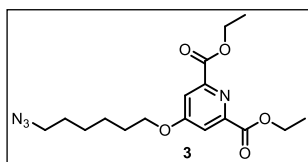
reaction was not complete, to prevent the alcohol from being converted into the methoxy the reaction was stopped anyway. The reaction was cooled to RT and quenched with water (50 mL). The ethanol was evaporated (not to complete dryness prevent insolubility of the product). What remains was dissolved in ethyl acetate (150 mL) and washed with a saturated solution of NaHCO₃ (30 mL). Next the water layer was extracted multiple times with ethyl acetate and DCM:MeOH 20:1 until no more product was in the aqueous layer (checked by TLC). The different organic layers were pooled, dried with MgSO₄, filtered and evaporated to obtain a white solid. Yield: 70% (4.5 g, 18.8 mmol). ¹H NMR is used to check the purity which indicated no further purification is needed.

¹H NMR (400 MHz, Chloroform-d) δ 9.45 (s, 1H), 7.26 (s, 2H), 4.43 (q, *J* = 7.2 Hz, 4H), 1.39 (t, *J* = 7.2 Hz, 6H).



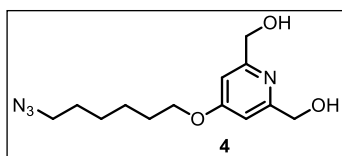
1,6-dibromohexane (15.4 mL, 100 mmol, 2.5 eq.) was dissolved in anhydrous DMSO (100 mL) and sodium azide (2.6 g, 40 mmol, 1 eq.) was added to the solution. The mixture was stirred at room temperature for one hour. Water (150 mL) was added to quench the reaction. The mixture was cooled in the fridge and extracted with diethyl ether (3x200mL). The diethyl ether was dried with MgSO₄, filtered, and evaporated under reduced pressure. The crude product was purified by column chromatography (silica gel, heptane with a gradient to ethyl acetate after the 1,6-dibromohexane is eluted, R_f=0.33). It is important to note that it was very difficult to separate the 1-azido-6-bromohexane from the by-product 1,6-diazo-hexane due to very similar R_f values. Since in the following steps **3-5** 1,6-diazo-hexane can't react, it was decided to purify it at the end of step **5** when there is a large difference between the R_f values (0.90 for 1,6-diazo-hexane and 0.3 for compound **5** in DCM). 1-azido-6-bromohexane is a colourless liquid but a small contamination of 1,6-diazo-hexane yields a yellow liquid. Yield: 67% (5.5 g, 27.5 mmol).

¹H NMR (400 MHz, Chloroform-d) δ 3.35 (t, *J* = 6.8 Hz, 2H), 3.21 (t, *J* = 6.8 Hz, 2H), 1.81 (m, 2H), 1.55 (m, 2H), 1.41-1.33 (m, 4H).



The pyridine diester **1** (4.5g, 18.8 mmol, 1 eq.) was dissolved in dry DMF (200 mL) and stirred under argon atmosphere. To the solution, K₂CO₃ (7.8 g, 56.4 mmol, 3 eq.) (previously dried in the oven at 100 °C) was added and stirred for several minutes. Then, 1-azido-6-bromohexane **2** (4.2 g, 18.8, 1 eq.) was added and the reaction was stirred at 100 °C overnight. TLC (ethyl acetate/heptane 1/2) was used to check if the reaction was completed. The reaction was cooled to room temperature and the K₂CO₃ filtered off. The reaction mixture was diluted with H₂O (200 mL) and extracted with ethyl acetate (2x150 mL). The organic layer was then washed with ice water (150 mL) and brine (150 mL) after which it was dried using MgSO₄, filtered and evaporated under reduced pressure. The resulting orange oil was further purified using column chromatography (silica gel, ethyl acetate/heptane 1/2, R_f = 0.3). The product **3** was obtained as a light yellow oil. Yield: 93% (6.4 g, 17.4 mmol).

¹H NMR (400 MHz, Chloroform-d) δ 7.75 (s, 2H), 4.45 (q, *J* = 7.2 Hz, 4H), 4.12 (t, *J* = 6.8 Hz, 2H), 3.28 (t, *J* = 6.8 Hz, 2H), 1.85 (m, 2H), 1.63 (m, 2H), 1.55-1.40 (m, 4H), 1.44 (t, *J* = 7.2 Hz, 6H).

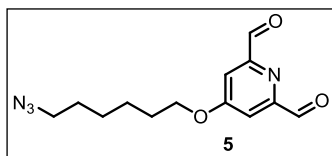


The pyridine diester **3** (6.4 g, 17.4 mmol, 1 eq.) was dissolved in absolute ethanol (400 mL) and carefully NaBH₄ (4 g, 104 mmol, 6 eq.) was added. The mixture was stirred at 40 °C overnight. The reaction was cooled on ice and quenched with H₂O (200 mL) and the ethanol was evaporated under reduced pressure. The water layer was then extracted with DCM until all the product was extracted (3x150 mL). The organic layer was washed with brine (150 mL) and dried with MgSO₄, filtered and the DCM is evaporated. The product **4** is a white oil that can crystallize. Yield: 90% (4.4 g, 15.7 mmol).

¹H NMR (400 MHz, Chloroform-d) δ 6.70 (s, 2H), 4.69 (s, 4H), 4.02 (t, J = 6.8 Hz, 2H), 3.33, (s, 2H), 3.28 (t, J = 6.8 Hz, 2H), 1.80 (quint, J = 6.8 Hz, 2H), 1.62 (quint, J = 6.8 Hz, 2H), 1.53-1.40 (m, 4H).

¹³C NMR (400 MHz, Chloroform-d) δ 166.6, 160.3, 105.6, 68.0, 64.4, 51.3, 28.7, 28.7, 26.4, 25.5.

HRMS (ESI): calculated for C₁₃H₂₀N₄O₃ [M+Na]⁺, 303.1433; found: 303.1430



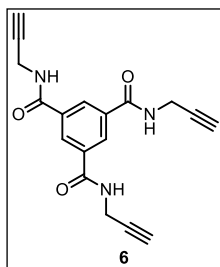
The dialcohol **4** (2.65 g, 9.5 mmol, 1 eq.) was dissolved in dry DCM (250 mL) and Dess Martin Periodane (DMP) (9.62 g, 22.7 mmol, 2.4 eq.) was added. The mixture was stirred at room temperature for three hours, TLC (DCM) was used to check if the reaction was complete. When the reaction was complete 1M NaOH in H₂O (200 mL) was added and stirred for 15 minutes. The DCM layer was separated and washed with a saturated NaHCO₃ (2x100 mL) solution and brine (100 mL) after which it was dried with MgSO₄, filtered, and evaporated. Yield: 96% (2.5 g, 9.1 mmol) as a yellow oil.

¹H NMR (400 MHz, Chloroform-d) δ 10.10 (s, 2H), 7.61 (s, 2H), 4.14 (t, J = 6.4 Hz, 2H), 3.29 (t, J = 6.8 Hz, 2H), 1.85 (m, 2H), 1.64 (m, 2H), 1.55-1.41 (m, 4H).

¹³C NMR (400 MHz, Chloroform-d) δ 192.5, 167.2, 154.9, 111.5, 69.2, 51.4, 28.9, 28.7, 26.5, 25.6.

FTIR (ATR) 661, 700, 715, 765, 833, 872, 947, 988, 1038, 1112, 1159, 1188, 1275, 1313, 1362, 1450, 1558, 1592, 1710, 1762, 2092, 2860, 2940, 3085 cm⁻¹.

HRMS (ESI): calculated for C₁₃H₁₆N₄O₃Na [M+Na]⁺, 299.1120, C₁₄H₂₀N₄O₄Na, [M+Na+MeOH]⁺, 331.1382, C₁₅H₂₄N₄O₅Na [M+Na+(MeOH)₂]⁺, 363.1644; found: 299.1122, 331.1385, 363.1648.



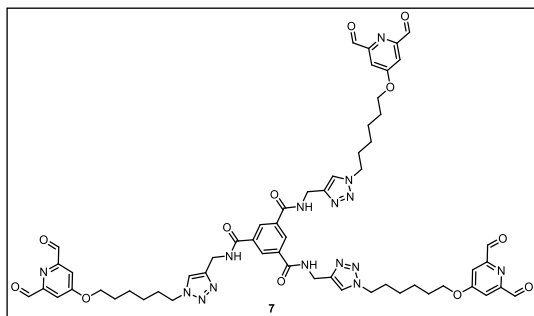
Propargylamine (2.17 mL, 33.9 mmol, 4.5 eq.), was dissolved in dry DCM (250 mL), next the mixture was cooled on ice and brought under argon atmosphere. Dry triethylamine (9.5 mL, 67.8 mmol, 9 eq.) was added and the mixture was stirred under argon for 20 minutes. 1,3,5-tris(chlorocarbonyl)benzene (2.0 g, 7.53 mmol, 1 eq.) was dissolved in dry DCM (250 mL) and added dropwise to the reaction, which was then stirred overnight at room temperature. The DCM was evaporated and the remaining yellow solid was transferred to a pore 4 glass filter. The solid was washed with ethyl acetate (2x60 mL) until the filtrate was clear. Next the solid was washed with 1M H₂SO₄ (2x60 mL) until the filtrate was clear. A white solid remained which was washed with H₂O (2x50 mL) to remove the final contamination after which the product was a pure white solid and dried under vacuum. Yield: 83% (2.0 g, 6.2 mmol).

^1H NMR (400 MHz, DMSO-d) δ 9.15 (t, J = 5.5 Hz, 3H), 8.44 (s, 3H), 4.09 (dd, J = 5.5 Hz, J = 2.4, 6H), 3.15 (t, J = 2.4, 3H).

^{13}C NMR (400 MHz, Chloroform-d) δ 165.05, 134.39, 128.91, 80.94, 73.02, 28.67.

FTIR (ATR) 613, 638, 658, 670, 694, 710, 724, 786, 869, 899, 914, 926, 979, 1009, 1017, 1058, 1067, 1142, 1253, 1291, 1337, 1363, 1416, 1444, 1548, 1632, 2942, 2989, 3059, 3246, 3277, 3289 cm^{-1} .

HRMS (ESI): calculated for $\text{C}_{18}\text{H}_{15}\text{N}_3\text{O}_3\text{Na}$ $[\text{M}+\text{Na}]^+$, 344.1011; found: 344.1010.



The BTA core **6** (0.61 g, 1.89 mmol, 1 eq.) and the pincer molecule **5** (1.60 g, 5.79 mmol, 3.06 eq.) were dissolved in DMF (250 mL) with argon bubbling through for a few minutes. Copper sulphate (42 mg, 0.17 mmol, 0.09 eq.) and Sodium ascorbate (65 mg, .33 mmol, 0.18 eq.) were dissolved in H_2O (250 mL) after which tris(3-hydroxypropyltriazolylmethyl)amine (THPTA) (0.216 g, 0.50 mmol, 0.27 eq.) was added and argon was

bubbled through for a few minutes. Both solutions were mixed under argon atmosphere and stirred at 80 $^\circ\text{C}$ overnight. A small sample was taken and checked with ^1H NMR to check if the reaction was complete (absence of the δ 3.15 (t, J = 2.4, 3H) peak belonging to the alkyne group indicates completion). N-hydroxyethyl-ethylenediamine-triacetic acid (HEDTA) (0.11 g, 0.5 mmol, 0.3 eq.) was added to capture the copper and prevent it from coordinating to the product during purification. The product was extracted from the reaction mixture using DCM (2x100 mL, 1x50 mL), the water phase had a blue colour due to the copper (II), and the first two DCM layers have a red colour. The organic layer was washed using a HEDTA solution in H_2O (0.11 g, 0.5 mmol, 0.3 eq. in 100 mL H_2O), a saturated NH_4Cl solution (100 mL), and brine (100 mL) after which it was dried with MgSO_4 , filtered, and evaporated under ultra-high vacuum. The resulting oil was further purified using an S-X3 Bio-Beads column to separate the product from the excess of pincer **6**. Upon full evaporation of the solvent the product, bubbles are formed which solidify causing the product to be extremely “fluffy” with a grey colour (a slightly brown colour indicates contamination with starting compound **5**). Yield: 71% (1.54 g, 1.34 mmol).

^1H NMR (400 MHz, DMSO-d) δ 10.01 (s, 6H), 9.13 (t, J = 5.5 Hz, 3H), 8.44 (s, 3H), 7.98 (s, 3 H), 7.62 (s, 6H), 4.52 (d, J = 5.5 Hz, 6H), 4.32 (t, J = 7.0, 6H), 4.21 (t, J = 7.0 Hz, 6H), 1.82 (m, 6H), 1.73 (m, 6H), 1.44 (m, 6H), 1.30 (m, 6H).

^{13}C NMR (400 MHz, Chloroform-d) δ 192.5, 166.7, 165.2, 154.4, 144.5, 134.5, 128.75, 122.8, 111.7, 68.8, 49.1, 34.9, 29.6, 27.9, 25.4, 24.6.

FTIR (ATR) 659, 700, 714, 785, 817, 870, 944, 988, 1038, 1157, 1189, 1217, 1277, 1314, 1363, 1450, 1527, 1593, 1656, 1709, 2859, 2939, 3079, 3139, 3306 cm^{-1} .

HRMS (ESI): calculated for $\text{C}_{57}\text{H}_{63}\text{N}_{15}\text{O}_{12}\text{Na}$ $[\text{M}+\text{Na}]^+$, 1172.4672; found: 1172.4645. (Figure 25)

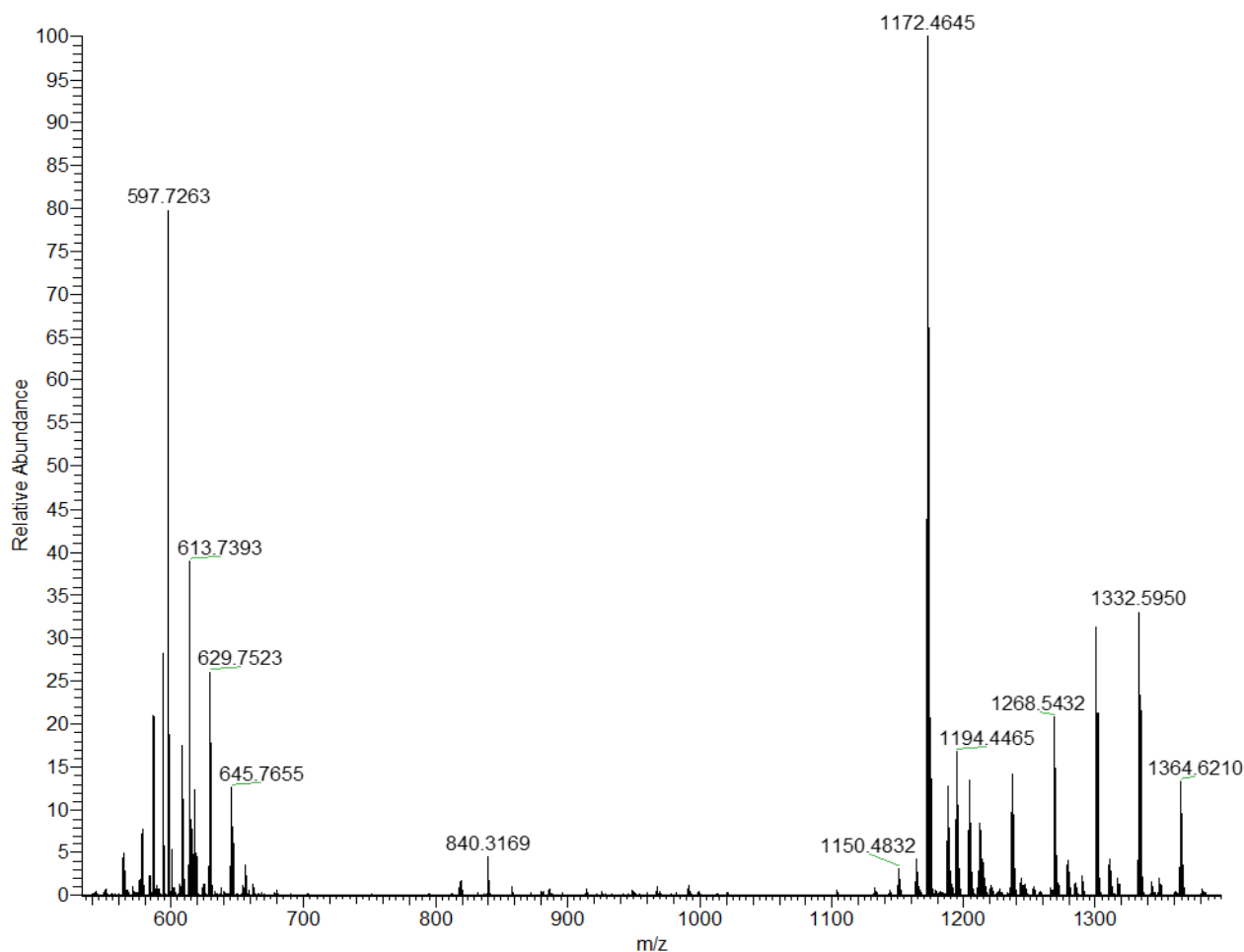
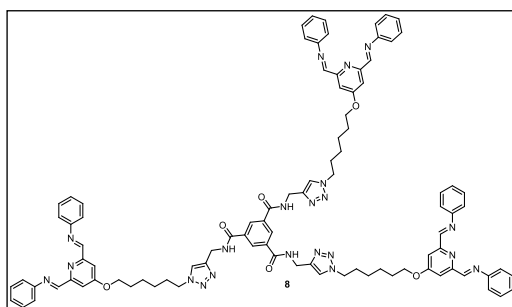


Figure 25: HRMS (ESI) spectrum of compound (**7**). A lot of additional peaks are observed (597.7263 – 645.7655 and 1194.4465 – 1364.6210) which originate due to the formation of acetal groups with MeOH or double binding of Na⁺. Some slight contamination is also observed (840.3169).



The tri-pincer compound **7** (100 mg, 0.095 mmol, 1 eq.) is dissolved in DMF (0.5 mL) to which aniline (48 μ L, 0.575 mmol, 6 eq.) is added in a small glass vial. The vial is shaken while heated with a heat gun for several seconds. The formation of the imine bond is an equilibrium which is why there is only about 95% conversion of the aldehyde bonds. For the purpose of coordination with metal ions this has no adverse effect since the imine bonds are stabilized when coordinated.

When the imine bonds are formed a colour shift from brown to pale green is observed. This colour change is dependent on the solvent, in chloroform the colour shifts from yellow to red.

¹H NMR (400 MHz, DMSO-d) δ 9.13 (t, J = 5.5 Hz, 3H), 8.59 (s, 6H), 8.46 (s, 3H), 7.97 (s, 3H), 7.70 (s, 6H), 7.44 (t, J = 7.6 Hz, 12H), 7.34 (d, J = 7.6 Hz, 6H), 7.30 (t, J = 7.6 Hz, 12H), 4.52 (d, J = 5.5 Hz, 6H), 4.31 (t, J = 7.0, 6H), 4.17 (t, J = 7.0 Hz, 6H), 1.81 (m, 6H), 1.73 (m, 6H), 1.45 (m, 6H), 1.29 (m, 6H).

¹³C NMR (100 MHz, DMSO-d) δ 165.7, 165.2, 159.8, 155.8, 150.1, 144.5, 134.6, 129.3, 128.8, 128.7, 126.9, 122.8, 121.2, 108.8, 68.2, 49.1, 34.9, 29.6, 28.1, 25.5, 24.7.

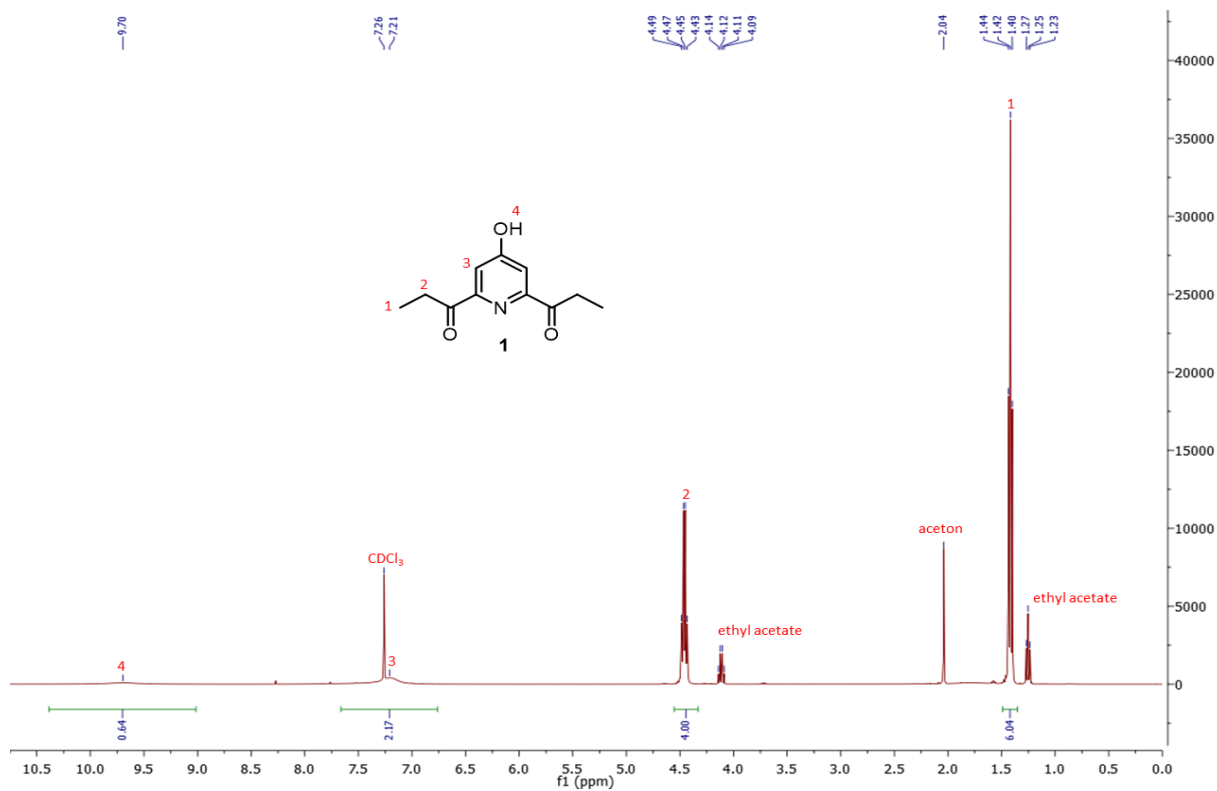
Appendix

1. NMR, IR and MS spectra

NMR

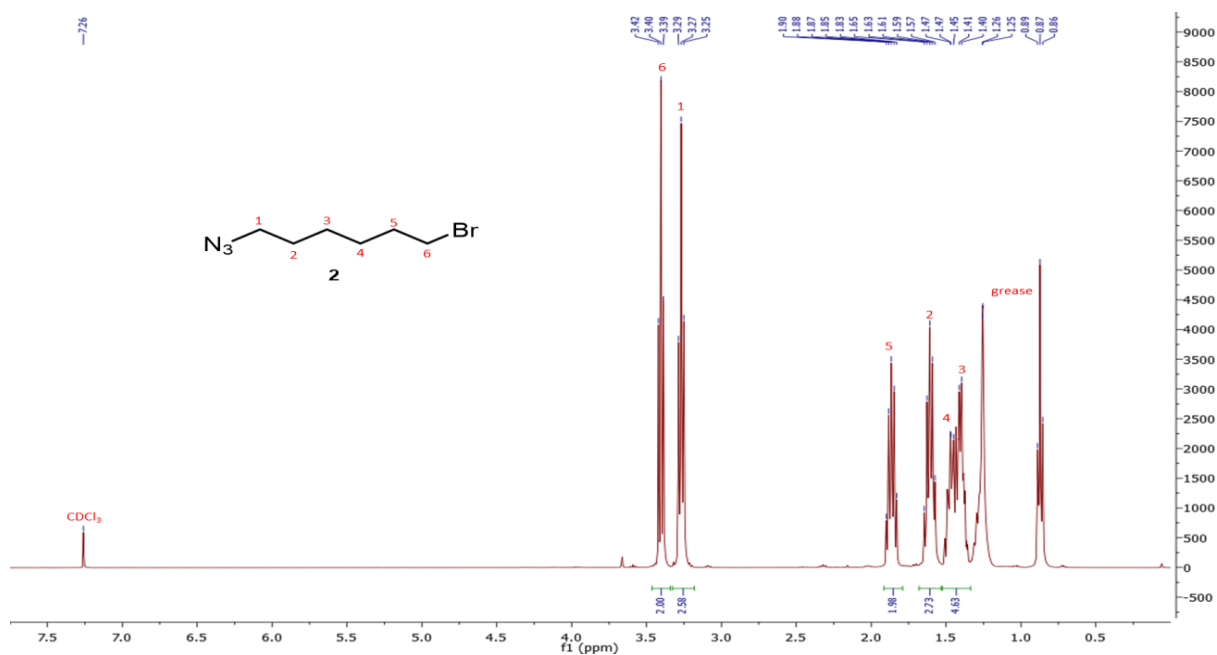
Compound **1**, the pyridine ester.

^1H NMR (400MHz) in CDCl_3



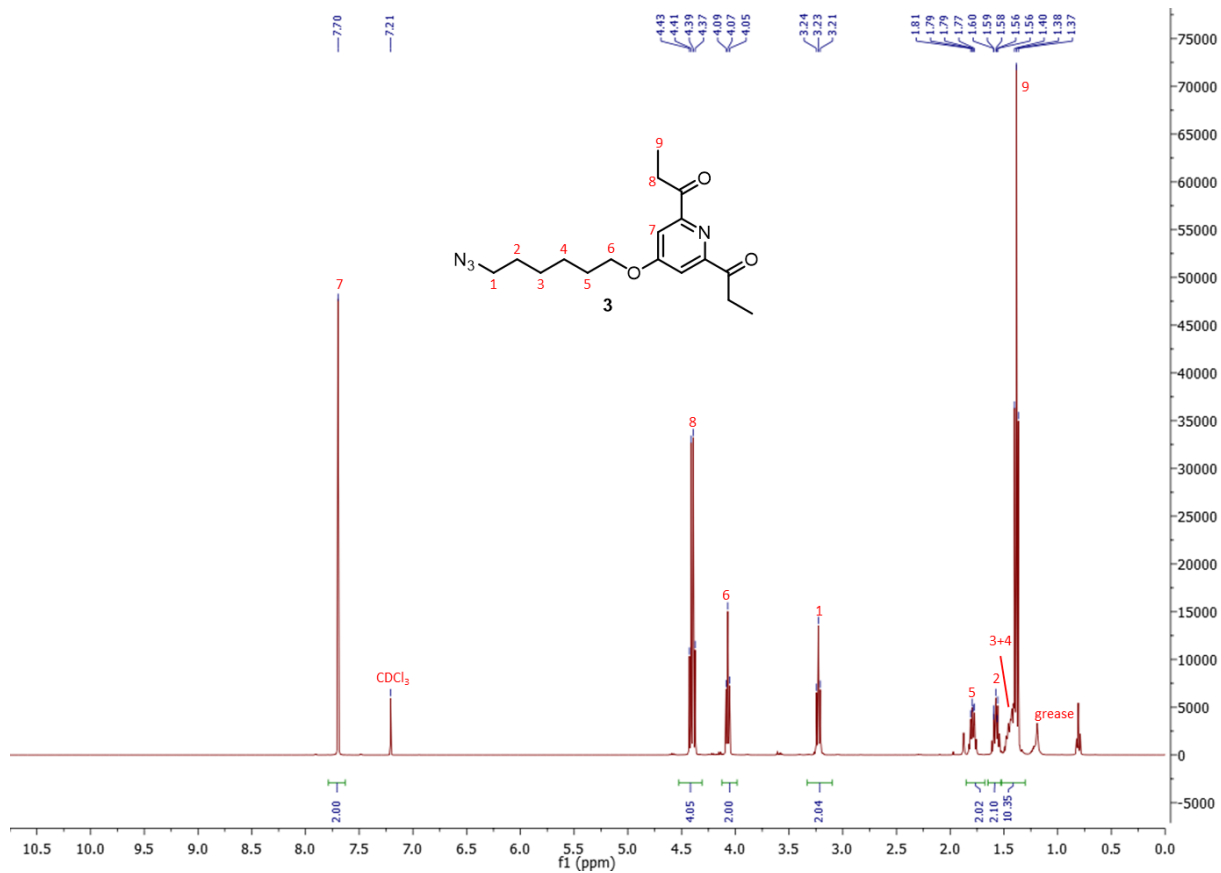
Compound **2**, 1-azido-6-bromohexane.

^1H NMR (400MHz) in CDCl_3



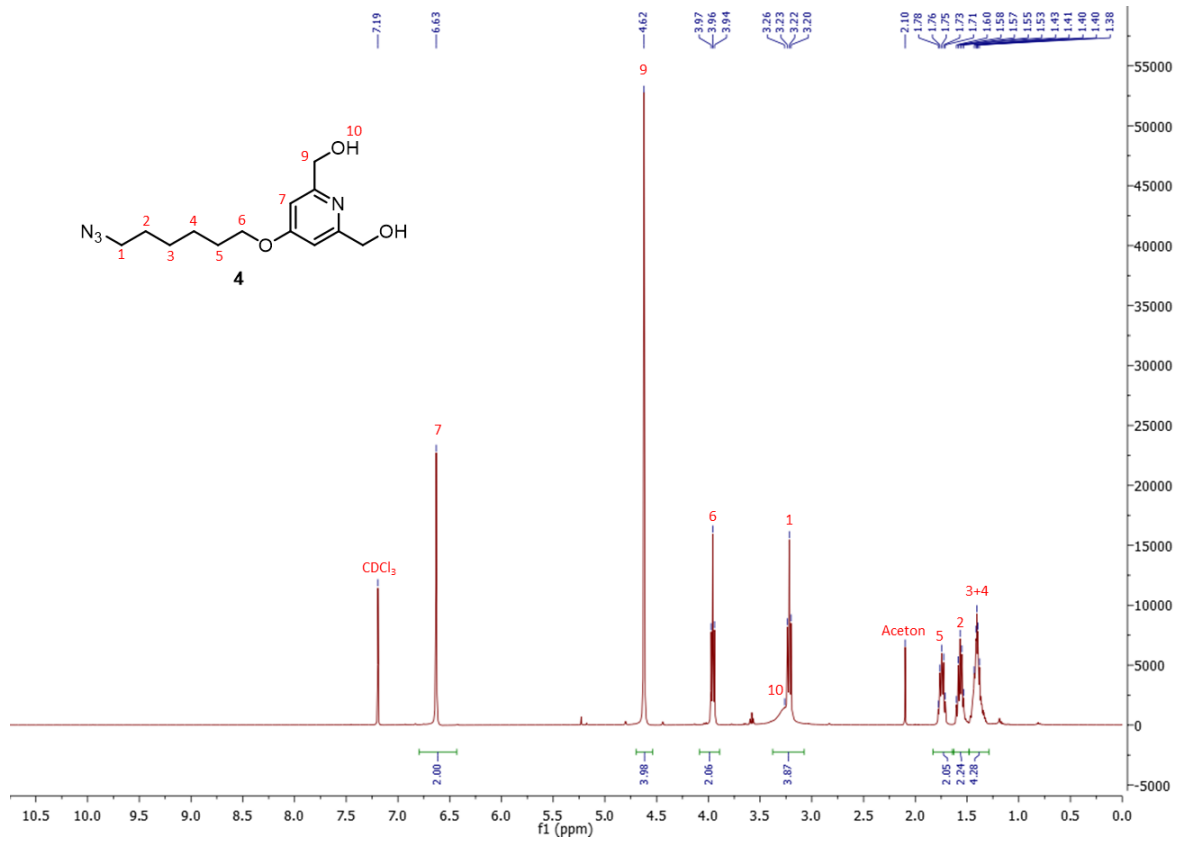
Compound **3**.

^1H NMR (400MHz) in CDCl_3

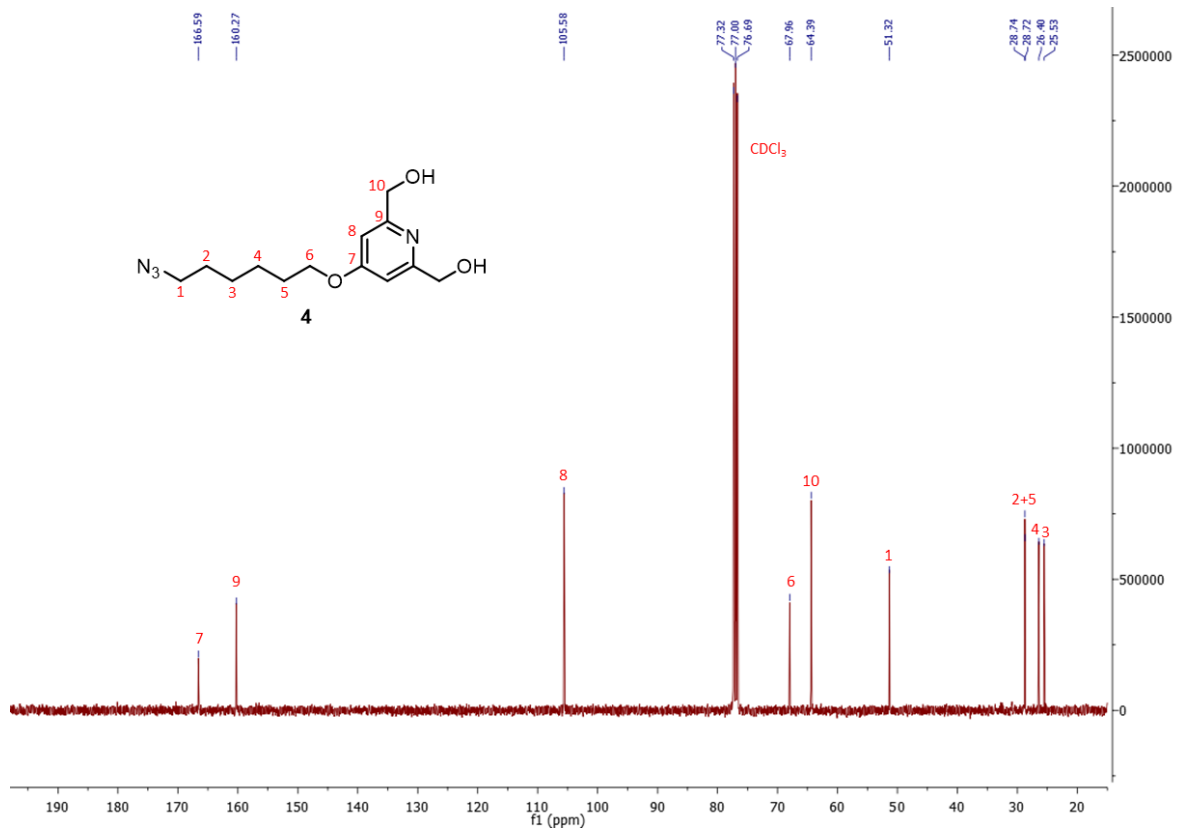


Compound 4.

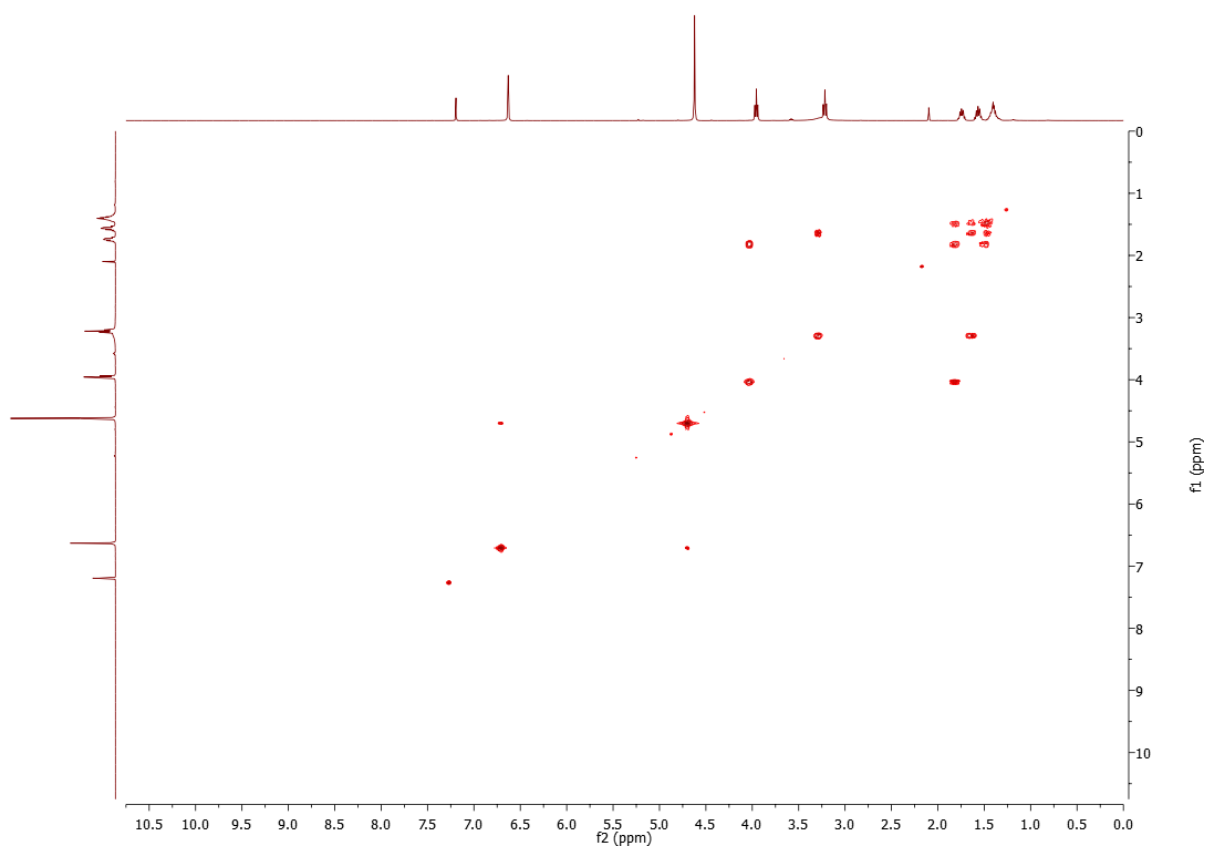
¹H NMR (400MHz) in CDCl₃



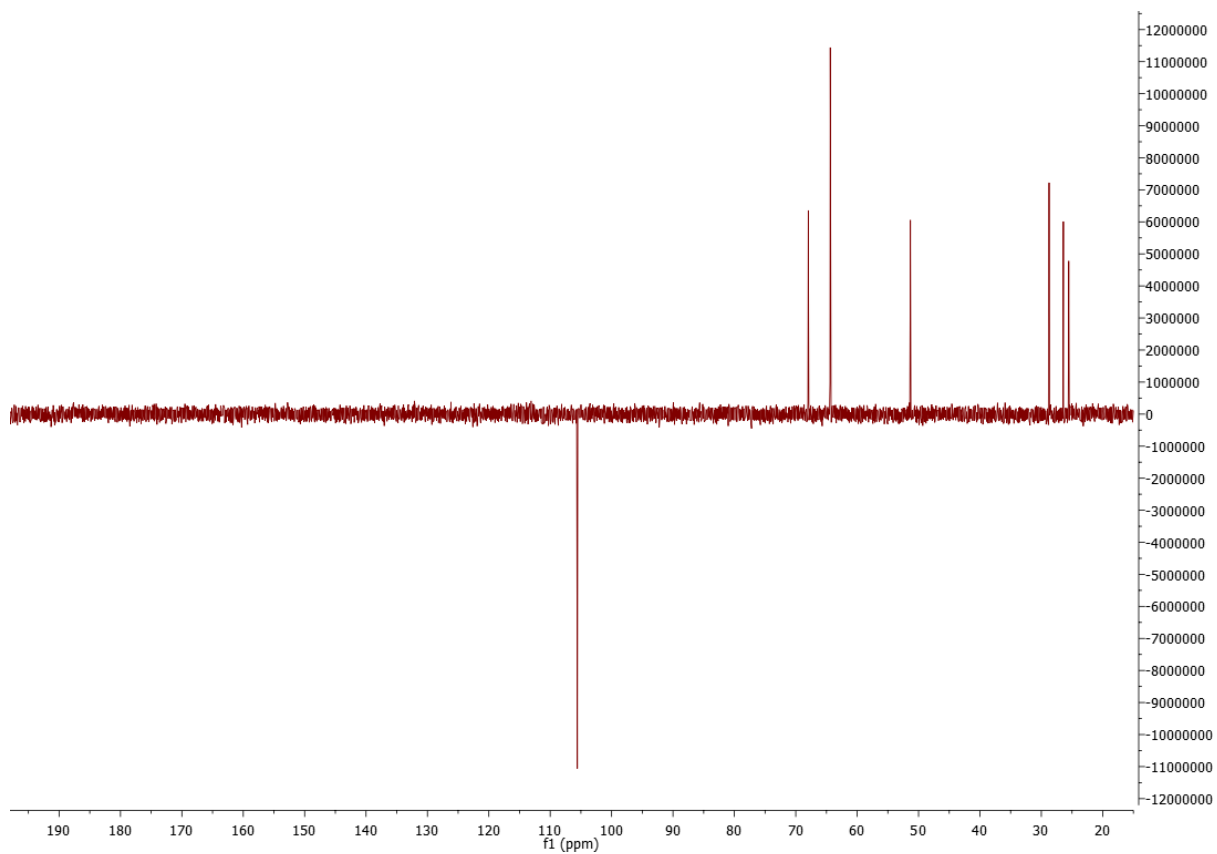
¹³C NMR (100MHz) in CDCl₃



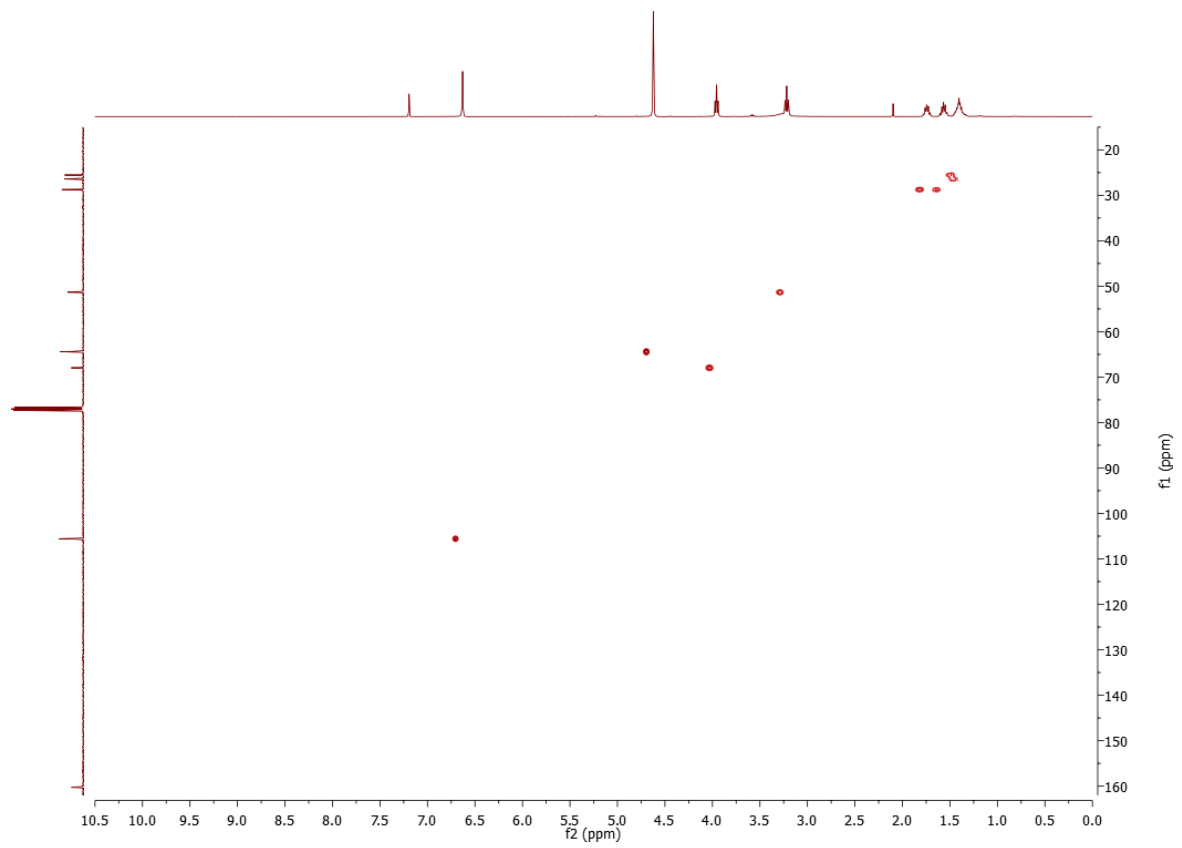
COSY (400MHz) in CDCl₃



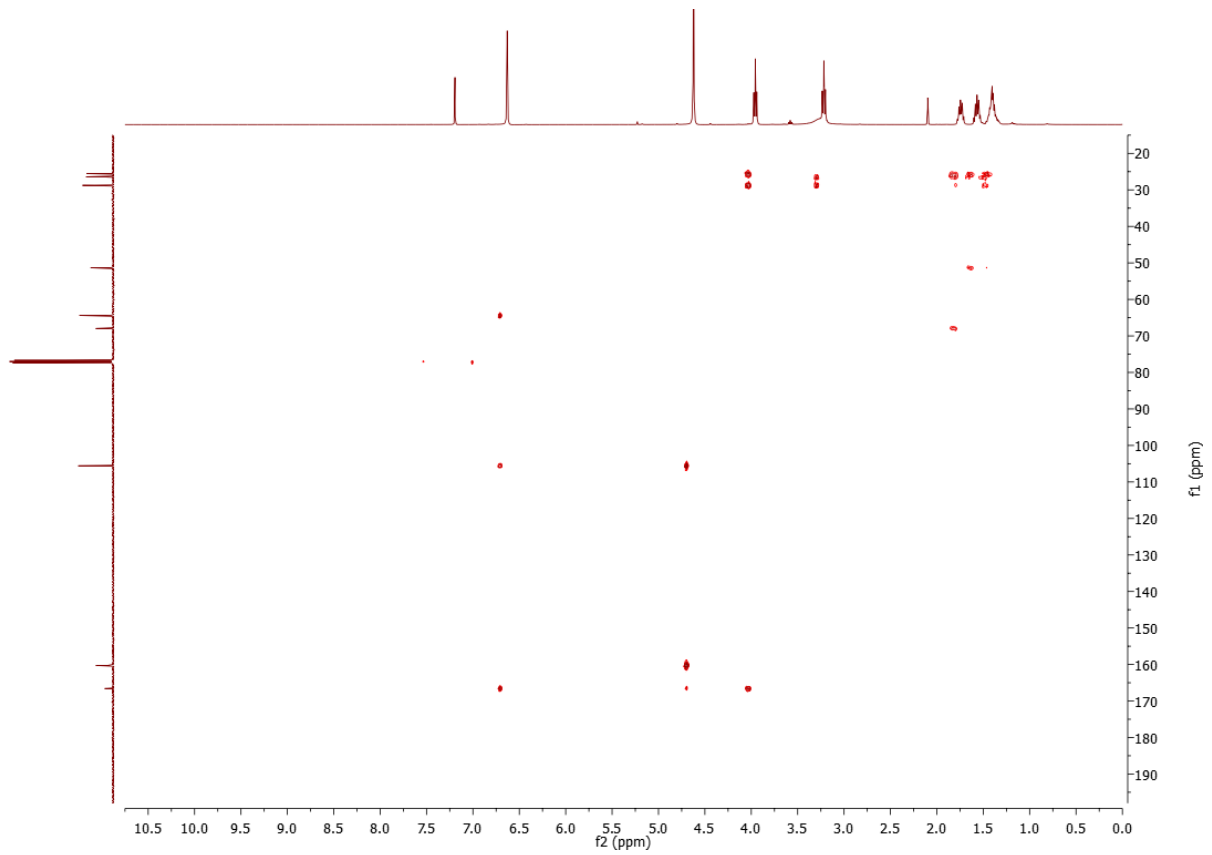
DEPT135 (100MHz) in CDCl₃



HSQC

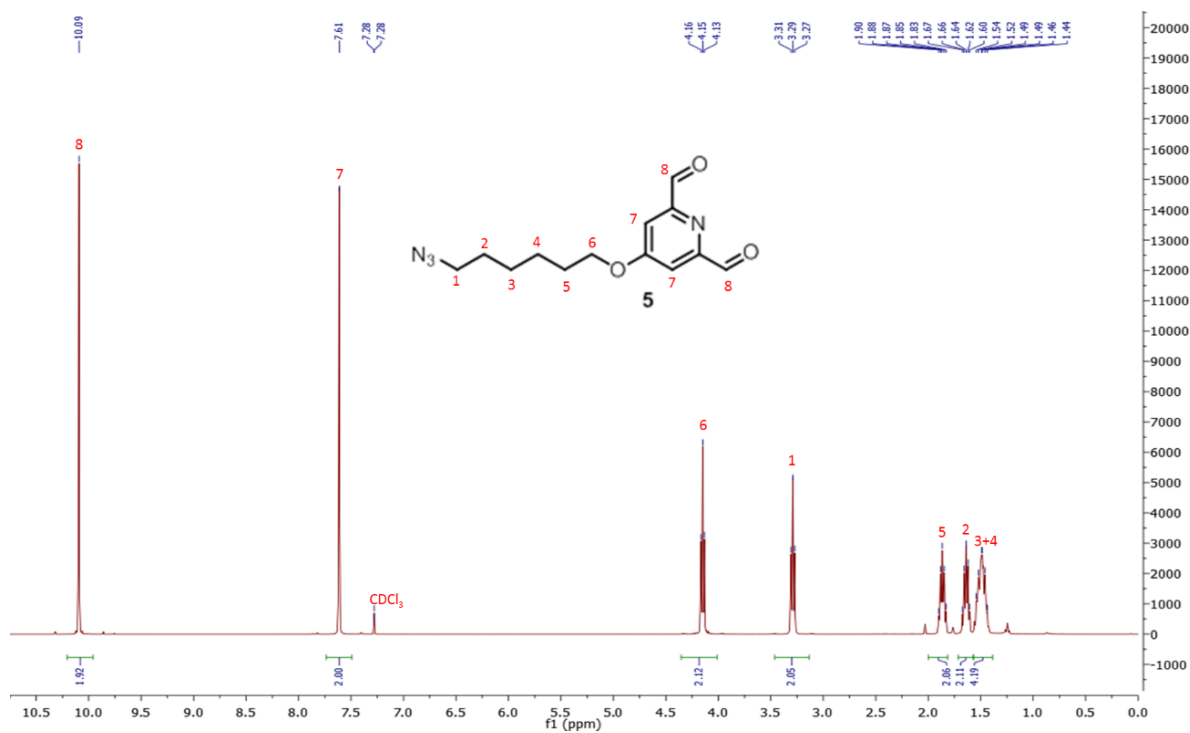


HMBC

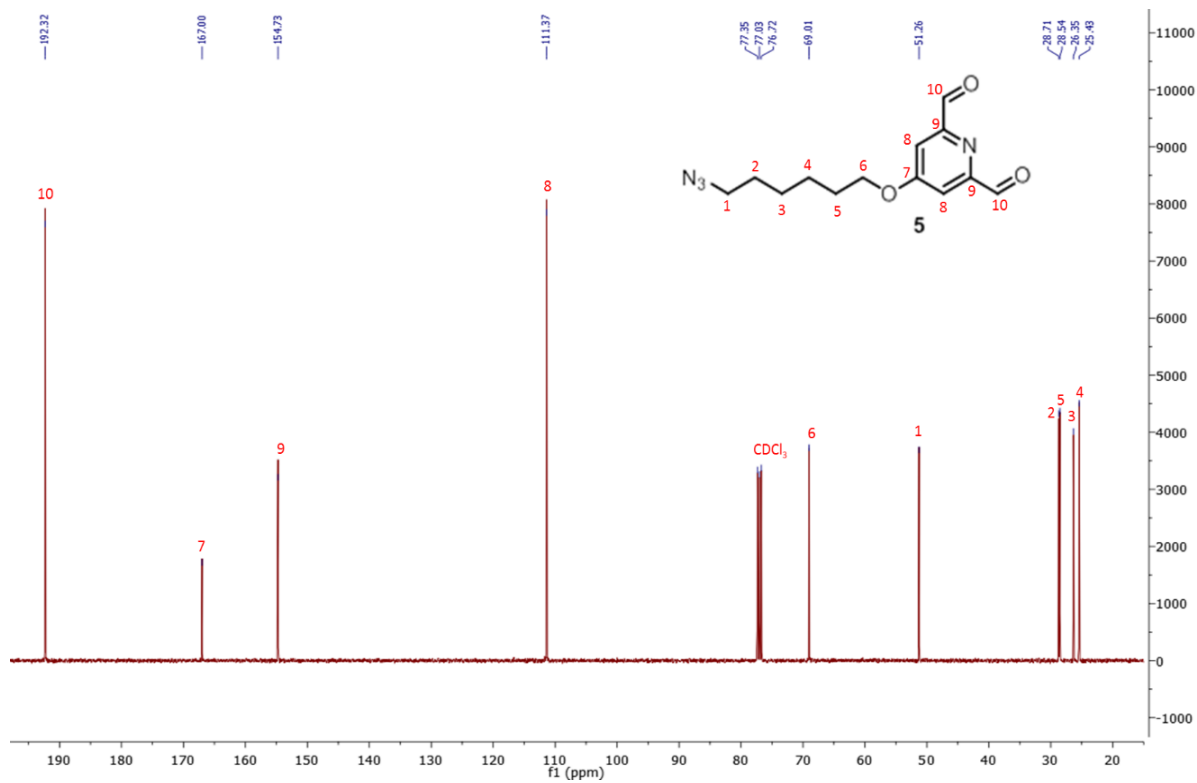


Compound **5**, the pincer molecule.

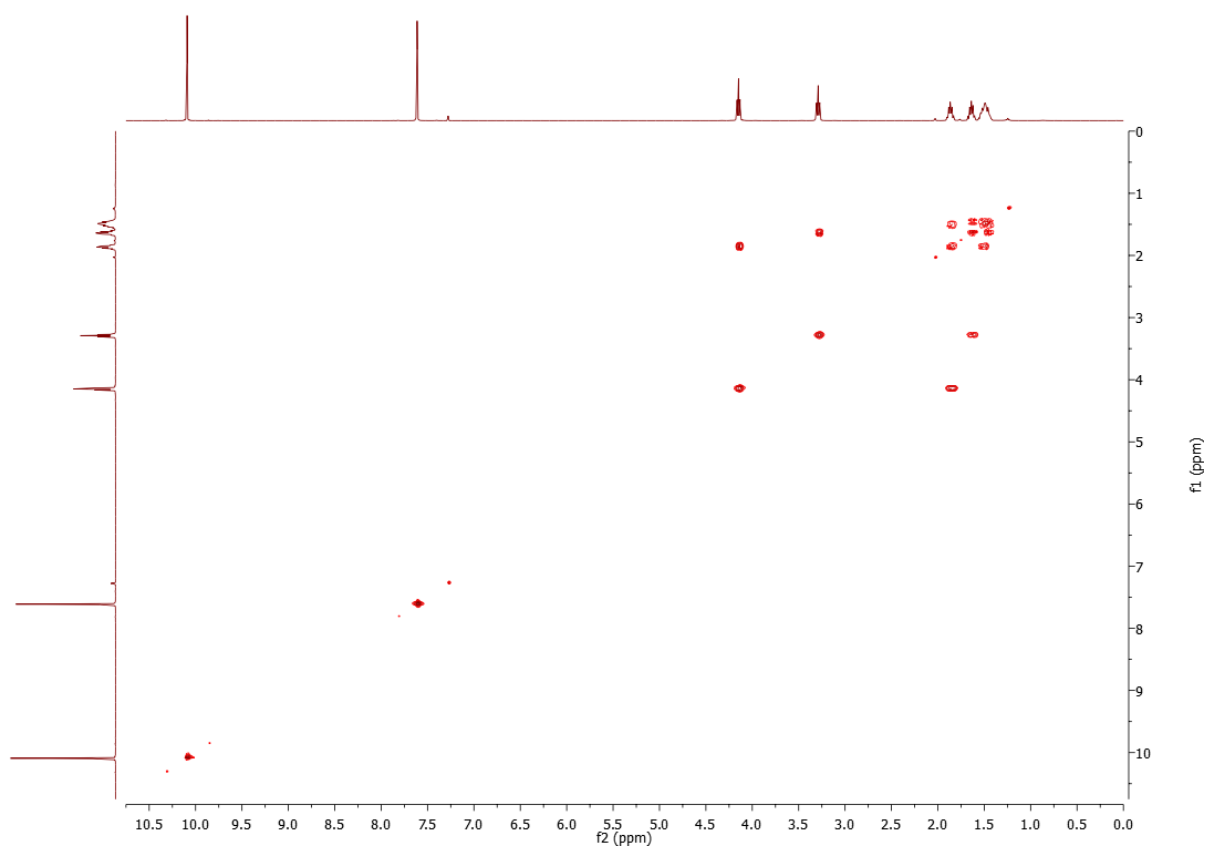
^1H NMR (400MHz) in CDCl_3



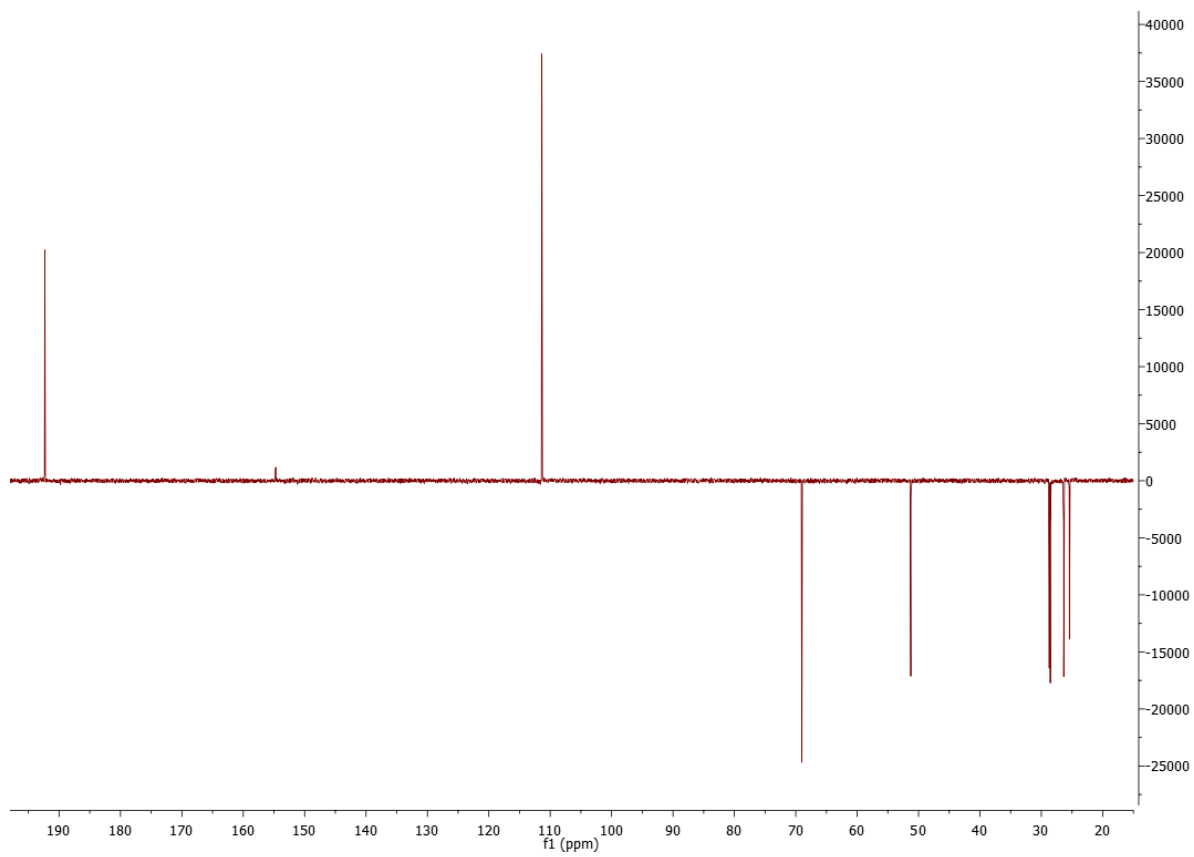
^{13}C NMR (100MHz) in CDCl_3



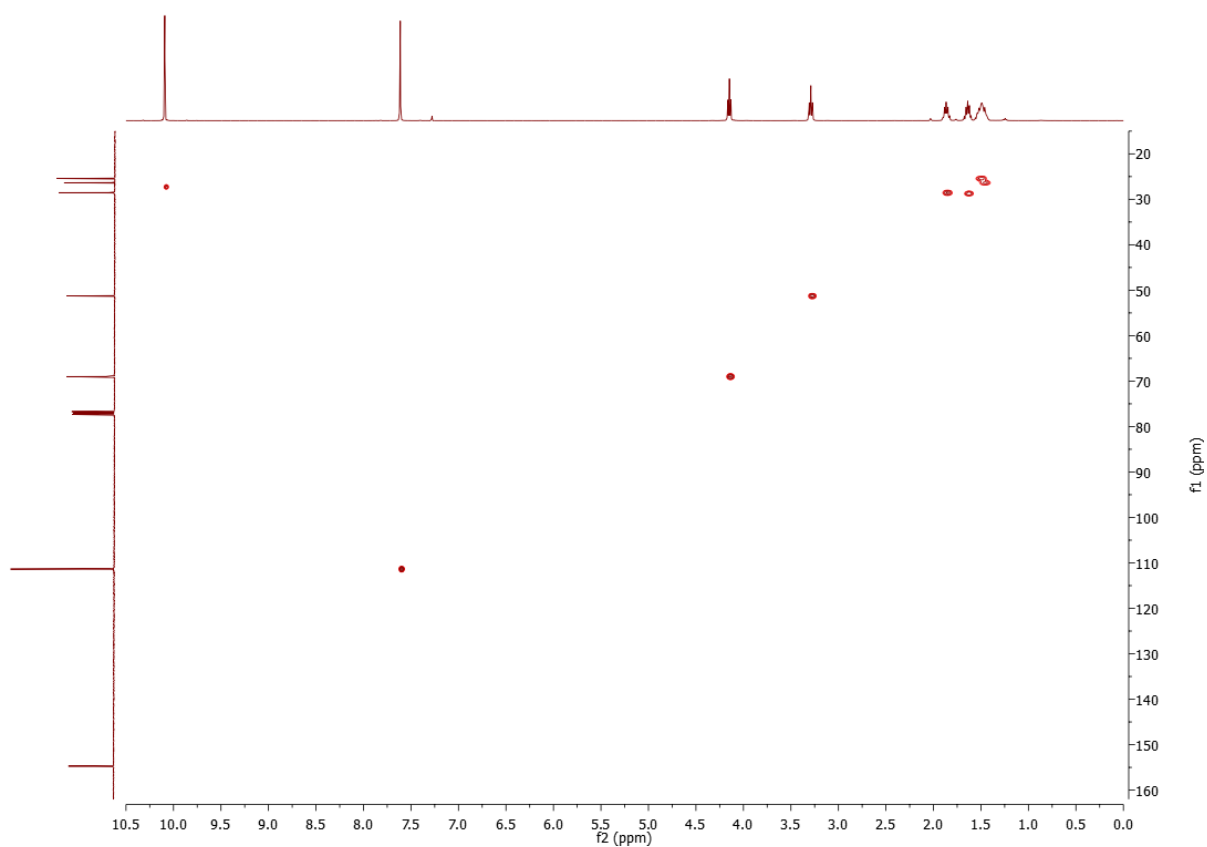
COSY (400MHz) in CDCl₃



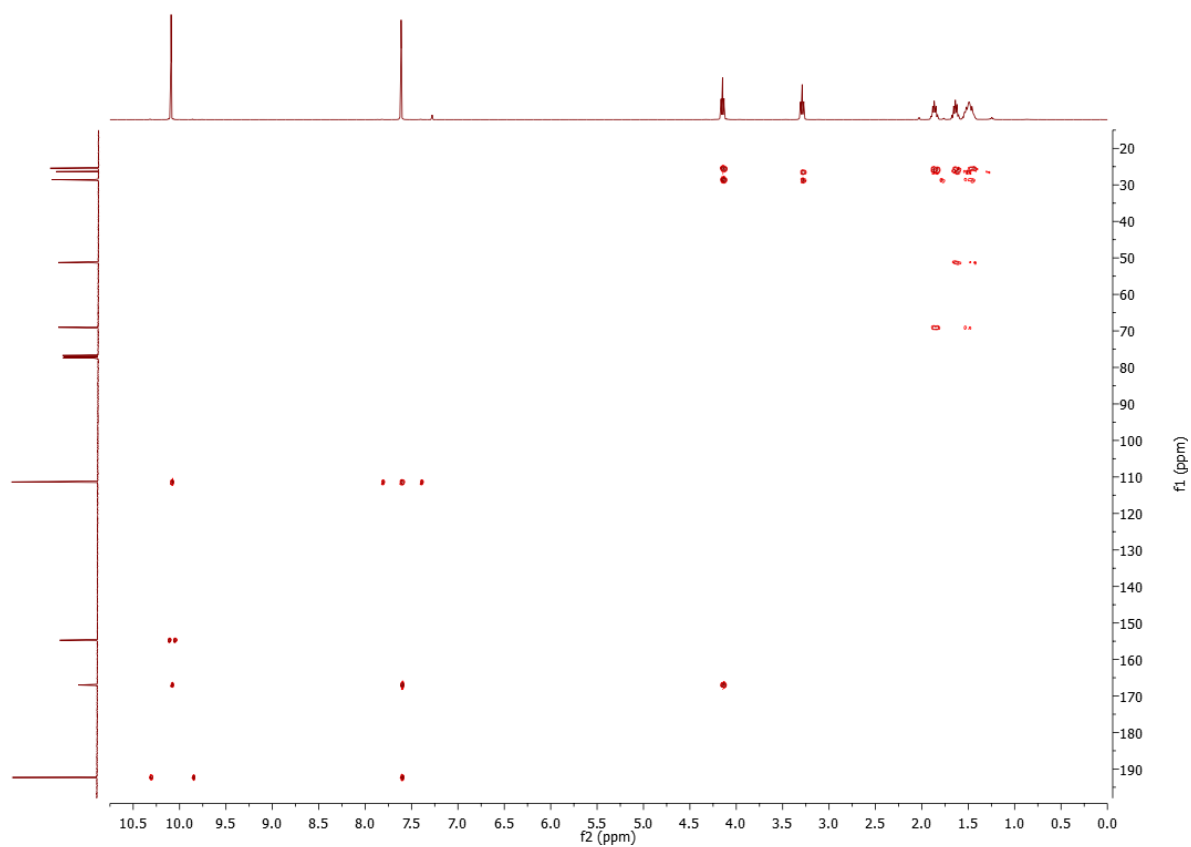
DEPT135 (100MHz) in CDCl₃



HSQC

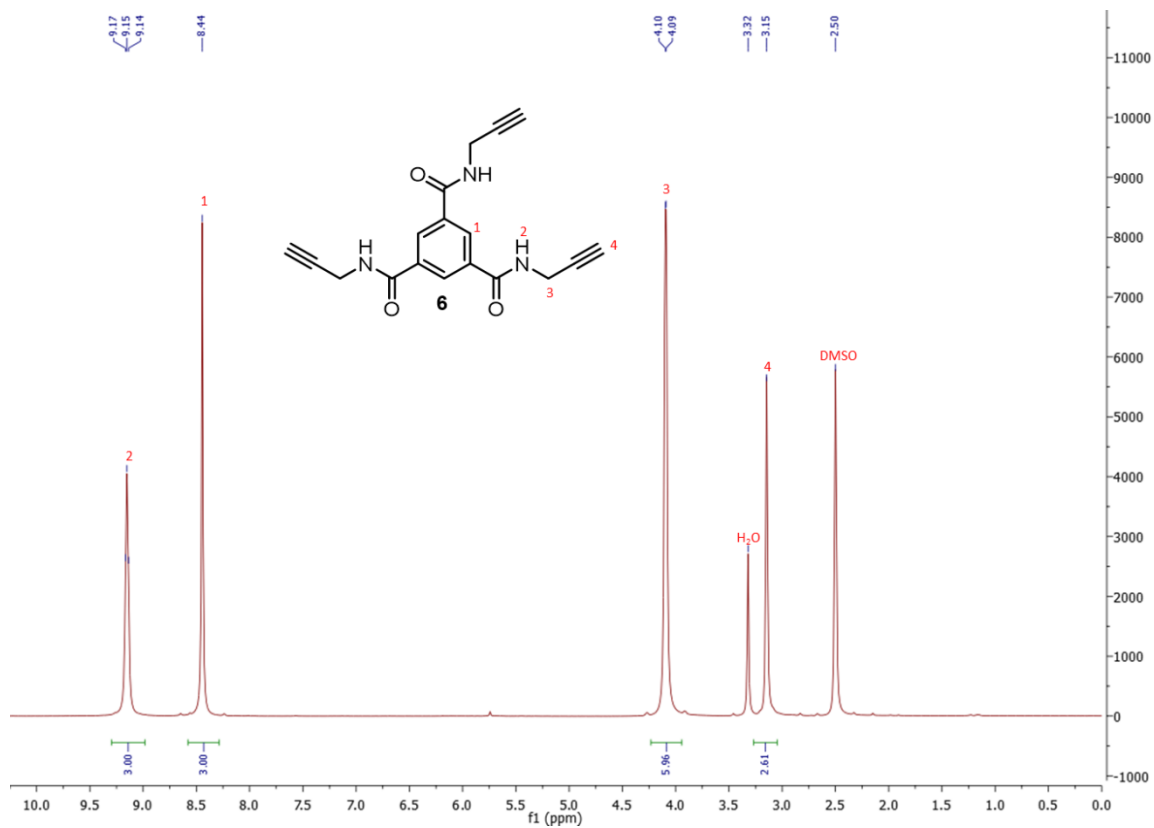


HMBC

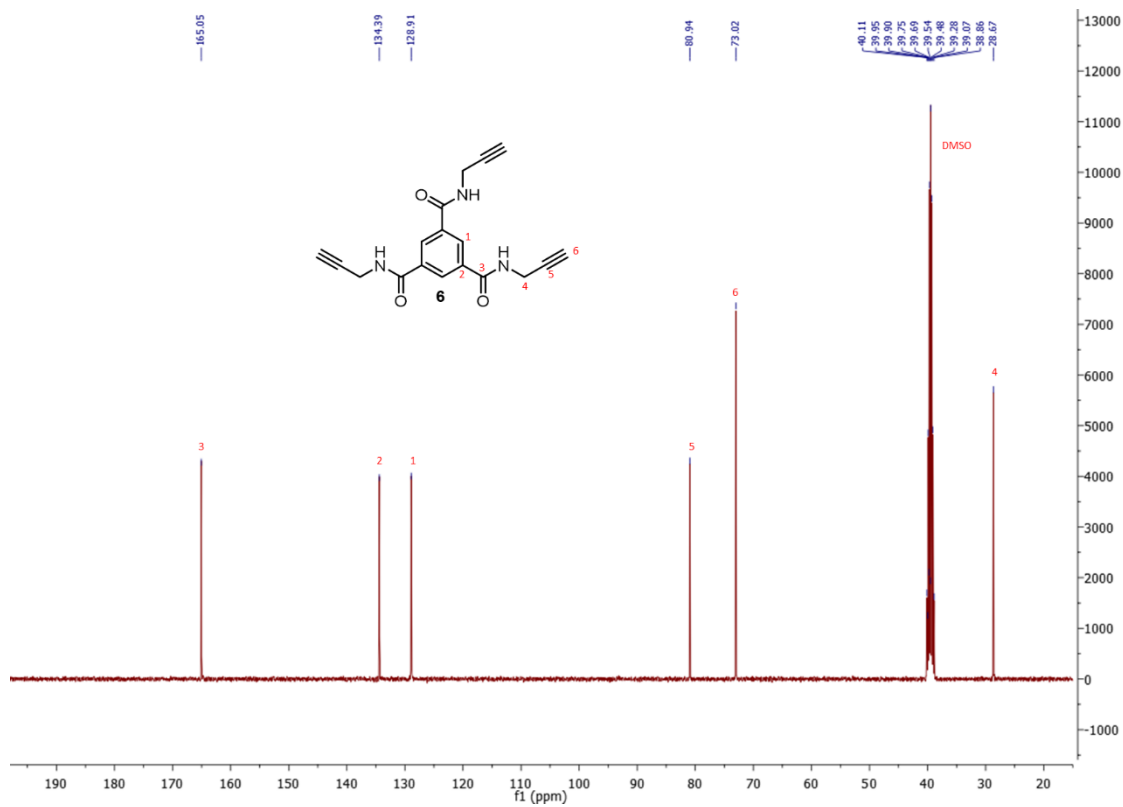


Compound **6**, the BTA core.

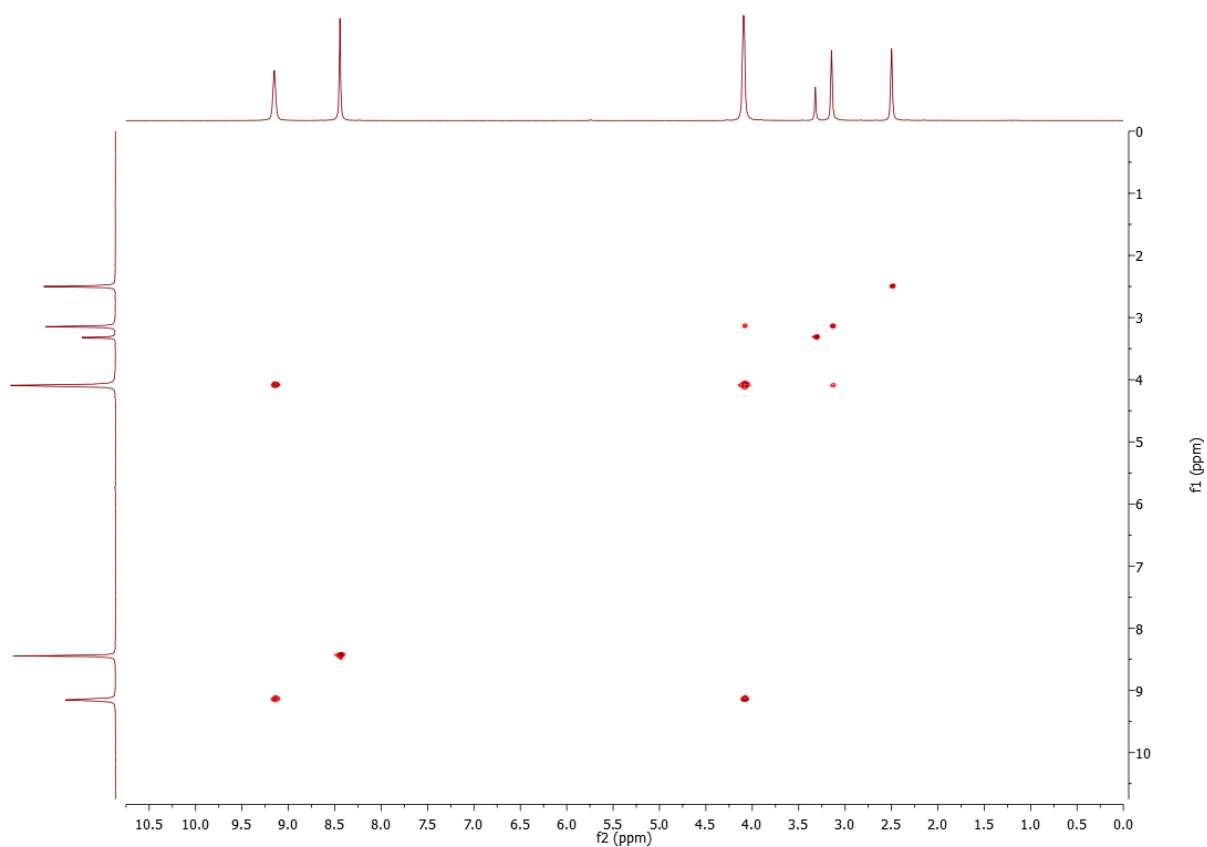
^1H NMR (400MHz) in DMSO



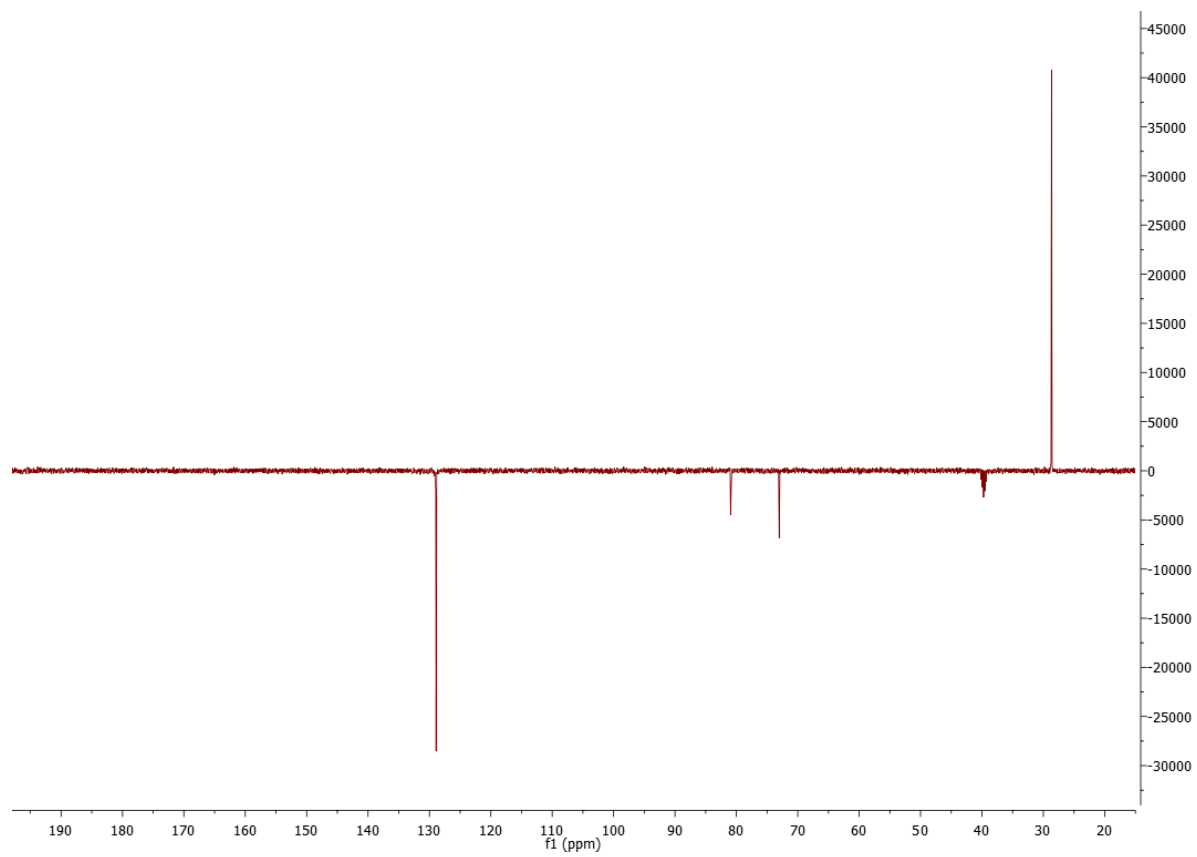
^{13}C NMR (100MHz) in DMSO



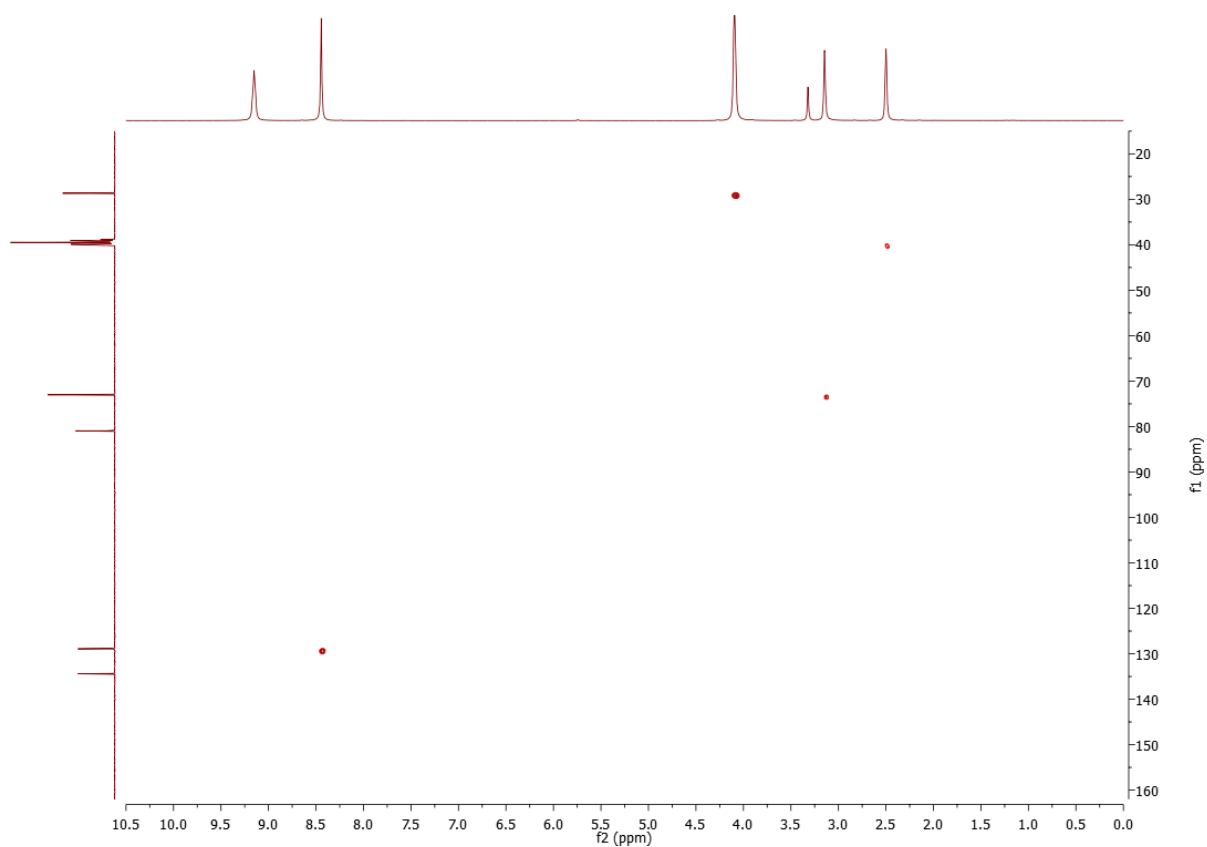
COSY (400MHz) in DMSO



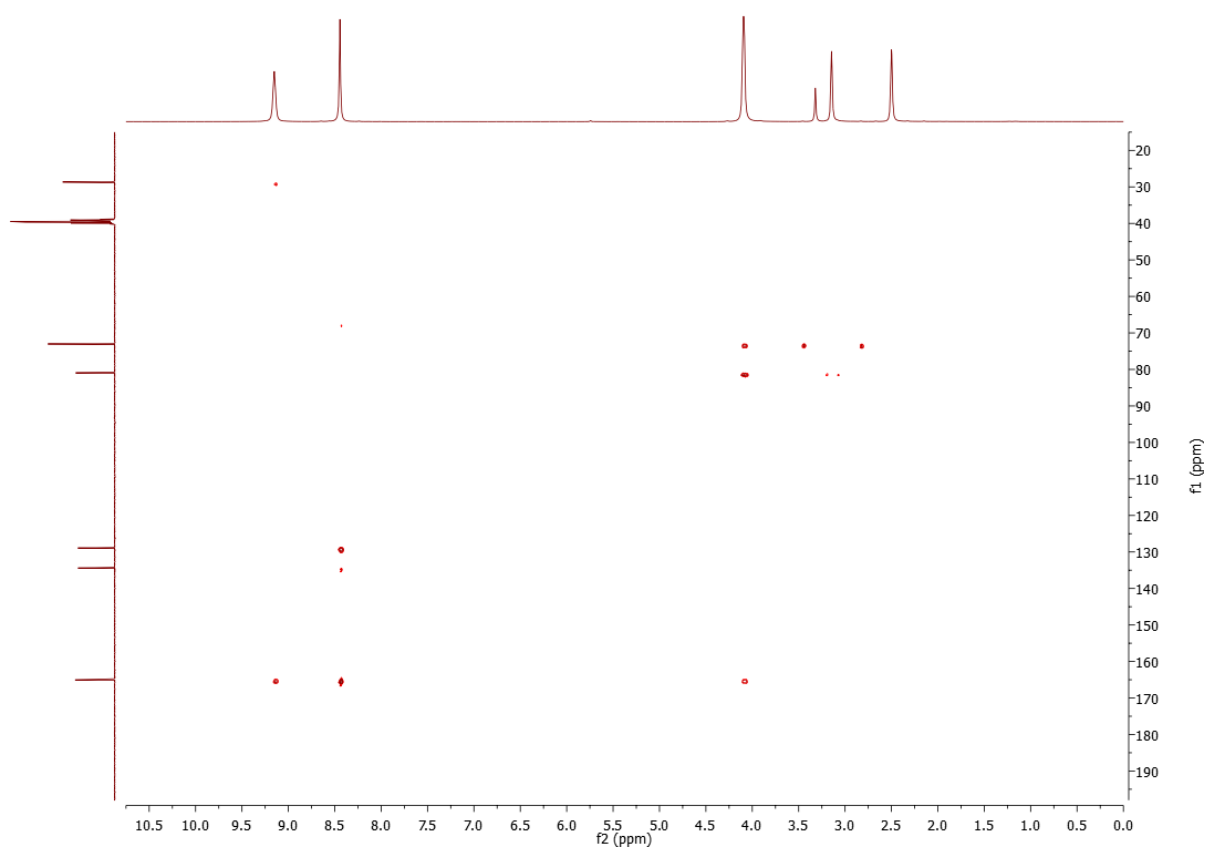
DEPT135 (100MHz) in DMSO



HSQC

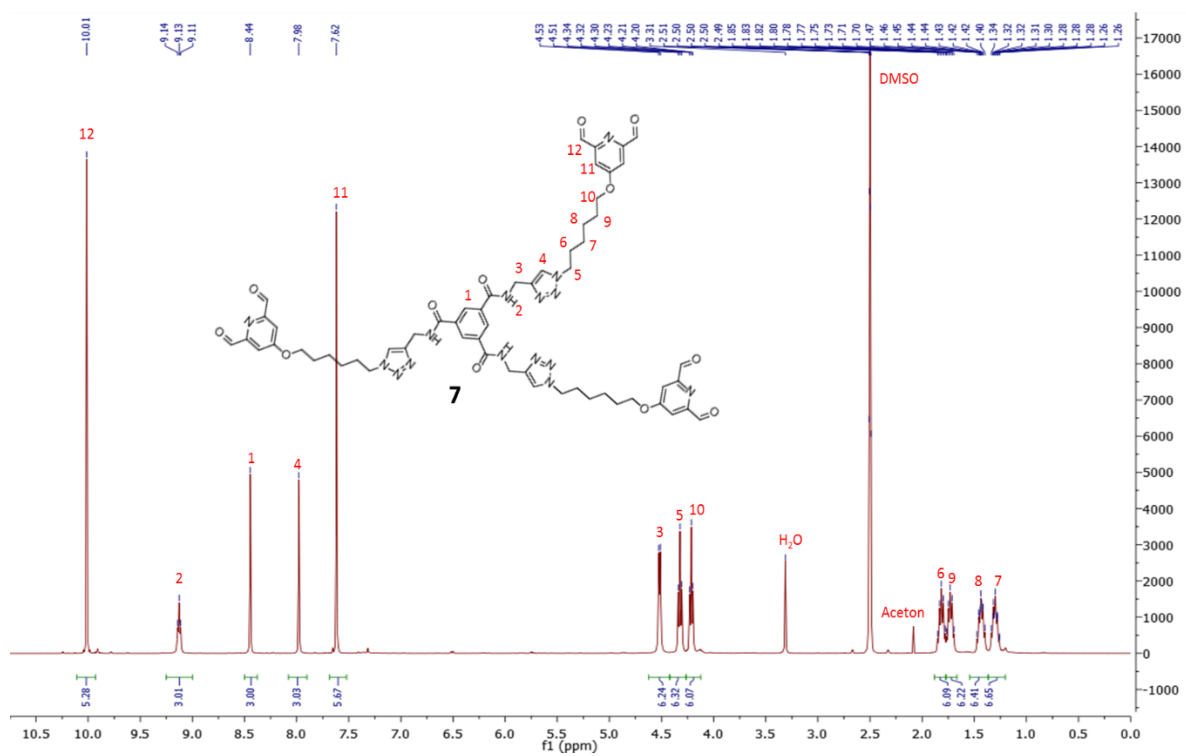


HMBC

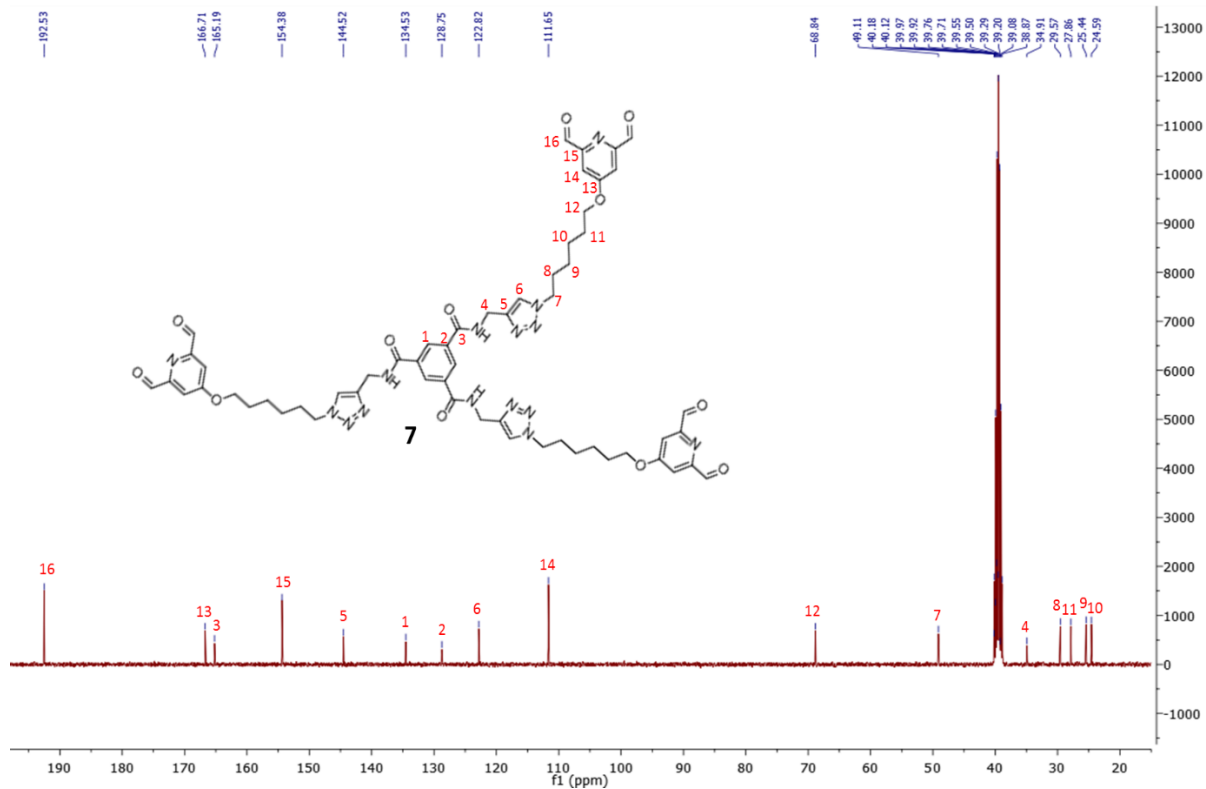


Compound **7**, the tripodal pincer unit.

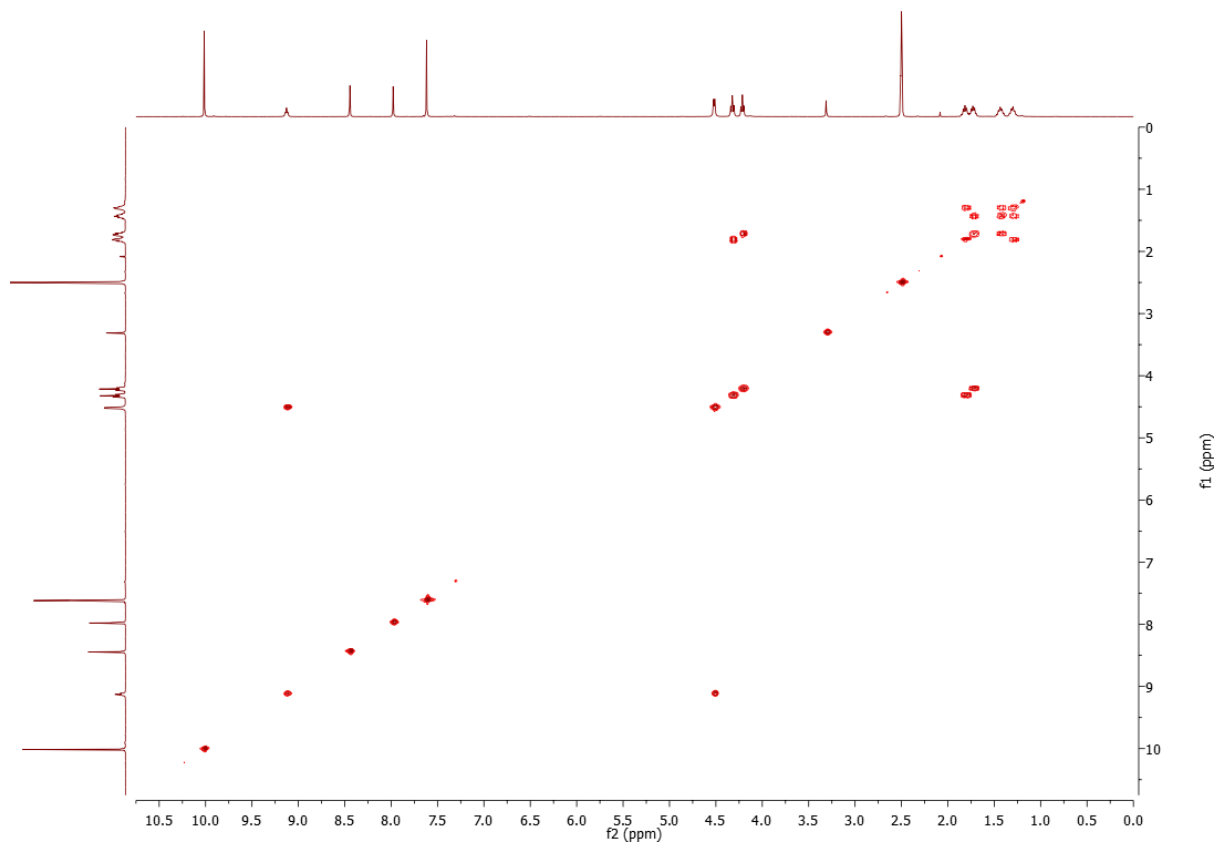
^1H NMR (400MHz) in DMSO



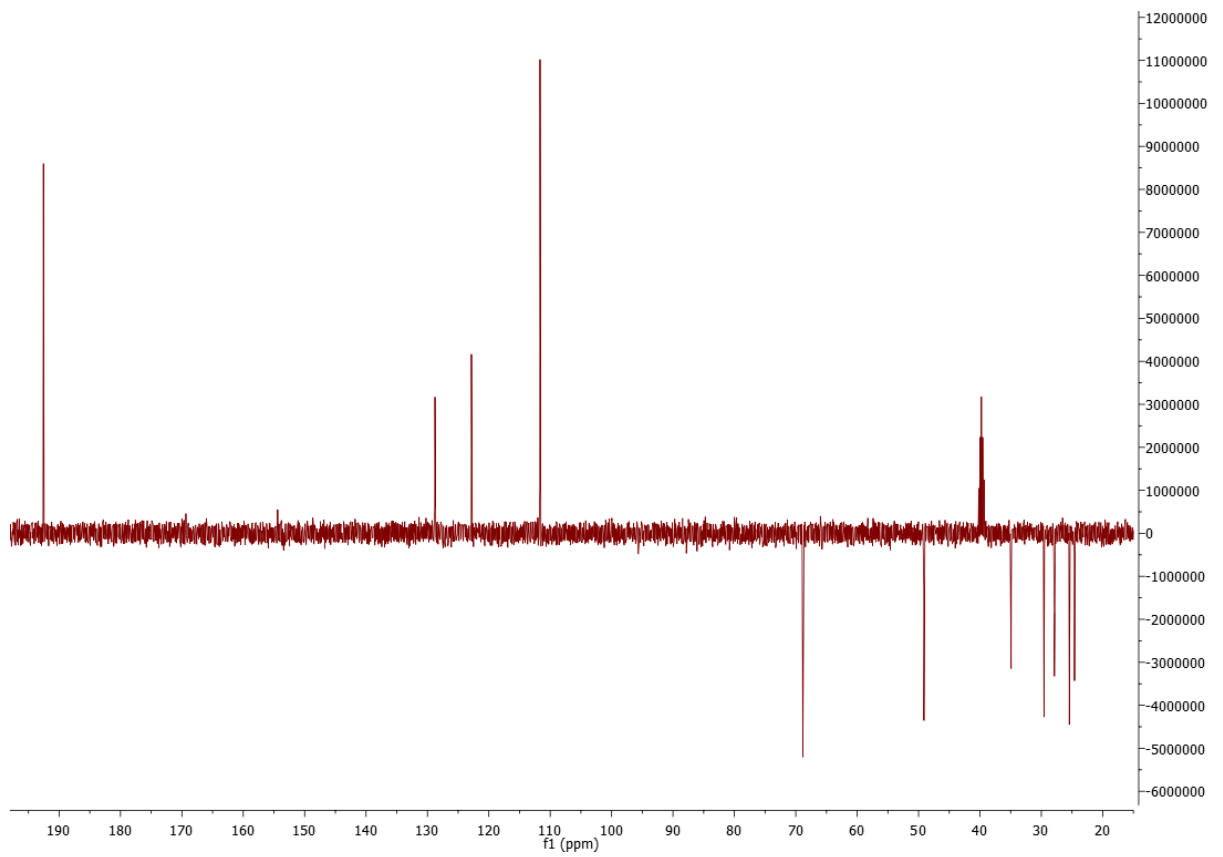
^{13}C NMR (100MHz) in DMSO



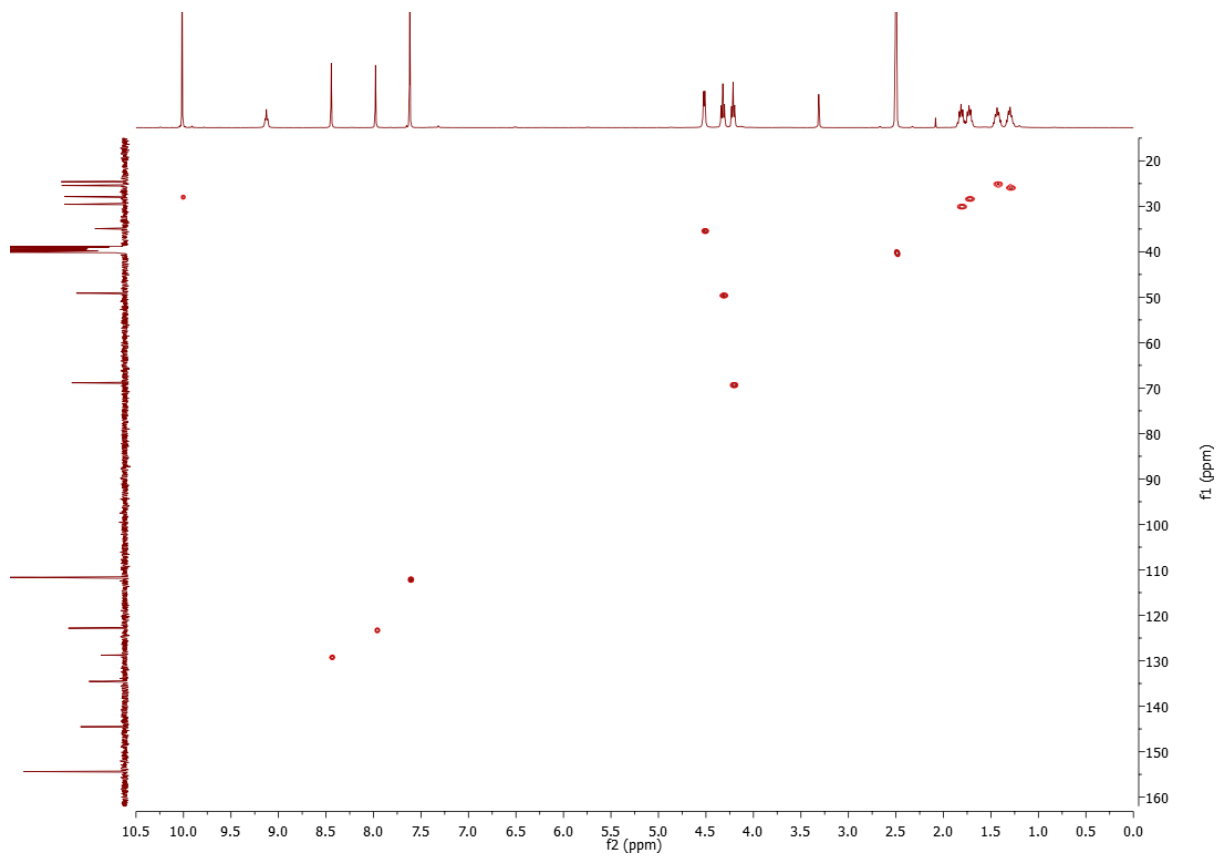
COSY (400MHz) in DMSO



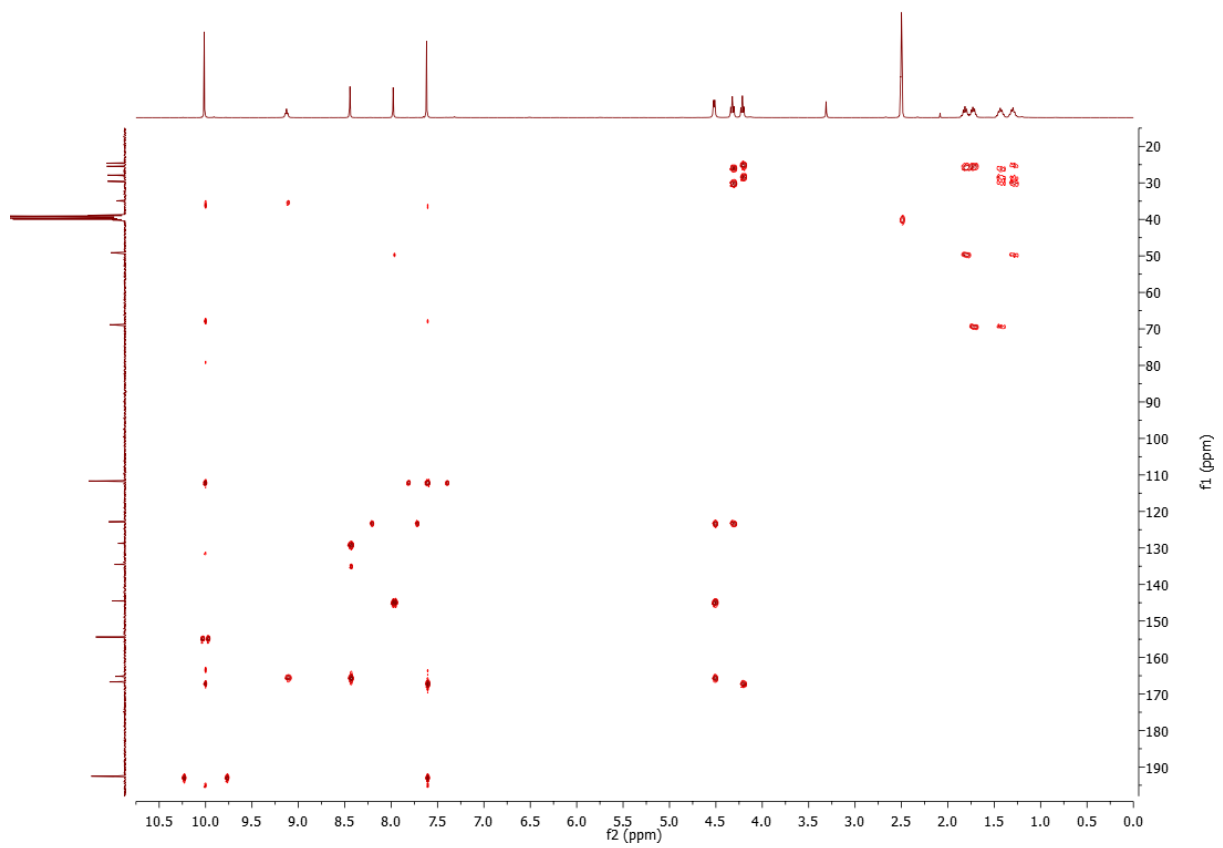
DEPT135 (100MHz) in DMSO



HSQC

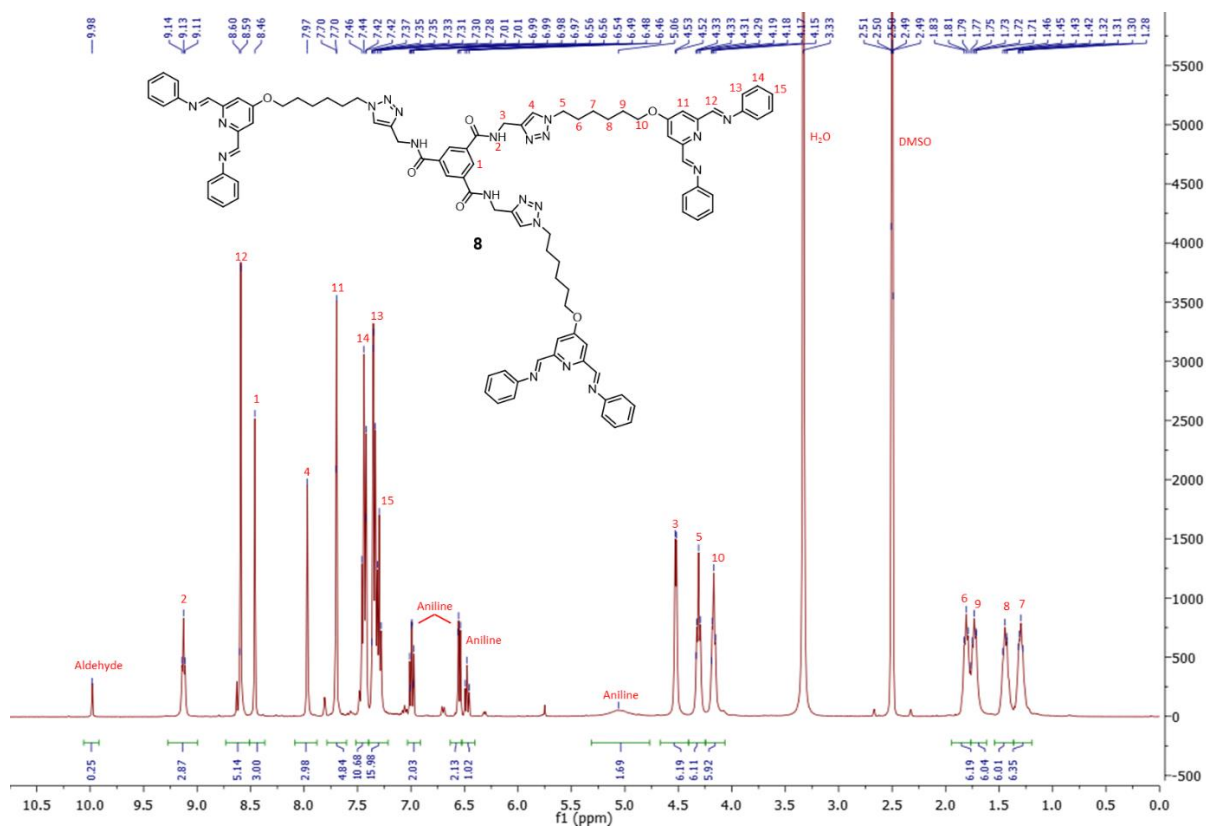


HMBC

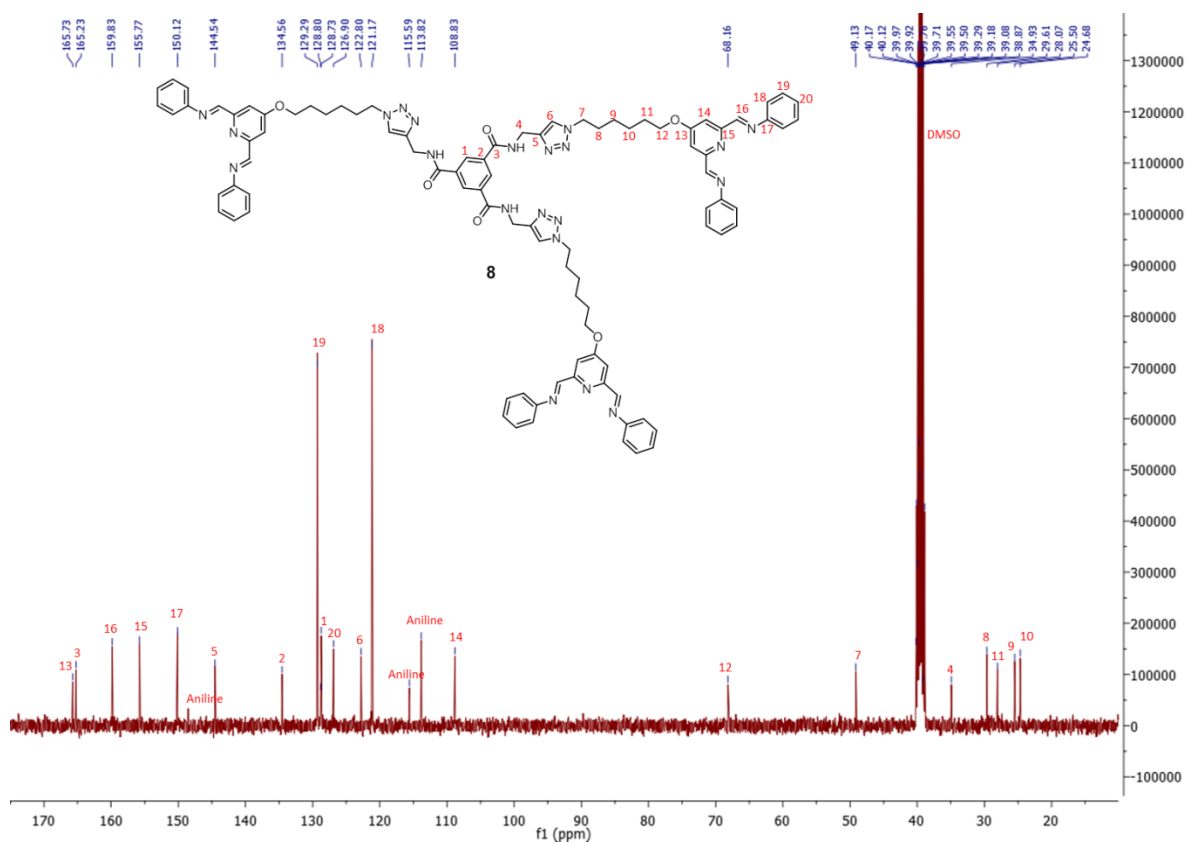


Compound **8**, the final product.

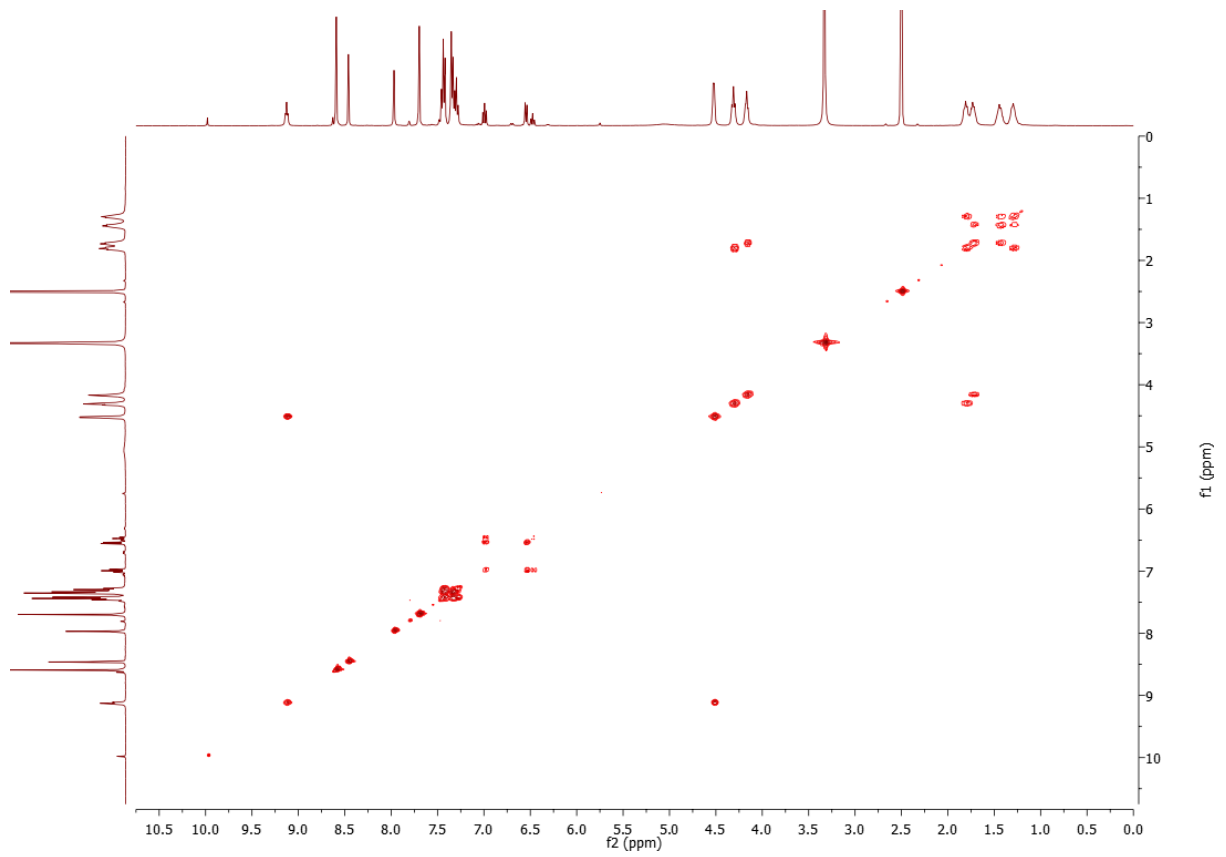
^1H NMR (400MHz) in DMSO



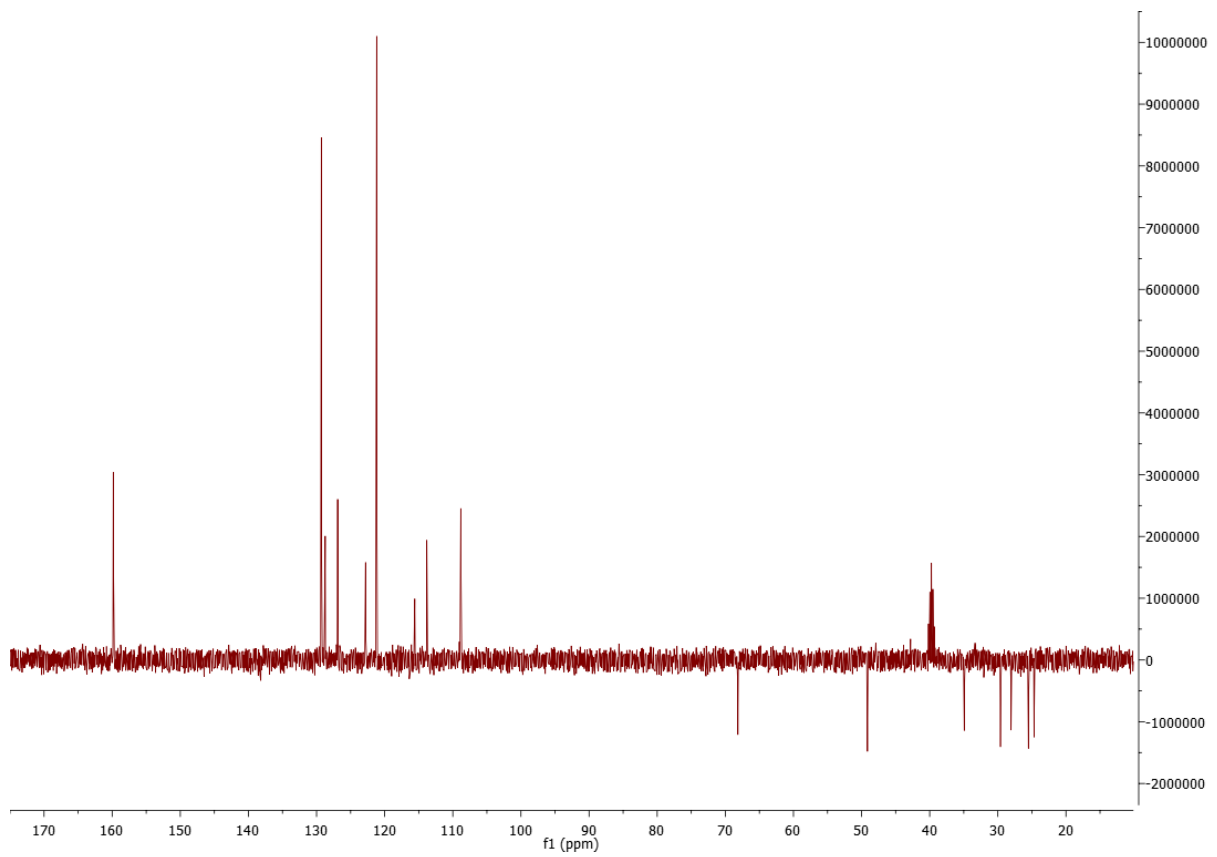
^{13}C NMR (100MHz) in DMSO



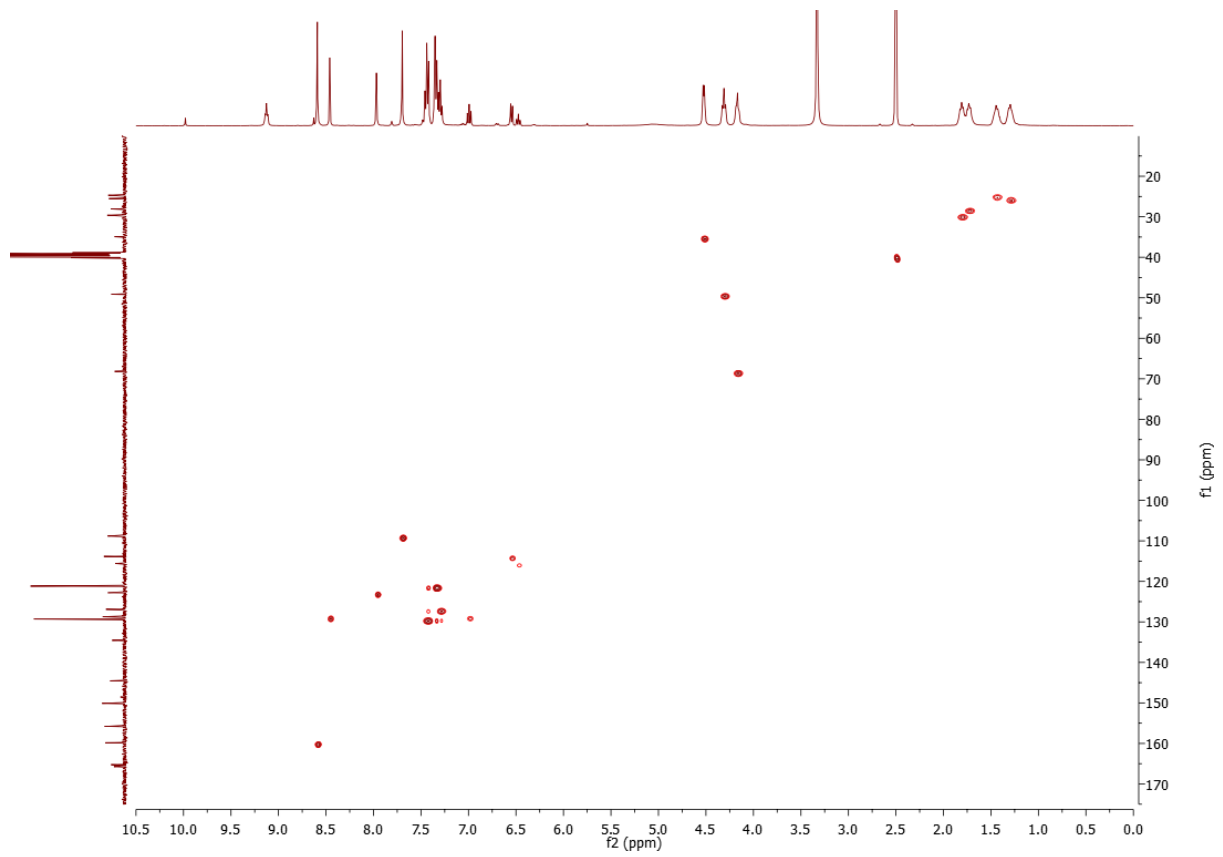
COSY (400MHz) in DMSO



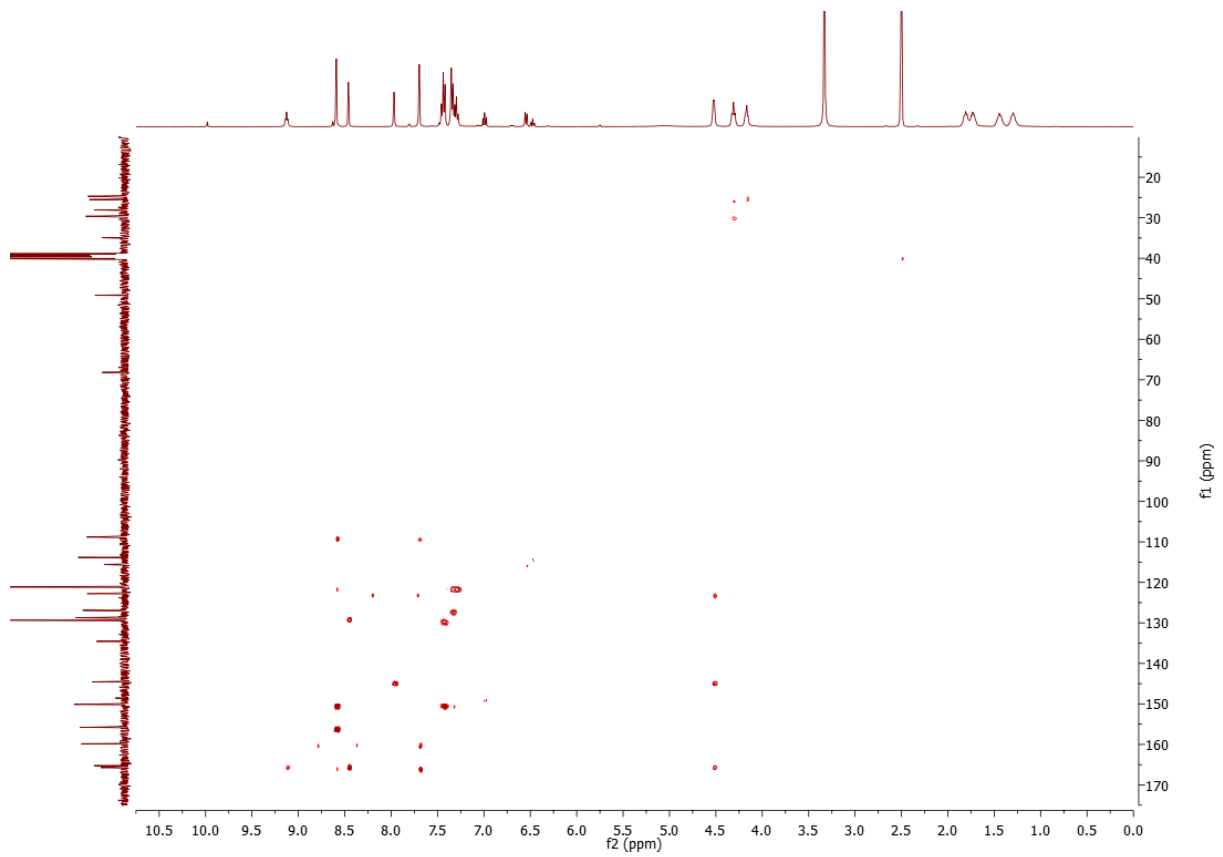
DEPT135 (100MHz) in DMSO



HSQC

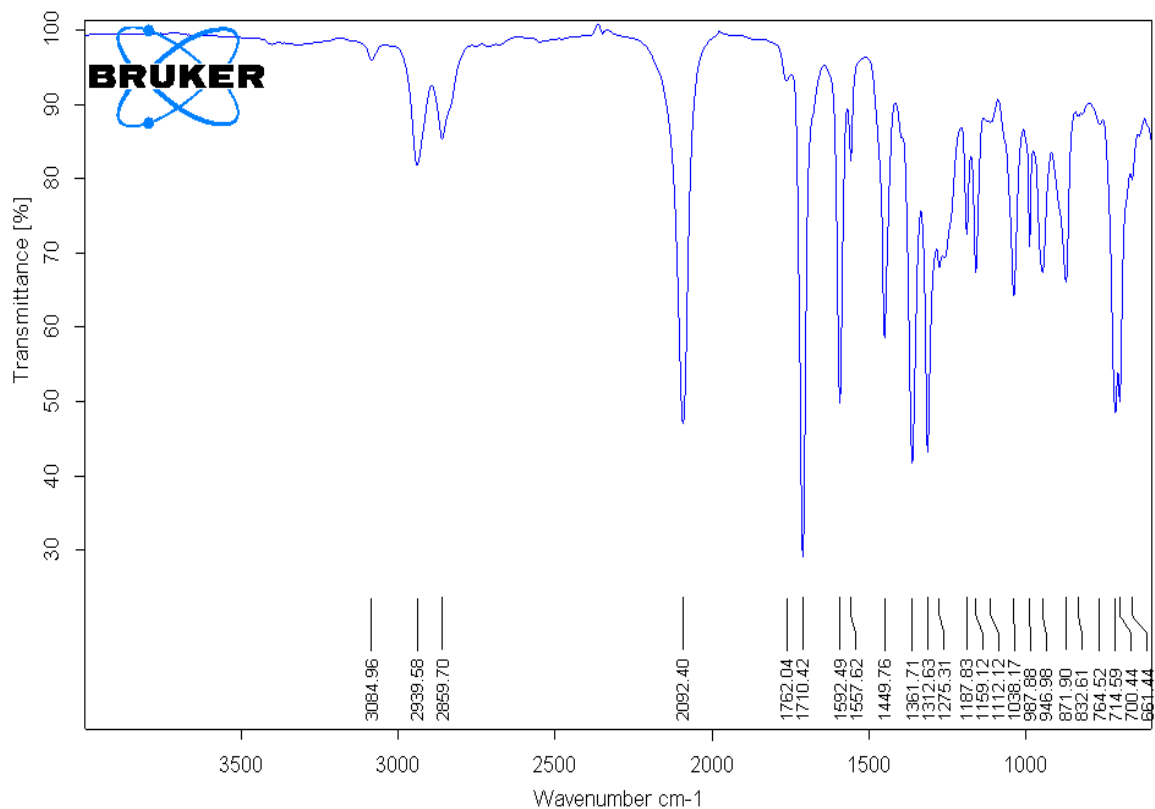


HMBC

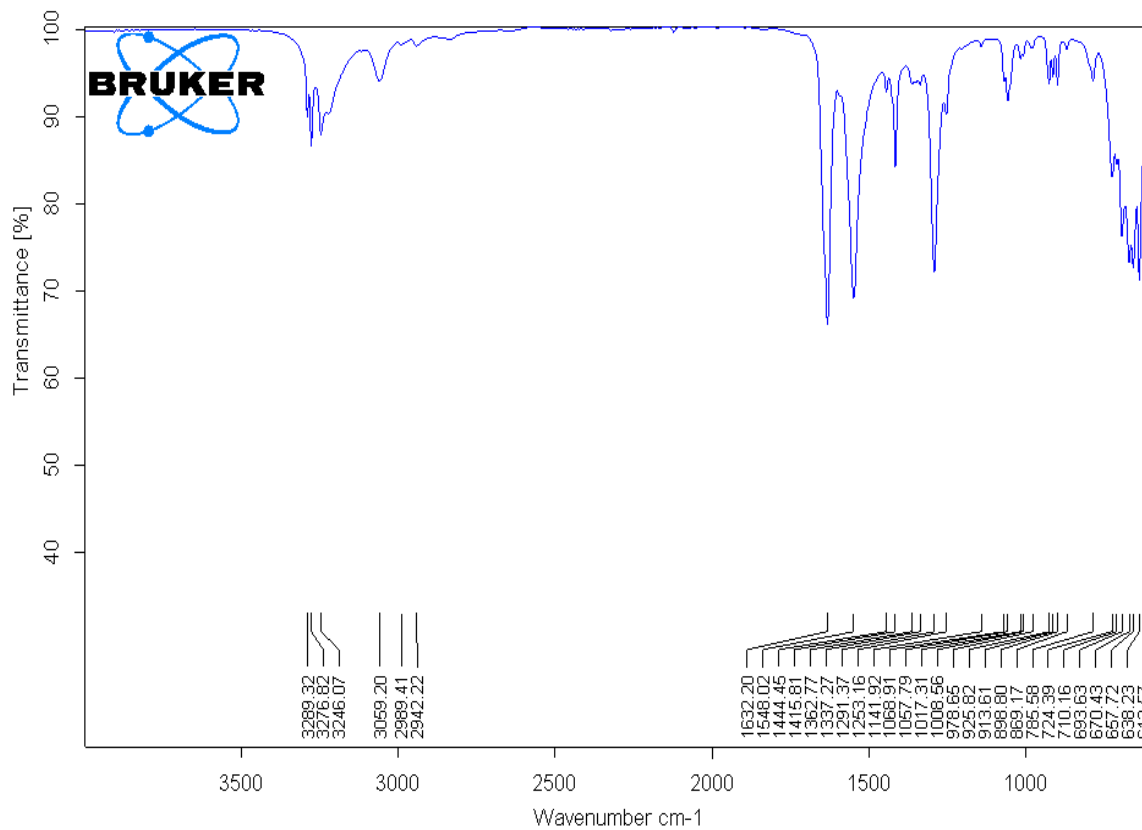


IR

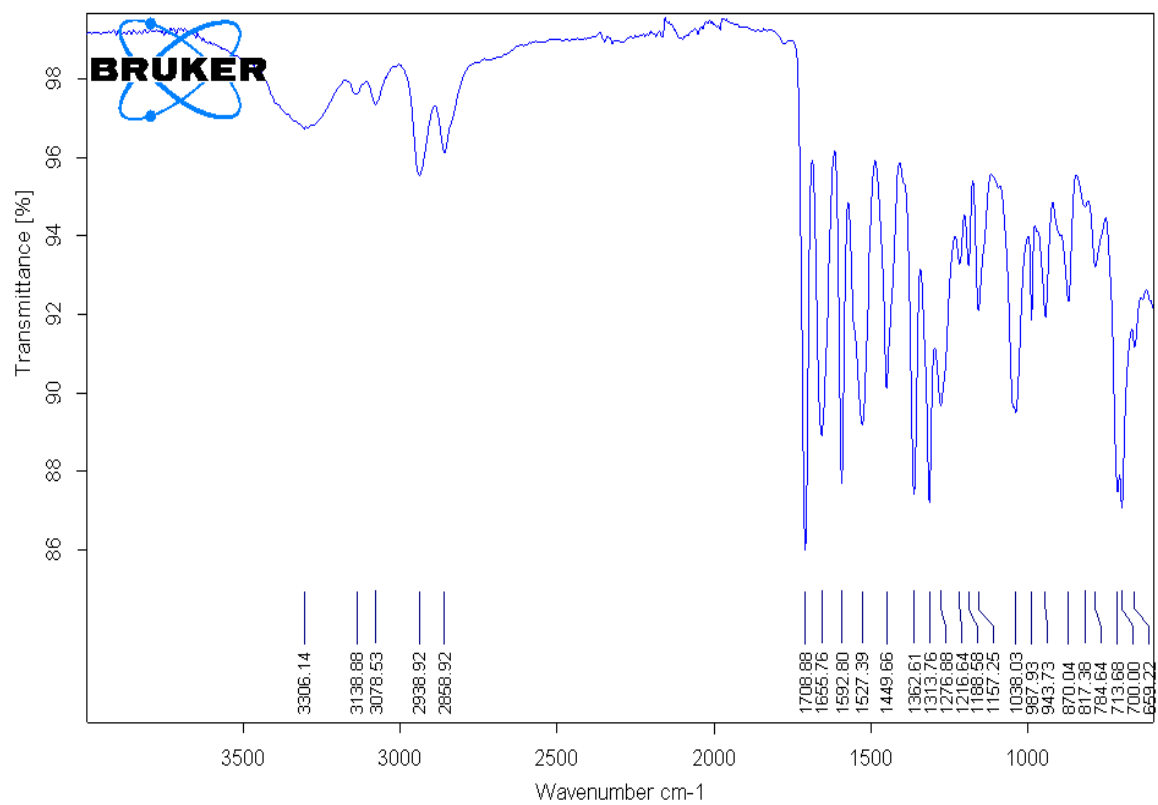
Compound 5.



Compound 6.

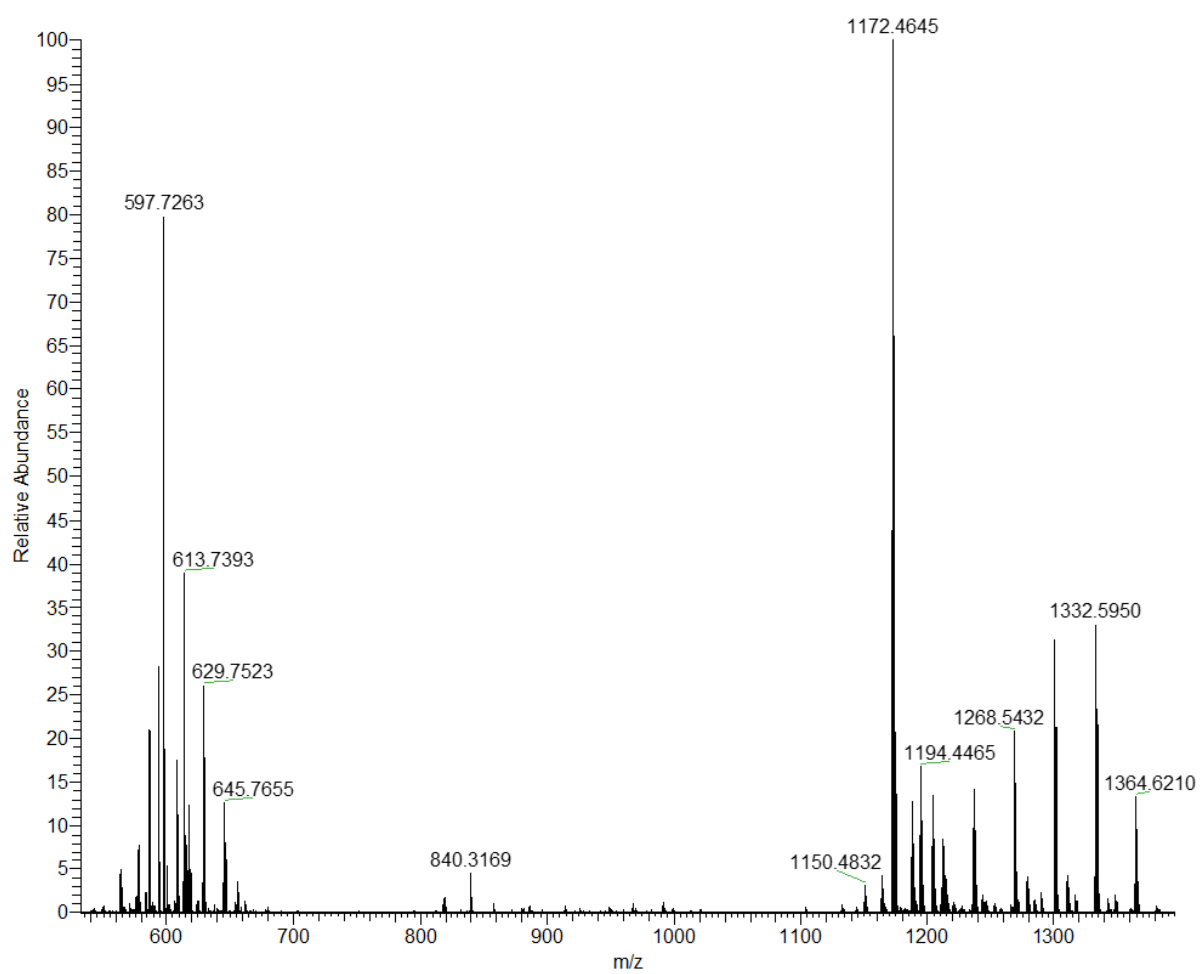


Compound 7.



MS

Compound 7.



2. Overview of gelation attempts

Metal/metal solvent	Metal eq.	Solvent	Gel w/v %	Solubility
CuSO₄	0.15	THF	1	insoluble
<i>In H₂O</i>	0.15	THF	5	insoluble
	0.15	MeOH	1	insoluble
	0.15	MeOH	5	insoluble
	0.15	DMSO	1	soluble
	0.30	DMSO	5	soluble
	0.30	DMSO	1	soluble
	0.30	DMSO	5	soluble
<i>In MeOH</i>	0.15	DCE	1	soluble
	0.15	DCE	5	soluble
	0.30	DCE	1	soluble
	0.30	DCE	5	soluble
	0.75	DCE	5	soluble
	1.05	DCE	5	insoluble
	0.30	DMF	5	soluble
	0.75	DMF	5	soluble
	1.13	DMF	5	soluble
	1.50	DMF	5	soluble
	0.75	DMF/DCE	2.5	soluble
<i>In H₂O</i>	1.50	DCE	5	insoluble

Metal/metal solvent	Metal eq.	Solvent	Gel w/v %	Solubility
Cu(OTf)₂	0.15	DCE	5	soluble (hard to dissolve)
<i>In DMF</i>	0.75	DCE	5	insoluble

Metal/metal solvent	Metal eq.	Solvent	Gel w/v %	Solubility
ZnCl₂	0.15	THF	1	soluble
<i>In H₂O</i>	0.15	THF	5	soluble
	0.30	THF	1	insoluble
	0.30	THF	5	insoluble
	0.15	MeOH	1	insoluble
	0.15	MeOH	5	insoluble
	0.15	DMSO	1	soluble
	0.15	DMSO	5	soluble
	0.30	DMSO	1	soluble
	0.30	DMSO	5	insoluble
	0.75	DMSO	1	soluble

	1.50	DMSO	1	soluble
<i>In THF</i>	0.15	DCE	1	insoluble
	0.15	DCE	5	insoluble
<i>In MeOH</i>	0.30	DMF	5	soluble
	0.75	DMF	5	soluble
	1.13	DMF	5	soluble
	1.50	DMF	5	soluble
	0.75	DMF	10	soluble
	1.50	DMF	10	soluble

Metal/metal solvent	Metal eq.	Solvent	Gel w/v %	Solubility
FeCl₂ (H₂O)₄	0.15	THF	1	soluble
<i>In H₂O</i>	0.15	THF	5	soluble
	0.30	THF	1	insoluble
	0.30	THF	5	insoluble
	0.15	MeOH	1	insoluble
	0.15	MeOH	5	insoluble
	0.15	DMSO	1	soluble
	0.15	DMSO	5	soluble
	0.30	DMSO	1	insoluble
	0.30	DMSO	5	insoluble
<i>In THF</i>	0.15	DCE	1	insoluble
	0.15	DCE	5	insoluble
<i>In MeOH</i>	0.30	DMF	5	soluble
	0.75	DMF	5	soluble
	1.13	DMF	5	soluble
	1.50	DMF	5	soluble
	0.75	DMF	10	soluble
	1.50	DMF	10	soluble

Metal/metal solvent	Metal eq.	Solvent	Gel w/v %	Solubility
Eu(OTf)₃	0.10	DMF/ Acetonitrile	1	soluble
<i>In acetonitrile</i>	0.10	DMF /Acetonitrile	5	phase separation (lost upon heating)
	0.50	DMF/ Acetonitrile	1	soluble
	0.50	DMF/ Acetonitrile	5	phase separation
<i>In DMF</i>	0.50	DCE	5	soluble
	1.00	DCE	5	soluble
	0.50	DMF	1	soluble
	0.50	DMF	5	soluble

	1.00	DMF	1	soluble
	1.00	DMF	5	soluble
	0.50	DMF	10	soluble
	1.00	DMF	10	soluble